Impact of El Nino and La Nina on selected commercially important marine fishery resources of Kerala

by

RESNA. K

(2015-20-016)

THESIS

Submitted in partial fulfilment of the

requirements for the degree of

B.Sc. – M.Sc. (Integrated) Climate Change Adaptation

Faculty of Agriculture

Kerala Agricultural University

ACADEMY OF CLIMATE CHANGE EDUCATION AND RESEARCH

VELLANIKKARA, THRISSUR – 680 656

KERALA, INDIA

2020

DECLARATION

I, Resna, K. (2015-20-016) hereby declare that this thesis entitled **"Impact of El Nino and La Nina on selected commercially important marine fishery resources of Kerala"** is a bonafide record of research work done by me during the course of research and the thesis has not previously formed the basis for the award to me of any degree, diploma, associateship, fellowship or other similar title, of any other University or Society.

Place: Vellanikkara
Date:

Resna. K
(2015-20-016)

CERTIFICATE

Certified that this thesis entitled **"Impact of El Nino and La Nina on selected commercially important marine fishery resources of Kerala"** is a record of research work done independently by Miss. Resna, K. under my guidance and supervision and that it has not previously formed the basis for the award of any degree, diploma, fellowship or associateship to her.

Place: Vellanikkara
Date:

Dr. Shelton Padua
Scientist
Fishery Environment Management Division (FEMD)
Central Marine Fisheries Research Institute (ICAR-CMFRI)
Ernakulam- 682018

CERTIFICATE

We, the undersigned members of the advisory committee of Miss. Resna, K. a candidate for the degree of **B.Sc – M.Sc (Integrated) Climate Change Adaptation** agree that the thesis entitled **"Impact of El Nino and La Nina on selected commercially important marine fishery resources of Kerala"** may be submitted by Miss. Resna, K. in partial fulfillment of the requirement for the degree.

Dr. Shelton Padua
(Chairman, Advisory Committee)
Scientist
Fishery Environment Management Division
Central Marine Fisheries Research Institute (ICAR-CMFRI)
Ernakulam- 682018

Dr. V. Kripa
(Member, Advisory Committee)
Member Secretary
Coastal Aquaculture Authority
Animal Husbandry and Fisheries Department, Nandanam,
Chennai-600035

Dr. P. O. Nameer
(Member, Advisory Committee)
Special Officer
Academy of Climate Change Education And Research (ACCER),
Kerala Agricultural University
Vellanikkara, Thrissur-680656

Dr. D. Prema
(Member, Advisory Committee)
Principal scientist
Fishery Environment Management Division
ICAR-CMFRI, Ernakulam – 682018

(EXTERNAL EXAMINER)

ACKNOWLEDGEMENT

First and foremost, I would like to thank ***God*** *Almighty for giving me the strength and opportunity to undertake this research study and complete it satisfactorily.*

I would like to express my profound gratitude and obligation to ***Dr. Shelton Padua****, Scientist, Fisheries Environment and Management Division, ICAR - Central Marine Fisheries Research Institute, and chairman of my advisory committee. Gratefully I acknowledge his exceptional guidance, constant encouragement, support, patience and time throughout the period of my M.Sc. thesis work.*

I must express my deep sense of gratitude and indebt to ***Dr. V. Kripa****, Member Secretary, Coastal Aquaculture Authority, Animal Husbandry and Fisheries Department, Chennai and member of my advisory committee for her patience, motivation and guidance throughout the study.*

I want to express my extreme gratitude to my advisory members ***Dr. D. Prema****, Principle scientist, Fishery Environment Management Division, CMFRI and* ***Dr. P. O Nameer****, Professor & Special officer, Academy of Climate Change Education and Research, KAU for their constant support and encouragement during my work.*

I respectfully thank ***Dr. A. Gopalakrishnan****, Director, Central Marine Fisheries Research Institute to permit me to undertake this work.I would also like to extend huge thanks on* ***Dr. T. V. Sathianandan****, Principle Scientist & Head in-charge, Fishery resource assessment division for providing necessary data for my work. I would also like to thank* ***Smt. Sindhu K. Augustine*** *&* ***Shri. Paulose Jacob Peter,*** *Technical assistants of FRAD in CMFRI for their valuable and timely suggestions given during my work.*

My sincere thanks also goes to my colleagues at CMFRI, ***Adithya M.V*** *and* ***Sajjan Joseph P*** *for their sincere help, support and kind gestures all throughout my study. Let me thank* ***Punya P, Keziya James*** *(JRF),* ***Vineetha Valsalan*** *(SRF),* ***Ros Kooren*** *(SRF),* ***Shameena M.K*** *(JRF),* ***Liya Benjamin*** *(JRF), and* ***Syamala M. P*** *for their help, support and generous care throughout the study. Also I would like to thank my beloved classmates of*

Academy of Climate Change Education and Research, KAU for their love and support throughout the period of my study.

I am thankful to ***Academy of Climate Change Education and Research*** *and* ***Central Marine Fisheries Research Institute*** *for providing me the opportunity and all the amenities to complete the research programme. I received generous support from all the teachers, scientists, staffs and workers of Academy of Climate Change Education and Research and Fishery Environment Management Division.*

Last, but not the least, I would like to thank my parents and my younger sister for their continuous help, support, steady encouragement and love showered on me during the course of my studies as well as my personal life.

Resna. K

TABLE OF CONTENTS

LIST OF TABLES

LIST OF FIGURES

SYMBOLS AND ABBREVATIONS

AIC	Akaike Information Criteria
APDRC	Asia-Pacific Data Research Center
CEP	Central Equatorial Pacific
CHL_A	Chlorophyll-a concentration
CMFRI	Central Marine Fisheries Research Institute
CP	Central Pacific
CPUE	Catch per Unit Effort
DMI	Dipole Mode Index
EEZ	Exclusive Economic Zone
EMI	El Nino Modoki Index
ENSO	El Nino Southern Oscillation
EOF	Empirical Orthogonal Function
EP	Eastern Pacific
EQUINO	Equatorial Indian Ocean Oscillation
ERSST	Extended Reconstructed Sea Surface Temperature
ESRL	Earth System Research Laboratory
FAO	Food and Agriculture Organization
GAM	Generalized Additive Model
GCOS	Global Climate Observing System
GDP	Gross Domestic Product
IM	Indian mackerel
IMD	India Meteorological Department
IOD	Indian Ocean Dipole
IPCC	Intergovermental Panel on Climate Change
ISMR	Indian summer monsoon rainfall
JAMSTEC	Japan Agency for Marine-Earth Science and Technology
LTA	Local Temperature Anomaly
MDTN	Multi day trawl net
MEI	Multivariate ENSO Index
MERIS	Medium Resolution Imaging Spectrometer

MGN	Mechanized gillnet
MHL	Mechanized hook and lines
MODIS	MODerate Resolution Imaging Spectro-radiometer
MOTHS	Mechanized other gears
MPS	Mechanized purse seine
MRS	Mechanized ring seine
MTN	Mechanized trawl net
NCAR	National Center for Atmospheric Research
NetCDF	Network Common Data Form
NFDB	National Fisheries Development Board
NM	Non-motorized gears
NMFDC	National Marine Fisheries Data
NOAA	National Oceanographic and Atmospheric Administration
OBBN	Outboard bag net
OBBS	Outboard boat seine
OBGN	Outboard gill net
OBHL	Outboard hook and lines
OBPS	Outboard purse seine
OBRS	Outboard ring seine
OBSS	Outboard shore seine
OC-CCI	Ocean Colour Climate Change Initiative
OCD	Ocean current direction
OCV	Ocean current velocity
OGD	Open Government Data
OLR	Outgoing long wave radiation
ONI	Oceanic Nino Index
OS	Oil sardine
PO.DAAC	Physical Oceanography Distributed Active Archive Centre
PP	Penaeid prawn
PSD	Physical Science Division
RF	Rainfall
SALT	Sea surface salinity

SeaWiFS	Sea-Viewing Wide Field-of-View Sensor
SLA	Sea-level anomaly
SLP	Sea Level Pressure
SODA	Simple Ocean Data Assimilation Ocean/Sea ice Reanalysis
SOI	Southern Oscillation Index
SSHA	Sea Surface Height Anomaly
SST	Sea Surface Temperature
SSTA	Sea surface temperature anomaly
TB	Threadfin bream
TNI	Trans Nino Index
VIIRS	Visible Infrared Imaging Radiometer Suite
WG-SP	Working Group on Surface Pressure

CHAPTER I

INTRODUCTION

Regional climates are the composite result of nearby physical processes and other global phenomena such as ENSO. Human influence on climate is apparent and the expanded emissions from anthropogenic activities are worsening the impacts of climate change on human populations and ecosystems (IPCC, 2014). There is high confidence that ENSO will stay as the dominant mode of interannual climate variability with great influence on human populations and ecosystems. And due to the increased moisture availability, the precipitation events associated with ENSO will intensify on a provincial scale (IPCC, 2014).

El Nino is the southward moving warm water current along the coast of Ecuador and Peru, usually occurred around Christmas time and thus given the name El Nino (the boy Child Christ in Spanish). This intermittently happening warm water current initially observed by Peru's occupants which bring additional rainfall on arid land, cause an ecological and economic fiasco by affecting the plenitude of Anchovies (largest single-species fishery of the world) and sea birds and seals population that relied upon anchovies for food. Now, the phenomenon is identified as basin-wide warming of equatorial eastern Pacific associated with the seesaw pattern of atmospheric pressure over the equatorial Pacific Ocean, called the Southern Oscillation. The combined oceanic and atmospheric effects are called El Nino Southern Oscillation (ENSO). The warm phase of ENSO is El Nino and the cool phase (opposite to the El Nino) is La Nina (the girl in Spanish) (Trenberth, 1997).

The ENSO, the coupled ocean-atmosphere phenomenon (Bjerknes, 1969), is regarded as a dominant source of interannual climate variability across the globe (Trenberth, 1997). These occur at the time scale of 2-7 years (Glantz 2001) and last for 6-12months. During warm El Nino, prevailing trade winds weaken, enhance deep atmospheric convection and westerly wind anomalies, the eastward warm surface current and deeper thermocline diminish the upwelling happening at eastern Pacific coast and alter ocean circulations (IPCC, 2014). El Nino and La Nina are accompanied by changes in sea surface temperature of tropical Pacific, strengthening or weakening of trade winds, shifts in walker circulation, east-west sea level pressure seesaw, and rainfall anomalies (Folland et al. 2002).

The last 5000 years have witnessed about 20 major El Niño events, which have severely affected different parts of the world. El Nino is one of the most deliberately studied climatic phenomena during the last fifty years. After the 1980s, National Oceanographic and Atmospheric Administration (NOAA) and National Center for Atmospheric Research (NCAR) started studying ENSO vigorously,

two severe El Nino events were observed: 1982/83 and 1997/98 and a strong La Nina in 1999. At the beginning of the twenty-first century (2002–2003, 2004–2005, 2006 and 2009–2010), El Niño events were weak. But in 2015/16, we witnessed another major El Nino event (Grove and Adamson, 2018). The 1982/83 El Nino event was addressed as 'El Nino Of the century' until 1997/98 El Niño happened (Wolter and Timlin, 1998; Grove and Adamson, 2018).

Recently, the scientists increasingly discriminate El Niño events as Eastern Pacific (EP) (Canonical El Niño) and Central Pacific (CP) El Nino (El Niño modoki) (Ashok *et al.,* 2007; Weng *et al.,* 2007; Kao & Yu, 2009; Kug *et al.,* 2009; Yeh *et al.,* 2009; McPhaden *et al.,* 2011; Yu and Kim, 2012). The CP event has sea surface temperature anomalies near the dateline and the EP event or cold tongue type has sea surface temperature anomalies over the eastern Pacific. Sea surface temperature anomalies during El Nino modoki events are characterized by the presence of cool surface water in both east and west Pacific (Ashok *et al.,* 2007). When both types co-exist (SST anomalies are relatively high in both central and eastern Pacific) it called Mixed type (MIXENSO) (Yu and Kim, 2012). The CP event occurs more frequently than the EP El Niño event and doubled the intensity over the past 30 years (Yeh *et al.,* 2009; Lee and McPhaden, 2010). Yu and Kim (2012) concluded that EP El Niño is more frequent in 20th and early 21st century and CP events are more robust in the late 21st century. These two types of El Nino have quite different global impacts, for example, the 1997/98 El Niño did not produce drought in India and the 2004 El Niño did (Kumar, *et al.,* 2006), maximum rainfall anomalies are near dateline for EP type and for CP type it shifts to 165°E (Yeh *et al.,* 2009).

The surface of the Indian, Atlantic, and the Pacific Ocean has warmed by 0.11°C, 0.07°C, and 0.05°C per decade (1950-2016) respectively (IPCC, 2018). SST in the western Pacific has increased by up to 1.5°C per century, and the warm pool has expanded (Cravatte *et al.,* 2009). The global climate model predicted that if the emissions of greenhouse gases continue to increase, there will be more frequent El Nino events and stronger La Nina conditions in the tropical Pacific Ocean (Timmermann *et al.,* 1999). The more frequent CP El Nino under global warming could induce more drought conditions over India and Australia (Ashok *et al.,* 2007; Weng *et al.,* 2007; Yeh *et al.,* 2009). Recent research (Wang *et al.,* 2017) also reveales that the frequency of extreme El Nino events increases with the global mean temperature and that the number of such events might double (one event every ten years) under 1.5°C of global warming. Even if the Global Mean Temperature stabilizes at 1.5°C, this trend will continue for a century, which indicates high risk even at the 1.5°C threshold. The frequency of the La Nina event persists as the same as the present-day under 1.5°C to 2°C warming.

ENSO affects global weather patterns through atmospheric teleconnections (Ashok *et al.,* 2001). These conditions have impacts on societies through agriculture and food security, water

resources, health, disaster occurrences including drought and floods, and numerous other means leading to worldwide economic damage (Zebiak *et al.,* 2014; Nobre *et al.,* 2019). The impact of El Nino events on Indian summer monsoon rainfall is one of the most studied areas. El Nino episodes are known to change the environmental characteristics of coastal waters which are the major habitats of the fishery resources. The variations in environmental factors including the ranges of SST, salinity, dissolved oxygen, nutrients, etc. can affect biological processes like maturation and spawning. The recruitment success of fishes and shellfishes also depends on the availability of food and other abiotic factors like current, all of which may be influenced in varying intensities by ENSO episodes.

Marine fisheries are one of the most important sectors of the Indian economy. India has a coastline of 8,118 km, an exclusive economic zone (EEZ) of 2.02 million square km, and four millions of people live in the coastal areas. There are 3288 marine fishing villages along the coast of India where people venture into coastal waters and harvest natural resources for their livelihood. There are 864,550 marine fisherman households in India out of which 118,937 households are in Kerala. Among these households in the country, 91.3% are traditional fishermen families (CMFRI, 2012). The fisheries sector contributes around 1% to national GDP (Gross Domestic Product) and 5.23% to Agriculture GDP. Fish and fish products contribute 20% to the national agriculture exports and recently emerged as the largest group in the agriculture exports (NFDB, 2019). There are about 4.0 million marine fishers along the coastal areas of India, indicating an increase of 14% over the last five years (Rao *et al.,* 2016). There are different types of fishing crafts and gears operated in each state and the CMFRI has a detailed census report of the number of fishermen and the fishing units of each state.

According to the Food and Agriculture Organization of the United Nations, in 2018 India stands the sixth position in world marine fish production, landings estimated as 3.49 million metric tonnes. The state Kerala contributed 6.43 lakh tonnes and was the third-largest contributor to Indian marine fish production in 2018. Kerala was positioned second in terms of species diversity. In 2018, 423 species were landed in Kerala. However, Kerala recorded a decline in species diversity compared to 2017 (CMRFI, 2019). Sathianandan*, et al.,* (2008) stated that out of 800 species landed along the Kerala coast around 200 are commercially important and they are classified in to 60 groups or species. Similarly, the study on the alpha, beta, and gamma diversity of the species in various locations of Kerala during the period 1970-2005 (Zacharia *et al.,* 2011) also indicated that there is a rich diversity of fished taxa along Kerala coast. Fishery along the west coast of India dominated by pelagic fish resources (53.4% in 2018), followed by demersal resources (27.1% in 2018) (CMFRI, 2019). The area within 200 m isobath, which properly covers the EEZ and highly productive coastal waters serves as spawning sites as well as feeding grounds for fish larvae, juveniles, and adults (George, *et al.,* 2019).

Kumar et al. (2014) have analyzed the impact of ENSO on tuna fisheries in the Indian Ocean and he found that high tuna landings were recorded during weak El Nino and La Nina periods. The reduction in Oil sardine catch along the Kerala coast during 2015-16 El Nino period was reported by Shetye et al. (2019). Though there are annual assessments of the fishery of each maritime state, the response of both pelagic and demersal fish species to warming or extreme events caused by climatic events such as El Nino Southern Oscillation (ENSO) and Indian Ocean Dipole (IOD) is poorly studied.

Considering the importance of marine fisheries to the national economy and the vulnerability of marine fishery resources and the coastal communities to ENSO, a study titled "Impact of El Nino and La Nina on selected commercially important marine fishery resources of Kerala" has been carried out with following objectives;

1. To assess the variations in ocean-atmospheric parameters during El Nino and La Nina years
2. To assess the impact of El Nino and La Nina on major pelagic and demersal resources of Kerala

This study attempted to generate information on how the ENSO events affected the ocean-atmospheric parameters, fish resources and fishery. The results of the study would help to expand the knowledge base, increase the preparedness of the fishers to face the decline in the fishery and also help policymakers and planners to prepare for the eventualities resulting from ENSO.

CHAPTER 2

REVIEW OF LITERATURE

El Niño Southern Oscillation (ENSO) is an important coupled Ocean-atmosphere phenomenon (Bjerknes, 1969) that happens every 2-7 years (Glantz 2001) and it is regarded as one of the main causes of interannual climatic variability across the globe (Kiladis and Diaz, 1989; Trenberth, 1997; Plisnier et al. 2000; Suarez et al. 2004). ENSO is also referred to as the see-saw pattern of atmospheric pressure over the equatorial Pacific Ocean. El Niño is the warm Ocean current that flows southward along the coast of Peru and Ecuador on Christmas time (the boy Christ child in Spanish). Opposite to this warm phase, the cold phase of ENSO is La Nina (the girl), it causes a basin-wide cooling of equatorial Pacific Ocean (Trenberth, 1997). Even though the origin of ENSO is in the equatorial Pacific Ocean, it generates far-reaching climate anomalies and has worldwide environmental impacts (McPhaden *et al.,* 2006). ENSO influences weather events such as drought, flood, tropical cyclones, forest fires, and affect the lives of millions of people. Recent research discriminates El Niño events as Eastern Pacific (Canonical El Niño) and Central Pacific ElNino (El Niño modoki) (Ashok *et al.,* 2007; Weng *et al.,* 2007; Kao & Yu, 2009; Kug *et al.,* 2009; McPhaden *et al.,* 2011). CP event occurs more frequently than EP El Niño event and doubled the intensity over the past 30 years (Lee & McPhaden, 2010). This may be due to increasing greenhouse gas concentrations in the atmosphere (Yeh *et al.,* 2009) or natural climatic variability (McPhaden *et al.,* 2011; Yeh *et al.,* 2011). El Niño induces immoderate rains and Floods in the Central and Eastern Pacific areas, patches of South America near to Argentina and Uruguay and west coast of the USA (Ward *et al.,* 2016), and drier conditions or droughts over South East Asia, Philippines, Indonesia, and Africa due to the greater atmospheric pressure over these regions (Baudoin *et al.,* 2017). The impacts of canonical El Niño are opposite to those of El Niño Modoki across many parts of the world such as tropical South America, Stretches of Africa near the equator, and India (Ashok *et al.,* 2007). The last five millennia have witnessed about 20 major El Niño events. It was also observed that no two El Niño events are identical and this diversity results in varied ecological and socio-economic responses to El Niño (FAO, 2020).

2.1 Impacts of El Niño and La Nina on coastal and marine resources

The ENSO phenomenon changes climate, weather patterns, oceanic conditions, and productivity across the globe (McPhaden, *et al.,* 2006) through atmospheric and oceanic teleconnections resulting in many ecological impacts worldwide (Trenberth, 2013). Haddad *et al.*

(2013), and Muis *et al.* (2018) noticed the correlation between El Niño induced SST anomalies, Global Mean Sea Level variations, and associated changes in the marine ecosystem.

Phytoplankton: phytoplankton is microscopic unicellular algae, the base of the oceanic food chain that living in the upper layer of the ocean, corresponding to oceanic uptake of ~25% of the carbon dioxide from the atmosphere (Le Quéré *et al.,* 2015). Ocean-color sensors on satellites can provide appraise of chlorophyll concentration at high spatial and temporal resolutions and on a global scale. Brainard *et al.* (2018) analyzed the changes in phytoplankton concentration in the Central equatorial Pacific associated with 1982/83, 1997/98, and 2015/16 El Niño events, and summarize that primary productivity decreased during strong El Niño events and vigorous phytoplankton blooms were observed during strong La Niña events. During 2010–2011 El Niño to La Niña transition period, across the entire Australian region, reported a 3% rise in chlorophyll a with the average fall in temperature (0.2%) from 2010 to 2011 (Peter *et al.,* 2015). The study by Roxy *et al.* (2016) illustrates a decreasing trend in chlorophyll through 1998-2013, but the earlier studies (Goes *et al.,* 2005) on the coastal region of the western Arabian Sea (47°-55°E, 5°-10°N) indicate an increasing trend in chlorophyll concentrations during 1998-2005. It can be elucidated by the strong El Niño event in the year 1998 and promptly followed La Nina conditions in the year 1999. The rise in chlorophyll anomalies during this period perfectly match with the fall in SST from 1998-1999 (Murtugudde *et al.,* 1999). Gierach *et al.* (2012) compared the biological production over the equatorial Pacific Ocean during CP El Niño (2009-10) and EP El Niño (1997-98). CP El Niño was associated with reduced chlorophyll concentration in central equatorial Pacific (CEP) and the reduction was confined to CEP. The massive drop in biological production in eastern equatorial Pacific was observed during EP El Niño, the declining trend was extended to CEP due to the strengthened and extended westerly wind anomalies. EP and CP El Niño events have the greatest impact on primary productivity of tropics and subtropics (67%). During EP El Niño, western Indian Ocean shows a declining trend whereas the eastern Indian Ocean has an increase in primary productivity (Racault *et al.,* 2017).

Zooplankton: Zooplankton plays a vital role as an intermediary link between primary producers and higher trophic levels to energy transfer (Heidelberg *et al.,* 2010). Both strong and weak El Niño events inducing eccentric warm water in Northern California Current demolish phytoplankton along with lipid-rich copepod species and confirm positive biomass anomalies of southern lipid poor copepod species. While analyzing the response of the copepod community in two different El Niño, they show immediate feedback in the EP events and there is a time lag of 2-8 months in case of CP events (Fisher *et al.,* 2015). During the 2015-2016 El Niño warning phase, a negative relation of the zooplankton

community with temperature was observed in Lakshadweep Sea around coral atolls, and also noted a higher profusion and heterogeneity in distribution during the peak period of El Niño compared to its warning phase (Vineetha *et al.,* 2018).

Benthos: Arntz (1986) has observed that invertebrate mortality in the intertidal and shallow subtidal off Peru was very high during El Niño 1982–1983, removing almost the whole cluster of macrobenthic grazers and many suspension feeders and predators. The research by Arntz *et al*. (1991) across Peruvian and Chilean Pacific Coast manifests that the species number increases strongly at the onset of El Niño, these new species from tropical areas continue to join the benthic community after the event. El Niño induced warming may exceed the temperature tolerance limits of *A. purpuratus* over Sechura Bay in northern Peru, where this scallop has become valued (Arntz *et al.,* 2006). Mussels, clams, snails, crabs, and echinoderms like cold-adapted benthic upwelling species off Peru suffered mass mortalities. Another way around, a few warm tolerant species like scallop (*Argopecten purpuratus)*, the purple snail (*Thais chocolata),* and the octopus (*Octopus mimus)* took advantage of the changing environment (Arntz *et al.,* 2006; Riascos *et.al.* 2017). Francisco and Netto (2019) reported that the benthic macrofauna community across the estuaries of southern Brazil fall after flooding in El Niño Modoki El Niño canonical events. They also observed that the diversity of macrofauna in the bay of southern Brazil was twice lower during El Niño canonical than El Niño Modoki, La Nina Modoki, and La Nina canonical.

Crustaceans: The clam *Mesodesma donacium* which inhabited the subtidal to intertidal zone on sandy beaches from Sechura Bay in northern Peru to Chiloe Islands shows a shift in their northern boundary of distribution area to southward because of consecutive El Niño events (Carre *et.al.* 2005). The increase in temperature (affects the physiology of bivalves) and food collapse due to algal disappearance results in the mass disappearance of filter feeders like bivalves (Arntz *et al.,* 2006). Impact of El Niño is more detrimental in bays, the semi-enclosed systems than other parts of Ocean (Rossi *et al.,* 2017).

Turtles: Reina *et al*. (2002) noticed the fact that the large scale multivariate ENSO (MEI) is independent of high variability observed in long-lived leatherback turtles (*Dermochelys coriacea*) at Playa Grande even though ENSO is the important climate driver in the eastern tropical Pacific. But Saba *et al.* (2007) observed the reproduction intervals of leatherback turtles at the eastern Pacific and found that it is highly variable and driven by ENSO events. The El Niño induced dip in primary productivity caused a collapse in foraging conditions (Saba *et al.,* 2007; Reina *et al.,* 2009) and El Niño

influencing local climatic conditions like low precipitation levels and higher temperature affects the nesting environment, thereby hatching success of leatherback turtles (Santidrian Tomillo *et al.,* 2012). During La Nina events, leatherback turtles reproduce sooner by shortening their remigration intervals due to the upwelling phenomenon (foraging areas become more productive). Conversely, during El Niño events they skip reproduction to overcome adverse climatic conditions (Saba *et al.,* 2007; Santidrian Tomillo *et al.,* 2017). Hatching success of most of the sea turtle species affected by higher temperatures (Howard et al. 2014; Montero *et al.* 2019). Northwest Costa Rica was hottest and driest than ever recorded in the years 2015-16, and the hatching success of leatherback turtles, olive ridley turtles were found to be largely affected (olive ridley turtles are less vulnerable than leatherback), but the Green turtles were largely unaffected by the El Niño and with minimal nesting abundance (Santidrián Tomillo *et al.*2020).

Seabirds: Changes in the sea surface temperature and sea level pressure preceding an ENSO event impact the foraging conditions and reproduction success of Sooty Shearwaters. So the massive reproduction failure of Sooty shearwater in 2013 was likely anticipated in the 2015/2016 El Niño event (Humphries *et al.,* 2015). Oceanographic conditions related to La Nina events bring foraging habitat of Laysan and black-footed albatrosses to the north (Thorne *et al.,* 2015), so the resulting higher energy requirements for longer foraging trips caused an increase in reproductive failure in both species (Thorne *et al.,* 2016). During the extreme El Niño event in the year 1998, the Cassin's Auklet (*Ptychoramphus aleuticus*) population on Triangle Island evince a marked breeding failure (Bertram *et al.,* 2017). The reproductive attempt was zero during 1998 ENSO for the sea bird species of the Galapagos Island except for Great Frigate birds and the sex ratio of the hatchlings affected even in a weak ENSO in 2003 (Wingfield, *et al.,* 2017). Thomson *et al.* (2018) explained the effects of an ENSO associated rainfall anomalies on marine and terrestrial food webs. The increased rainfall in the 2009–2010 ENSO events caused a hike in numbers of predators and leading to enhanced predation of a vulnerable nocturnal seabird on its terrestrial breeding grounds in 2011 and 2012 (Thomson *et al.,* 2018).

Sea snakes: Sea snakes are the largest group of marine reptiles that inhabited tropical and subtropical waters of Indian and Pacific oceans, they are decreasing in number (Rasmussen *et al.,* 2011) and there are changes in their typical distribution area (Park *et al.,* 2017). Gordon L. blame El Niño for the venomous sea snake, *Hydrophis platurus* captured from southern California beach that moved far north of its usual range (2015 Oct 16).

Seagrass and mangroves: One of the natural factors that impart to mangrove ecosystem wane in the Western Indian Ocean is ENSO. The El Niño event in the year 1997/98 grounded for the disappearance of 500 ha of mangroves in Kenya (FAO, 2007). Studies conducted by Lovelock *et al.* (2007) in New Zealand noticed that the mangroves are shifting landward and the movement was conspicuous during El Niño events. López-Medellín, *et al.,* (2011) also, confirm this result. He disclosed a 20% landward expansion of mangroves in Baja California (Mexico Pacific coast). The extreme events like Floods and droughts induced by ENSO events can severely affect the mangrove ecosystem by altering salinity, nutrients, and organic matters (Pereira *et al*. 2013; Costa *et al*. 2016). Droughts caused by El Niño had a drastic impact on the ecology of mangrove forest estuaries on the Amazon coast (Costa *et al*. 2016). The dieback of mangroves in the Gulf of Carpentaria shorelines in 2016 was coincident with the 2015/16 El Niño event (Duke and Larkum, 2019).

Corals: The cases of coral bleaching and mortality were recorded in many of the regions across the globe due to the extended thermal stress endured by the coral reef communities during El Niño events: Thousand Islands, Indonesia in 1982/83 (Brown and Suharsono, 1990), corals in eastern equatorial Pacific during 1997/98 (Glynn *et al*. 2001), the Phoenix Islands during 2002/03 (Obura and Mangubhai, 2011), Howland and Baker Island in 2009/10 (Vargas-Ángel *et al.* 2011), corals of Jarvis, Howland, Baker, and Kanton Islands in 2015/16 (NOAA, 2017). There is a decline in total reef fish biomass in 2016 compared to other years (Brainard *et.al*. 2018). Equatorial reefs undergo more crucial ENSO associated deterioration compared to higher latitude reefs (Claar *et al*. 2018). 1997/98 major El Niño event caused 90% coral mortality on shallow Indian reefs (Wilkinson *et al*. 1999). Bleaching related mortality was higher in lagoon reefs of Lakshadweep related to the other reef regions of India, Gulf of Kutch, and Gulf of Mannar (Arthur, 2000).

Fishes: ENSO induced variability in Ocean, atmosphere parameters alter the abundance and distribution of fish species (Arntz, 1984; Lehodey *et al.,* 1997; Davis, 2000; Brander 2007), affect various commercially important fish stocks of Indian and Pacific Ocean (Miller, 2007). The strong El Niño events caused a drastic reduction in the biomass of Anchovy, the largest fishery on Earth (Csirke *et al.,* 1994; Perea *et al.,* 1998; Niquen and Bouchen, 2004) and jack mackerel (Arcos *et al.,* 2001) on the Peruvian coast. There is a dip in species richness during the El Niño period than normal years on the coast of Central Mexican Pacific and the top listed species in terms of catch *Lutjanus guttatus* shifted to tenth place in 1998. The species such as *Elops affinis, Caranx caballus, Caranx vinctus, Trachinotus rodophus,* and *Nematistius pectoralis* occur in a deviant season in inshore waters and *Katsuwonus pelamis and Opisthonema libertate* show atypically towering their number during El Niño

(Domı´nguez *et al.,* 2000). Recent studies documented that Tuna population dynamics are affected by ENSO (Lehodoy *et al.,* 2008; Kumar *et al.,* 2014). Niquen and Bouchen (2004) found that the major pelagic resources of Peru, such as Anchovy and Sardine shoals travel towards the coast, shifted to the south, and in central-northern parts they are getting deeper. Apart from these changes in species distribution, there is a surprising result in the size structure of species, a large number of juveniles were observed among sardine, longnose anchovy, and pacific mackerel. Contradictory to impacts on Anchovy, El Niño conditions favored the reproduction of Pacific mackerel and Sardine. When comparing the abundance of Little Tuna (*Euthynus affinis*) and Spanish mackerel (*Scomberomorus commerson)*, the two dominant pelagic fishes of Jawa Sea during 2014 El Niño and 2010 La Nina year, both the species showed a higher catch rate in El Niño than La Nina (Syamsuddin *et al.,* 2018). Fish landing data from Ecuadorian fleets during 1981-2012 manifests *Cetengraulis mysticetus*, the local species of El Niño 1-2 region which have high landings during El Niño years and low landings during La Nina years (Ormaza-González *et al.,* 2016). Kumar *et al*. (2014) summarized in his study conducted in the Indian Ocean that the highest tuna landings reported in 2004, and 2006 that were weak El Niño years, landings were optimum at SST 25°-26°C in ENSO phenomenon. In 2015 the poor maturation and recruitment of Indian Oil sardine were partially influenced by El Niño (Kripa, 2018).

Fisheries: As FAO's (2020) figures World Marine landings were roughly 0.7 million tonnes lower during El Niño and were 1.3 million tonnes higher during La Niña years when match with the mean landings of the normal years. It also reveals that marine landings of the Western Indian Ocean shows a decrease in extreme CP El Nino (-21,000 tonnes) and landing increase during EP El Nino (+25,000 tonnes). ENSO induced variations in ocean biology change the stock size of the species leading to a time lag in fisheries (Chavez *et al.,* 2002). The catch composition of the artisanal coastal fin-fish fishery of Galapagos Island changed because of the dominance of predatory fishes like groupers during the 2016 El Niño year (Marin Jarrin and Salinas-de-Leon, 2018). Due to the severe impact on reproduction and biomass of anchovy, the world's largest single-species fishery the Peruvian fisheries shifted from single species-specific to multispecific fisheries (Niquen and Bouchen, 2004).

2.2 Impacts of El Niño and La Nina on environmental parameters

Temperature: General circulation model study by Annamalai (2004) using SST anomalies over Nino 3.4 region in the period of 1976/77 indicated that after 1976 there were would be reasonable SST anomalies in the eastern equatorial Indian Ocean and Western Pacific that stands above the normal and before 1976 there was basin-wide warming in the Indian Ocean. The basin-wide warming generally

happened after the mature phase (winter and spring) of El Niño. And the SST cooling in the post-1976 period was due to the influence of IOD. This basin-wide warming of the Indian Ocean due to surface heat flux anomalies associated with El Niño is a typical characteristic of El Niño (Klein *et al.,* 1999). Through the El Niño years, an area extending from the Philippines to Western Australia covering Maritime Countries experiences deficit rainfall, the region from central to eastern equatorial Pacific experiences surplus rainfall anomalies. Impacts of El Niño Modoki is different from this response, the equatorial eastern Pacific experiences less than normal rainfall, Philippines, Sri Lanka, East Africa, southern Thailand, southern India experiences severe dry conditions, and northeast Africa to central India and southern China have notable wet conditions during El Niño Modoki (Ashok *et al.,* 2007). While relating ENSO warm events to drought and flood conditions across the globe, drought disasters of India show a significant relationship with ENSO (Dilley and Heyman, 1995). El Niño the warm phase causes the warming of coastal waters of Peru and extreme rainfall occurs along with the normally arid coastal patches .1997/98 and 2015/16 El Niño (EP El Niño and mixed EP and CP El Niño) events are the two strongest recorded ever, both caused SST to rise 3.5°C from normal (Peak *et al.,* 2017). 1997/98 El Niño resulted in positive SST anomalies nearly 2°C and the 1982/83, 1987, 1992 events also resulted in temperature anomalies reaching more than 1°C (Arcos, *et al.,* 2001). Investigation on teleconnections between the Indian Ocean and the Pacific Ocean indicate that SST anomalies of Indian Ocean can influence SST variations in equatorial Pacific (Annamalai, 2004). El Niño years induce more hydro-climatological changes than La Nina or normal years.

Nutrients: Eastern boundary regions of the Pacific has higher primary productivity than Western boundaries (Barber and Kogelschatz, 1989). Barber and Kogelschatz (1989) observed that the 1982/83 El Niño event resulted in a dramatic reduction in nutrients in the offshore and middle portions of eastern equatorial Pacific. He also noticed that from December 1982 to June 1983, the surface layer concentration of nitrate was below the detection limit (0.2 µM). Along with nitrate, the supply of other nutrients to the euphotic zone also significantly reduced. Even though the 40 km inshore band remained relatively productive in the coastal region, the size of the upwelling environment was reduced to 10% of normal, reduced the quantity of nutrients upwelled. The study on Vancouver Island during the 1997/98 El Niño event was also evident to variations in nutrient concentration. Dissolved nitrate and silica concentrations showed a declining trend throughout the year 1997 (Harris *et al.,* 2009). Sub-Antarctic waters are the primary source of nutrients to the global thermocline and the Australian part of Sub Antarctic mode water nutrients had a greater correlation with ENSO. El Niño events were associated with a decrease in nutrients and an increase in temperature of Sub Antarctic Mode Waters.

Wind Stress Curl anomalies linked with El Niño strengthen the South Pacific Subtropical gyre there by affecting the East Australian Current (western boundary current). EAC brings more nutrient-poor water and led to a decline in nutrient availability of sub-Antarctic waters (Ayers and Strutton, 2013).

Salinity: Sea surface Salinity (SSS) indices are used to characterize ENSO (Delcroix *et al.,* 1998), SSS anomalies are significantly negative in western equatorial Pacific near the dateline and there is an eastward movement of SSS front (34.8 psu isohaline) with the eastern edge (longitudinal location of the 29°C isotherm) during El Niño development phase (Chi *et al.,* 2015), retreats westward during La Nina. SSS front separates the fresh western Pacific water from central Pacific saline water (Tang and Yueh, 2017). The barrier layer formed due to salinity stratification of the Pacific warm pool mixed layer blocks the subsurface cooling into the mixed layer (Maes *et al.,* 2005). In 2014/15, the strong subsurface processes during summer led to the formation of positive SSS anomalies in central equatorial Pacific and caused westward movement of salinity front. It indicates that variations in sea surface salinity over equatorial Pacific largely depends on changes in subtropical circulation and had fewer impacts on SST during 2014/15 (Chi *et al.,* 2015). Tang and Yueh (2017) investigated the role of SSS in water cycle anomaly connected with ENSO using the SSS datasets from SMAP, Aquarius (NASA) and ESA's SMOS. The study concluded that salinity plays an active role in the onset and evolvement of an ENSO event. Zhu *et al.* (2014) also provided evidence for the role of salinity on ENSO evolution, he demonstrated that the data on salinity variations were essential to correctly forecast the 2007/08 La Nina starting from April 2007. SSS variability in the southeastern Pacific is the deciding factor to identify El Niño type. The South Eastern Pacific SSS Index (SEPSI), defined based on the SSS variations over the region extended from 0°-10°S to 150°-90°W is significantly correlated with the El Niño Modoki Index (Qu and Yu, 2014). Based on 33 years (1980-2012) of PEODAS reanalysis it is evident that temperature variations are highest in the eastern Pacific thermocline, the salinity variations are strongest in the western Pacific mixed layer and strongly associated with the accompanying east-west shift of western Pacific fresh pool during El Niño and La Nina (Zhao *et al.,* 2016). In normal years salinity over Pacific Ocean freshwater lens is determined by seasonal rainfall events. After 1983, 1987 El Niño events salinity remained above normal until the 1989 La Nina that recharged the freshwater lens (Van der Velde *et al.,* 2006).

Turbidity: Spatio-temporal variability of turbidity in Rio de le Plata estuary in Argentina analyzed and explained in terms of ENSO using MODIS data from 2000-2014. The El Niño events associated with low turbidity amplitudes in the upper and middle estuary, opposite occurs in La Nina. During 2003, 2007, and 2010, the moderate and weak El Niño years, low turbidity was observed with increased

outflow. In La Nina years (2000, 2008, 2009, and 2012) the outflow mean value was lower than the normal, led to higher turbidity. The high turbidity observed in 2004 due to low outflow was not related to a La Nina event (Dogliotti, 2016).

2.3 Ocean atmospheric variations: Indian Scenario

The Pacific Ocean and the Indian Ocean is connected through walker circulation and the passage of Indonesian Archipelago. Our country gets more than 75% of annual rainfall during the four months (June-September) of Indian Summer Monsoon Rainfall (ISMR). So ISMR plays a crucial role in the Nation's economy. It is evident that ENSO influences the Indian summer monsoon rainfall through atmospheric teleconnections (Ashok *et al.* 2001). Rasmusson and Carpenter (1983) observed an El Niño phenomenon connected to positive pressure anomalies over the Indian Ocean, get below normal rainfall over India during ISMR and the opposite happens during La Nina. Contrary to this general impact, India received positive rainfall anomalies in the El Niño year 1997 (Li *et al.,* 2001). Later this paradoxical observation was explained by Maity and Nagesh Kumar (2006). He concluded that both ENSO and Equatorial Indian Ocean Oscillation (EQUINO), the atmospheric part of Indian Ocean Dipole (IOD) have a significant effect on monthly ISMR and gave weightage as 0.61 and 0.39 respectively. While El Niño weakens Indian Summer Monsoon, co-occurring IOD events dampen this impact (Ashok *et al.,* 2004). This influence of IOD explains why all the years associated with El Niño didn't cause a drought in India. SST anomalies in the central equatorial Pacific enhance the likelihood of droughts during monsoon and SST anomalies in eastern equatorial Pacific reduces the chances of drought during monsoon (Kumar *et al.,* 2006). Izumo *et al*. (2010) on his model analysis suggest that IOD and the interannual climate fluctuations in the Indian Ocean can predict ENSO. Negative IOD precedes the El Niño (14 months before its peak) and positive phase of IOD come before La Nina. The century wide analysis (1901-2002) by Tamaddun *et al*. (2019) reveals that most of the north Indian districts experienced significant decreasing trends in the temperature in all ENSO phases. The western parts of North India experienced enhanced rainfall events and eastern parts have decreasing trends in precipitation in various ENSO phases. During El Niño years, the maximum number of north Indian districts showed an increasing trend in rainfall events. Moreover, during El Nino years, tropical cyclone activities increased in the southwestern Indian Ocean and the opposite happened during La Nina (Lin *et al.,* 2020). There was a considerable warming in the tropical Indian Ocean, somewhat because of impacts of the 2015 El Niño. The mean SST in the tropical Indian Ocean exceeded by 0.13–0.2°C in 2015 (Xue *et al.,* 2016).Extreme El Nino events stimulate the occurrence of marine heat waves in the Indian Ocean (Zhang *et al.,* 2017). During 2015/16 El Nino rainfall received over Indian subcontinent

was lower than the normal rainfall, ten states experienced drought, affecting 330 million people during the period. Due to the IOD response to El Nino, the south east of Indian peninsula experienced torrential rainfall and flooding, Northern part of India experienced drought (Grove and Adamson, 2018).

2.4 Impacts of El Niño and La Nina on socioeconomics

The occurrence and the intensity of ENSO has a crucial impact on the economy of a country, notably in countries in the tropical region (Suarez *et al*. 2004). Globally about 200 million people are directly and indirectly employed in different activities related to fisheries right from harvesting from natural areas to distribution, most of this population lives close to the sea (FAO, 2018). Localized coastal El Niño on February and March 2017 on Peru resulted in heavy rainfall and flooding in Sechura. Most of the villagers lost the fishing days due to this El Niño shocks, their income reduced because fisheries products could not reach national markets out of Sechura (Kluger *et al.,* 2018). In California, the most damaging El Niño events were in the years 1982/83 and 1997/98 and resulted in the loss of $2 billion and $1.1 billion (1998 dollars) respectively. When summarizing national impacts, the benefits from positive outcomes supersede the losses. Approximately there is a difference of $15.4 between economic gain and loss (Changnon, 1999). The developed nations like Europe and the USA betrayed an escalating response on the nation's economy, However India, Japan, Indonesia, Australia, Chile, South Africa, and New Zealand faced a period of economic stagnation during El Niño shocks (Cashin *et al.,* 2017). For example, the study (Gutierrez, 2017) investigating impacts of El Niño on the global wheat market summarized that Argentina show an increase in wheat production and Argentina experienced rise in export. The US had higher export in La Nina. Coinciding El Niño conditions with summer monsoon rainfall of India affect the agriculture production of the nation and India's GDP growth falls by 0.15% (Cashin *et al.,* 2017). The growth-limiting impacts of back to back El Niño events in Africa can be reduced by La Nina after an El Niño. The similar response were also found in Asia-Pacific region. The adverse effect of back to back La Nina on the nation's economy can be mitigated by El Niño after a La Nina (Hsiang and Meng, 2015). During the 1997–98 *El Niño* event, Tumbes, Peru received 16 times the normal rainfall of the year. The negative effects that enhanced swiftly were hindered access to transport, health care and ameliorated infectious diseases. Tumbes residents who encountered the El Niño impact needed more time to restore their houses, agriculture, livestock, and revive their income stability (Bayer *et al.,* 2014). El Niño events caused droughts in South Africa including the country's summer rainfall region (Richard *et al.,* 2000) El Niño induced droughts in South Africa created increased unemployment, less purchase power, and rise in debit

service coast for farm implements, led to increased mounting pressure on the country's agro-economic system (Agri SA, 2016). The agricultural productivity of local subtropical regions were affected with 1997/98 El Niño, the sharp reduction in production cause disruption of rural income and employment. Specifically, due to the shortfall in rice production during this El Niño period, Malaysia required to import over a million tons of rice to satisfy their food requirement. Based on the study results the estimated direct economic loss was RM87 million. Rice, oil palm, and horticulture sector and more than 17,000 people including farmers were also directly affected (Quasem, 2016). Not only the agriculture production, the children were exposed to El Niño floods of 1997/98 in Equador, specifically third trimester in utero were born with low birth weight (Rueda, 2018). Smith and Ubilava (2017) confirms that El Niño can negatively affect the nation's economy as a whole. The heavy flooding during the 2015/16 El Niño period severely affected the southern and central parts of Kenya. The landslides associated with heavy precipitation caused the collapse of buildings, infrastructure, failure of crop and livestock production, business, and schools were forced to close (Siderius, *et al.,* 2018). From the records of India's associated Chambers Of Commerce, Grove and Adamson (2018) stated that India had drought damages estimated to be $100 billion US during 2015/16 El Nino.

CHAPTER 3

MATERIALS AND METHODS

ENSO events identified since 2007 using various ENSO Indices such as Oceanic Nino Index (ONI), Multivariate ENSO Index (MEI), Southern Oscillation Index (SOI), El Nino Modoki Index (EMI), Dipole Mode Index (DMI), Trans Nino Index (TNI), Nino 1+2 Index, Nino 3.4 Index, Nino 4 Index and their types from literature. The different methods followed to meet the objectives of research are described below. The Whole work divided into following sections- 1) variations on ocean-atmosphere parameters and 2) impacts on fishery in Kerala coast. In this chapter details of data collected and analyzed and the statistical packages used for different sections are presented.

3.1 Data used for assessing the impact of Ocean-atmospheric parameters

3.1.1 ENSO indices

ONI (Oceanic Nino Index)

The Oceanic Niño Index (ONI), which is based on sea surface temperature (SST) in the east-central Tropical Pacific Ocean, which is 3 month running mean of ERSST.v5 SST anomalies in the Niño 3.4 region (5°N-5°S, 120°-170°W), based on 30-year base periods. El Niño conditions to be present when the Oceanic Niño Index is +0.5 or higher, La Niña conditions exist when the Oceanic Niño Index is -0.5 or lower. 2007 to 2018 ONI Index values downloaded from NOAA (National Oceanic and Atmospheric Administration), Climate Prediction Center (https://origin.cpc.ncep.noaa.gov/products/analysis_monitoring/ensostuff/ONI_v5.php).

MEI (Multivariate ENSO Index)

The bi-monthly Multivariate El Niño/Southern Oscillation (ENSO) index (MEI.v2) is the time series of the leading combined Empirical Orthogonal Function (EOF) of five different variables [sea level pressure (SLP), sea surface temperature (SST), zonal and meridional components of the surface wind, and outgoing long wave radiation (OLR)] over the tropical Pacific basin (30°S-30°N and 100°E-70°W). MEI is a method used to characterize the intensity of an ENSO event. 2007-2018 MEI values downloaded from the Physical Science Laboratory of NOAA (National Oceanic and Atmospheric Administration) (https://psl.noaa.gov/enso/mei/).

TNI (Trans –Nino Index)

The timeseries is calculated from the HadISST Dataset. It is the standardized Nino 1+2 minus the Nino 4 with a 5 month running mean applied which is then standardized using the 1950-1979 period. 2007-2018 TNI index values downloaded from the ESRL (Earth System Research Laboratory), Physical Science Division of NOAA (National Oceanic and Atmospheric Administration), (https://psl.noaa.gov/gcos_wgsp/Timeseries/Data/tni.long.data) (Trenberth and Stepaniak, 2001).

EMI (El Nino Modoki Index)

The El Nino Modoki Index is defined as,

$$EMI = [SSTA]_A - 0.5 * [SSTA]_B - 0.5 * [SSTA]_C$$

The brackets in equation represent the area-averaged SSTA over each of the region A (165˚E–140˚W, 10˚S– 10˚N), B (110˚W–70˚W, 15˚S–5˚N), and C (125˚E– 145˚E, 10˚S–20˚N), respectively (Ashok *et.al*, 2007).1870-2019 EMI index values downloaded from JAMSTEC (Japan Agency for Marine-Earth Science and Technology) (http://www.jamstec.go.jp/frsgc/research/d1/iod/DATA/emi.monthly.txt).

DMI (Dipole mode Index)

The Dipole Mode Index (DMI) is a measure of the anomalous zonal SST gradient across the equatorial Indian Ocean. It is defined as the difference between SST anomaly in a western (60˚E-80˚E, 10˚S-10˚N) and an eastern (90˚E-110˚E, 10˚S-0˚S) box (Figure 3.1). When the DMI is positive then, the phenomenon is referred as the positive IOD (Indian Ocean Dipole) and when it is negative, it is refereed as negative IOD. Data from 2007-2018 collected from Global Climate Observing System (GCOS) Working Group on Surface Pressure (WG-SP) hosted by NOAA ESRL Physical Sciences Laboratory (https://psl.noaa.gov/gcos_wgsp/Timeseries/DMI/).

SOI (Southern Oscillation Index)

The oldest indicator of the ENSO state the Southern Oscillation Index (SOI) is defined as the normalized pressure difference between Tahiti and Darwin (Figure 3.1). 2007-2018 SOI index values downloaded from the Global Climate Observing System (GCOS) Working Group on Surface Pressure (WG-SP) hosted by NOAA ESRL Physical Sciences Laboratory (https://psl.noaa.gov/gcos_wgsp/Timeseries/SOI/). Here the SOI calculated based on the method given by Ropelewski and Jones (1987). During El Niño, the pressure becomes below average in Tahiti and

above average in Darwin, and the Southern Oscillation Index is negative. During La Niña, the pressure behaves oppositely, and the index becomes positive.

Nino 1+2 Index

Nino 1+2 index is based on SST anomalies averaged over the Nino1+2 region (0°-10°S, 90°W-80°W), which is the smallest and eastern most of the Nino SST regions (Figure 3.1). 2007-2018 Nino 1+2 values downloaded from the Global Climate Observing System (GCOS) Working Group on Surface Pressure (WG-SP) hosted by NOAA ESRL Physical Sciences Laboratory (https://psl.noaa.gov/gcos_wgsp/Timeseries/Nino12/).

Nino 3.4 Index

Nino 3.4 index is based on SST anomalies averaged over the Nino 3.4 region (5°N-5°S, 170°W-120°W), representing the average equatorial SSTs across the Pacific from about the dateline to the South American coast (Figure 3.1). The Niño 3.4 index typically uses a 5-month running mean, and El Niño or La Niña events are defined when the Niño 3.4 SSTs exceed +/- 0.4C for a period of six months or more. 2007-2018 Nino 3 values downloaded from the Global Climate Observing System (GCOS) Working Group on Surface Pressure (WG-SP) hosted by NOAA ESRL Physical Sciences Laboratory (https://psl.noaa.gov/gcos_wgsp/Timeseries/Nino34/). (Trenberth and Stepaniak, 2001)

Nino 4 Index

Nino 4 index is based on SST anomalies averaged over the Nino 4 region (5°N-5°S, 160°E-150°W) (Figure 3.1). It captures SST anomalies in the central equatorial Pacific. This region tends to have less variance than the other Niño regions. 2007-2018 Nino 4 index values downloaded from the Global Climate Observing System (GCOS) Working Group on Surface Pressure (WG-SP) hosted by NOAA ESRL Physical Sciences Laboratory (https://psl.noaa.gov/gcos_wgsp/Timeseries/Nino4/).

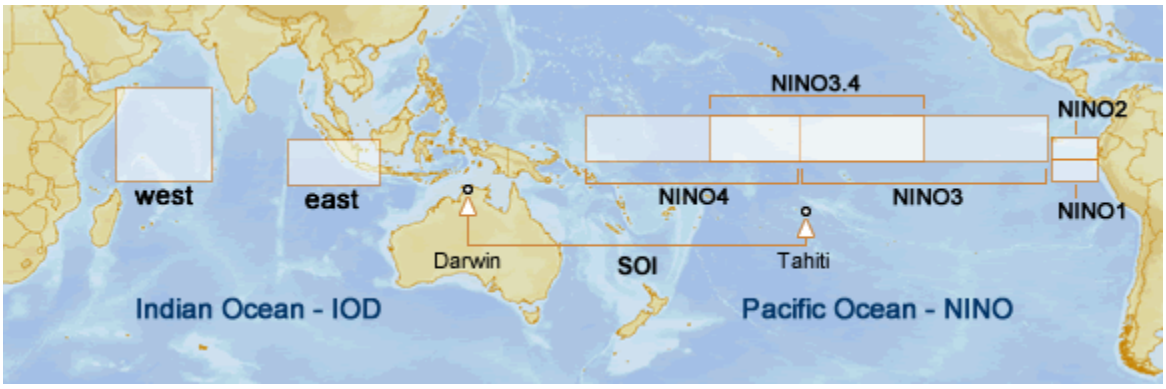

Figure 3.1: Regions used to monitor ENSO and IOD (Source: Australian bureau of meteorology)

3.1.2 Ocean-atmospheric Parameters

Sea Surface Temperature (SST)

Global ocean Sea Surface Temperature data was downloaded from the Asia-Pacific Data Research Center (APDRC) which is a part of the international Pacific Research Center at the University of Hawai'i at Maona, funded in part by the National Oceanic and Atmospheric Administration (NOAA). Monthly mean SST data with 4km resolution derived from MODIS Aqua (MODerate Resolution Imaging Spectro-radiometer) sensor was downloaded for the year 2007 to 2018.

Chlorophyll-a concentration (CHL_A)

The monthly climatological chlorophyll data with a spatial resolution of 4x4km from 2007 to 2018 were downloaded from the website Ocean Colour Climate Change Initiative (OC-CCI) (https://www.oceancolour.org/), used latest version of the dataset, version 4.0 comprising globally merged MERIS, Aqua-MODIS, SeaWiFS and VIIRS data.

Sea Surface Height Anomaly (SSHA)

The monthly sea surface height anomaly having a spatial resolution of 0.25°lat X 0.25°lon was derived from Level 4 Global Ocean Gridded Maps REP (Reprocessed) SLA (Sea-level anomaly) from 2007 to 2018 was downloaded from Copernicus Marine Environment Monitoring Service (https://resources.marine.copernicus.eu/?option=com_csw&view=details&product_id=SEALEVEL_GLO_PHY_L4_REP_OBSERVATIONS_008_047).

Sea Surface Salinity (SALT)

Global Sea surface salinity data with spatial resolution of 0.33°lat x 1.0°lon from GODAS (Global Ocean Data Assimilation System) was also extracted from the NOAA ESRL Physical Science Division (PSD) website (https://psl.noaa.gov/data/gridded/data.godas.html) for the period 2007 to 2018.

Ocean Current

Ocean current information from SODA3.4.2 was extracted from the SODA3 website (http://www.atmos.umd.edu/~ocean/index.html). The monthly climatological data of 0.5˚spatial resolution from 2007-2016 was downloaded as NetCDFv4 files. Ocean surface current data was also downloaded from the OSCAR (Ocean Surface Current Analysis Real-time) satellite sensor of 0.33˚

spatial resolution and 5 day temporal resolution from the website of PO.DAAC (Physical Oceanography Distributed Active Archive Centre) (https://podaac.jpl.nasa.gov/) for 2017 to 2018. Using R software, these 5day files were compile in to monthly data. The current data are represented as zonal (u) and meridional (v) components. Current speed and direction were derived from u and v components using the formula:

$$\text{Current velocity} = \sqrt{(u^2+v^2)}$$

$$\text{Current direction} = 180+ [180*\arctan^2 (u,v)]/\pi$$

Current velocity and direction were calculated using R programming and Python.

Local Temperature Anomaly (LTA)

Local Temperature Anomalies (LTAs) are intended as the coastal upwelling indices by comparing coastal and offshore temperature. The positive LTA values suggest coastal upwelling processes (Shah *et al.,* 2015; Smitha *et al.,* 2008; Naidu *et al.,* 1999). And the equation is:

$$LTA = SST_{off} - SST_{coast}$$

Where, SSToff represents sea surface temperature associated with an off-shore station at a distance of 3˚ with respect to that recorded at a coastal station (denoted using SSTcoast) within the same latitudinal belt. LTA serves as a proxy to represent oceanographic forcing. LTA values greater than 1˚C indicate a strong upwelling in the coastal areas (Shah *et al.,* 2015).

Rainfall Data

Meteorological sub division wise monthly rainfall data was downloaded from Open Government Data (OGD) Platform-data.gov.in website (https://data.gov.in/). Also, rainfall data of India Meteorological Department (IMD) was collected from the IMD's Annual publication "The Rainfall statistics of India" (Kaur and Purohit, 2012, 2013, 2014, 2015, 2016, 2017). Monthly rainfall data of Kerala in 2018 was collected from Indiastat.com which is an authentic storehouse for socio-economic statistics about India (https://www.indiastat.com/meteorological-data/22/ rainfall /238/ stats.aspx).

3.2 Fisheries Data

The fisheries data encompassing the resource wise, gear wise, district wise catch, number of units operated (effort), and actual fishing hours collected from National Marine Fisheries Data Centre (NMFDC) of Central Marine Fisheries Research Institute (CMFRI), Kochi, India. The multistage stratified random sampling (stratification is done over time and space) developed by CMFRI is used to collect fisheries data (Srinath, *et al.,* 2005; Mini, 2014). Normally 16 to18 days in a month are selected at random for observation. The trained staffs collect resource wise landings, the number of fishing days and effort per month from the landing centers of entire Indian coast and this is raised to derive estimate for the month. Monthly data from 2007 to 2018 was extracted for Kerala state it was used for further analysis. Normally the catch is harvested by a variety of craft and gear combinations. Based on fishing crafts used there are three main fishing sectors termed as Mechanized, motorized and non-motorized sector. Different gears used from both mechanized and motorized crafts are given below.

Table 3.1 Types of gears operated in the mechanized and motorized fisheries sectors

Mechanized sector	Motorized sector
Multi day trawl net (MDTN)	Outboard bag net (OBBN)
Mechanized gillnet (MGN)	Outboard boat seine(OBBS)
Mechanized hook and lines (MHL)	Outboard gill net (OBGN)
Mechanized purse seine (MPS)	Outboard hook and lines(OBHL)
Mechanized ring seine (MRS)	Outboard purse seine (OBPS)
Mechanized trawl net (MTN)	Outboard ring seine(OBRS)
	Outboard shore seine (OBSS)

Apart from these, other gears are sometimes observed and these are mechanized other gears (MOTHS) and outboard other gears (OBOTHS).

The fish resources inhabited in the water column (in surface waters, not near the bottom or the shore) are termed as pelagic resources and adult fish having vertical habitats below 30 m of depth have been assigned under demersal category. Types of gears, area and depth of operation influence the catch variations. The NM and most outboard crafts and gears are operated in the near shore waters and resources influenced by coastal waters will be the major catch and the resources will vary in the mechanized crafts which fish in off shore waters. Within the pelagic and demersal resources based on the mesh size of the gear the catch may vary. The seines which are encircling gears, small pelagic fishes are caught while in hook and line large pelagic fishes like tunas and seer fishes are caught. Trawl net is the most effective gear to exploit demersal resources. Operate trawl net to exploit the marine crustaceans, cephalopods and demersal finfishes

Resource assemblage of a particular group of resources can be understood from the catch and from the catch per unit effort (CPUE) the abundance of the resource can be inferred. The major marine resources of interest considered for the present study include prawns, pelagic planktivores such as anchovies, mackerel, and sardines along with demersal resources such as Threadfin breams.

Catch per Unit Effort

Catch per Unit Effort (CPUE) is the ratio of total catch and effort (number of units operated), is an indirect measurement of fish abundance. CPUE is much more powerful tool than catch data alone. Deviations in CPUE over a time period is usually a good indication to changes in the fish stocks. The total catch is expressed as weight (in KG) and the effort portion refers to the time that the fishing craft deployed in the water.

CPUE = TOTAL CATCH ÷ EFFORT

Study Area

The study area comprises the coastal area of Kerala between 8° N and 12° N latitudes and 74° E and 77° E longitudes. The area within the 200 m depth contour provide the best feeding and spawning site for the fishes and hence considered as the most productive coastal region (George, *et al.,* 2019). The ocean-atmospheric parameters, fish catch and effort datasets are limited with in the area of shore line to 200 m isobath (Figure 3.2).

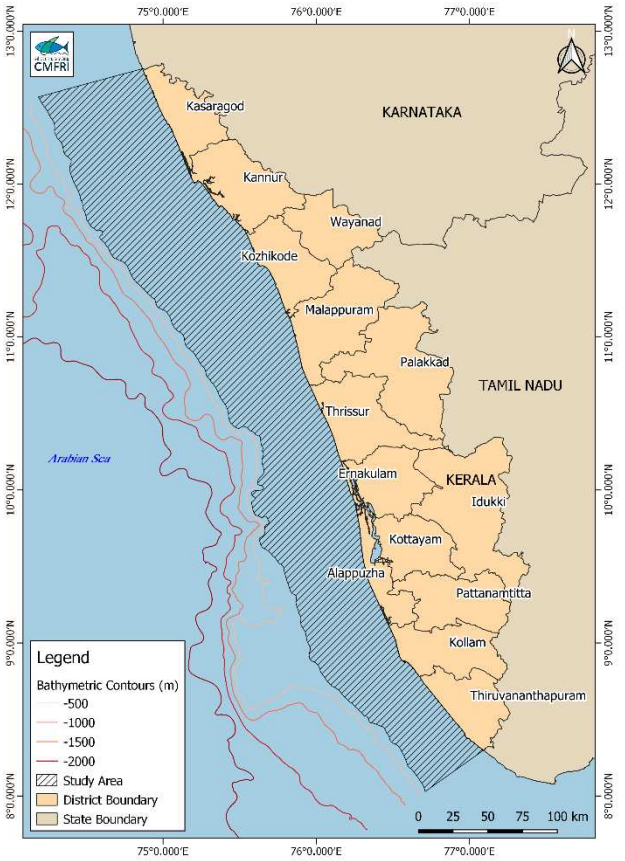

Figure 3.2: Location of the study area. The study region (stippled area) is enclosed by the coastline on the east and 200 m isobath on the west.

Software Used

The software *viz.* R 3.6.1, Python 3.7, QGIS 3.4.12 and MS-EXCEL were used for the data processing. Using R software, datasets falling within the area of shore line to 200 m depth contour were extracted.

Pearson's Correlation Test

Pearson's correlation test or parametric correlation test is a measure of the linear correlation between two variables. It was developed by Karl Pearson. Pearson's correlation coefficient is a statistical measure of the strength of a linear relationship between paired data. Correlation coefficient *r* ranges from +1 to -1. +1 indicates a positive correlation, -1 indicates a negative correlation and 0 shows no correlation. According to Evans (1996), the strength of the correlation could be categorized in to very weak/no correlation ($r \leq 0.19$), weak correlation ($r = 0.2$ to 0.39), moderate correlation ($r =$ 0.4 to 0.59), strong correlation ($r = 0.6$ to 0.79), very strong correlation ($r = 0.8$ to 1).

Each ENSO indices and ocean-atmosphere parameters considered in this study, evaluated the degree of collinearity between all ENSO predictors and between all ocean-atmosphere predictors. The preliminary analysis was necessary because the multicollinearity can cause problem when we fit the model. Then estimated the Pearson's correlation coefficients between all ENSO predictors and

between ocean-atmosphere predictors and discarded those predictors for which we found pairwise correlations exceeding 0.9 in absolute value.

General Additive Model (GAM)

Generalized Additive Models (GAM) encompass the series of non-parametric and semi-parametric regression techniques and describe many data in the environmental science which do not fit simple linear model. General Additive Model (GAM) is used to estimate ENSO effects on ocean atmosphere parameters and impacts on fishery resource abundance in Kerala coast with Gaussian error distributions. GAM was performed with mgcv (Wood and Augustin, 2002) package in R (3.6.1). The predicted variable is modeled by sum of smooth functions of covariates. A stepwise fitting procedure was used to remove insignificant variables. The model fits were analyzed using the Akaike Information Criteria (AIC), Adjusted R^2 and Deviance. The model with lowest AIC value was selected for the study purpose.

CHAPTER 4

RESULTS

4.1 Variations in Ocean-atmospheric parameters during El Nino and La Nina years

4.1.1 Variations in the different ENSO indices

ENSO events are identified based on different El Nino indices corresponding to the particular time period. Nino 1+2, Nino3, Nino 3.4, Nino 4, Oceanic Nino Index (ONI), Trans Nino Index (TNI), Multivariate ENSO Index (MEI), El Nino Modoki Index (EMI), Dipole Mode Index (DMI) and Southern Oscillation Index (SOI) are considered in this study. These indices describe quality and period of ENSO warm and cold phases on a monthly scale and depend on oceanic or atmospheric parameters estimated over different parts of the Pacific Ocean. Nino 1+2, Nino 3, Nino 3.4, Nino 4 and ONI indices are SST based indices and Nino3.4 and ONI are the most commonly used indices to define ENSO events. Other indices are used to characterize the unique nature of each event (Trenberth and Stepaniak, 2001).

The warm and cold events of El Nino Southern Oscillation inferred through the Oceanic Nino Index during the period 2007-2018 is illustrated in the fig. 4.1a. ENSO events are defined as five consecutive overlapping three month periods at or above the +0.5 anomaly for warm (El Nino) events and at or below the −0.5 anomaly for cold (La Nina) events. The threshold is further broken down into Weak (with a 0.5 to 0.9 SST anomaly), Moderate (1.0 to 1.4), Strong (1.5 to 1.9), and Very Strong (≥2.0) events. The positive values greater than +0.5 in the y-axis occurred during 2006-2007, 2009-2010, 2014-15, 2015-2016, and 2018 depict the warm phases (El Nino) of ENSO. Weak events were observed during the year 2007, 2015, and 2018 whereas a moderate event was observed during 2009-2010. A very strong warm event was experienced in 2015-2016. The negative values below −1.5 were observed in the years 2007-2008 and 2010-2011 indicating a strong cold event (La Nina) of ENSO. A moderate cold phase was experienced during 2011-2012 whereas weak La Nina years were observed in the years 2008-2009 and 2017-2018.

The El Nino and La Nina episodes of ENSO inferred the Nino3.4 index during 2007-2018 are described in the figure 4.1b. Events are defined as six consecutive overlapping five-month running mean of SST in Nino3.4 region at or above the +0.4 SST anomaly for warm events and at or below -0.4 SST anomaly for cold events. All the El Nino and La Nina events had a strong signature on the Nino 3.4 index. The positive values greater than 0.4 in the y-axis represents the El Nino phases. From

2007 to 2018 the weak El Nino episodes such as 2006-2007, 2014-2015, and 2018-2019 had temperature anomaly between +0.5 and +0.1 in Nino 3.4 index. A moderate El Nino event was experienced in 2009-2010 and a very strong El Nino in 2015-2016 which was also well marked in the Nino 3.4 index. The negative values below -0.4 observed in the year 2007-2008 and 2010-2011 showed a strong La Nina and 2011-2012 indicate moderate La Nina events. Weak cold events were experienced during 2008-2009, 2011-2012, and 2016-2017.

Time series of area-averaged sea surface temperatures over the Nino 1+2 region are illustrated in the figure4.1c. The five El Nino events experienced during 2007-2018 was well marked in the Nino 1+2 region, SST anomaly recorded during these periods were at or above 0.5 anomalies. The moderate El Nino during 2009-2010 did not have a strong signature on Nino 1+2index, temperature anomaly during this period was between 0.5 and 1. It is the easternmost region among all SST index regions, thereby it had the greatest variance of Nino SST indices. For the years 2012 and 2017, the SST anomaly over this region was above the threshold. In the case of cold La Nina events, the strong La Nina in the years 2007-2008 and 2010-2011 had a strong signature on the Nino1+2 index. Weak La Nina event of 2016-17 was not well marked in the index, there was no such signal during the period. The very next cold event during 2017-2018 was well marked on the Nino 1+2 index.

Nino 4, the westernmost part of SST index regions captures SST anomalies in the central equatorial Pacific. The time series of area-averaged sea surface temperature over the Nino 4 region is elucidated in the figure 4.1d. The Nino 4 index has less variance on SST average than other Nino regions. The values at or above 29°C on the y-axis represented the El Nino event during 2007-2018. Values below 28°C represents the La Nina. The very strong El Nino experienced during 2015-2016 reached the value above 30°C. The area-averaged SST in the weak El Nino years such as 2006-2007, 2014-2015, and 2018-19 were found to be between 29°C and 30°C. During moderate El Nino years, the area averaged SST values were very close to 30°C. The strong La Nina in 2007-2008 and 2010-2011 had SST below 27°C, weak La Nina in the years 2008-2009, 2016-2017, 2017-2018, and moderate La Nina in the year 2011-2012 had SST below 28°C.

Trans Nino index (TNI) is the gradient of equatorial SST across the Pacific from about dateline to the American coast (the difference between normalized SST anomalies of Nino 1+2 and Nino4 regions) (Figure 4.1e). El Nino events are represented by negative TNI values and La Nina by positive TNI values. The five El Nino events that occurred during the period 2007-2018 had TNI value below -1. The very strong El Nino in 2015-2016 showed a very less SST gradient between Nino1+2 and

Nino4. Moderate El Nino in 2009-2010 and weak El Nino in 2014-2015 had a strong signature on the TNI index. The gradient in SST anomalies is used to define different flavors of El Nino events (Trenberth and Stepaniak, 2001), the events with a larger SST gradient due to positive anomalies in Nino4 region and negative anomalies in Nino 1+2 region is considered as CP type of El Nino. The classification of types of El Nino that occurred during 2007-2018 collected from FAO (2020) state that El Nino during 2006-2007 was an EP type and moderate El Nino in 2009-2010, weak El Nino in 2014-2015 and 2018-2019 were CP type. The years of occurring CP type event had a larger SST gradient as it is evident from the figure (Figure 4.1e). The five La Nina episodes during 2007-2018 had a strong signature on TNI but there was no such signal in 2017-18.

Multivariate ENSO Index (MEI) is based on five variables such as sea level pressure (SLP), sea surface temperature (SST), zonal and meridional components of the surface wind, and outgoing long wave radiation (OLR) from the tropical Pacific. The time series of MEI for 2007-2018 is illustrated in the figure 4.1f. El Nino events are indicated using positive MEI values and La Nina events by negative. The weak warm events had MEI values close to 1, moderate events had values between 1and 2 and the very strong El Nino during 2015-2016 had MEI value greater than 2. The El Nino episode in 2014-2015 was not well marked on the MEI time series. The strong La Nina in the year 2010-2011 was very clear in the time series of MEI, but there was no such evidence for the La Nina in the year 2007-2008 which was strong. The six La Nina events that happened during the study period had MEI value below -1 except for the weak La Nina in 2016-2017.

Southern Oscillation Index (SOI) is the normalized pressure difference between Tahiti and Darwin, Australia. The time series data for the Southern Oscillation Index is illustrated in the figure 4.1g. El Nino events are represented by persistent negative values of SOI and La Nina episodes coincide with sustained positive values. The weak El Nino events in 2006-2007, 2014-2015, and 2018-2019 had SOI values at or below -1 and very strong event exceeded the value -2. All the six La Nina events were well evident in the SOI time series. During weak La Nina events, the SOI values were between 1 and 2, and during moderate and strong La Nina events, the SOI values were above 2.

El Nino Modoki Index (EMI) assess the SST anomalies over the central Pacific deducted from the area-averaged SST anomalies over eastern and western Pacific. The time series of the EMI values are elucidated in the figure 4.1h. Sustained positive values represent the El Nino episodes and La Nina events are indicated by negative values. The representing values for each El Nino event lie above 0.5. The El Nino event in 2009-2010 showed the highest EMI value (1.2) among all El Nino years. The

weak La Nina episode in 2017-18 was not well evident in the EMI index, other La Nina episodes lie below the value -0.5 and Strong events had EMI value between -1.0 and -1.5. Dipole Mode Index (DMI) is the SST gradient between southeastern equatorial Indian Ocean (90°E-110°E and 10°S-equator) and the western equatorial Indian Ocean (50°E-70°E and 10°S-10°N). Positive values of Index represented the Positive IOD and negative values indicate the negative IOD event (Figure 4.1i). 2006, 2012, 2015, and 2019 were positive IOD years. The El Nino in 2006-2007, 2015-16, and 2018-19 coincided with positive IOD. 2010, 2014, and 2016 were negative IOD events. La Nina events in 2010-2011 and 2016-2017 coincided with negative IOD.

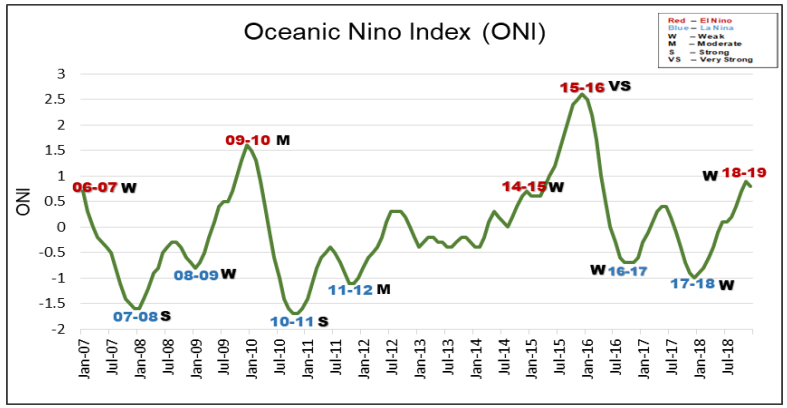

Figure 4.1a: Time series of Oceanic Nino Index for 2007-2018

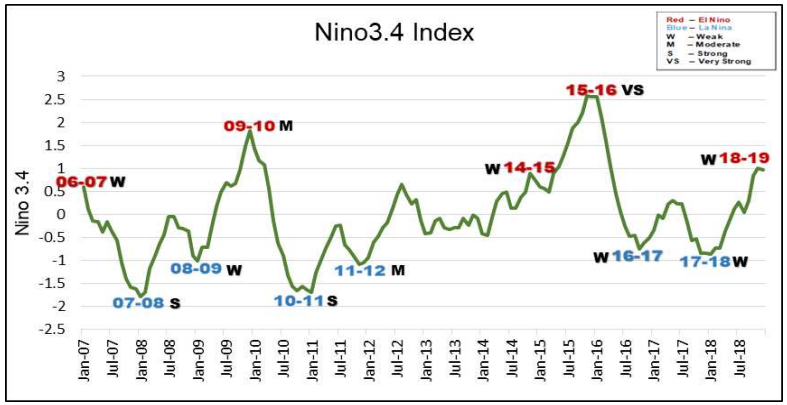

Figure 4.1b: Time series of Nino 3.4 Index for 2007-2018

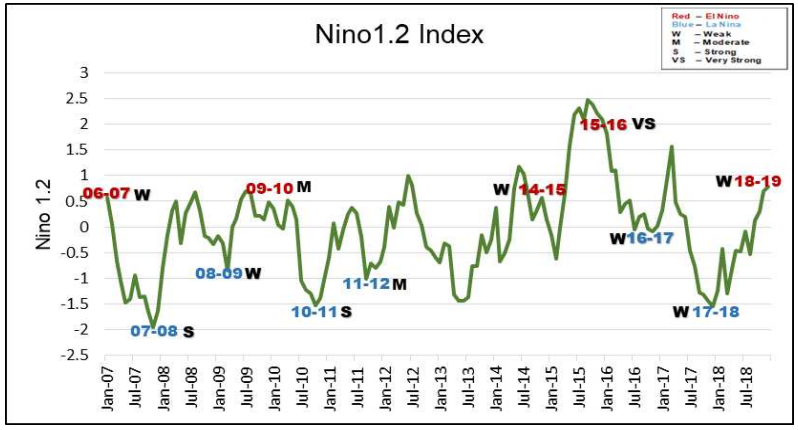

Figure 4.1c: Time series of Nino 1+2 Index for 2007-2018

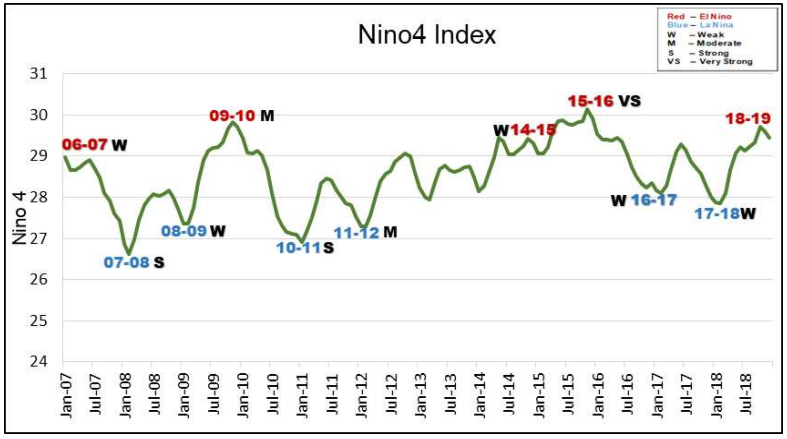

Figure 4.1d: Time series of Nino 4 Index for 2007-2018

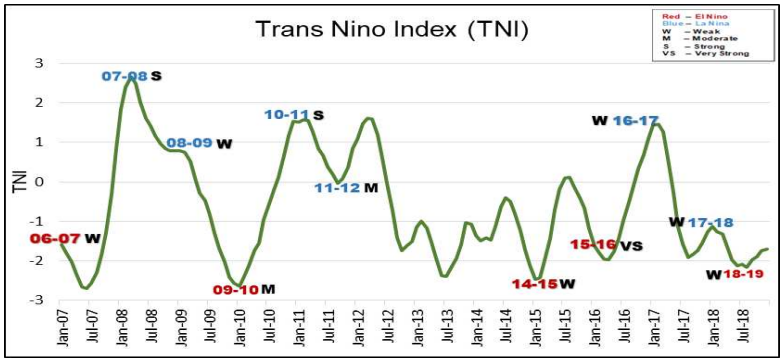

Figure 4.1e: Time series of Trans Nino Index for 2007-2018

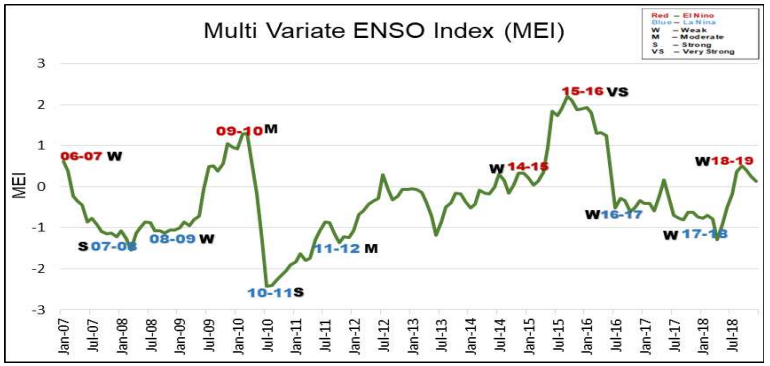

Figure 4.1f: Time series of Multivariate ENSO Index for 2007-2018

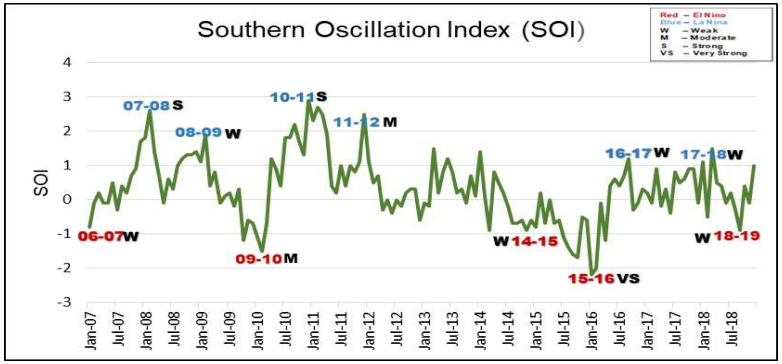

Figure 4.1g: Time series of Southern Oscillation Index for 2007-2018

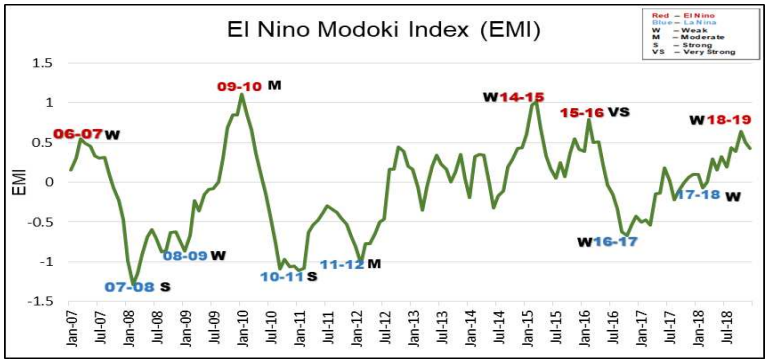

Figure 4.1h: Time series of El Nino Modoki Index for 2007-2018

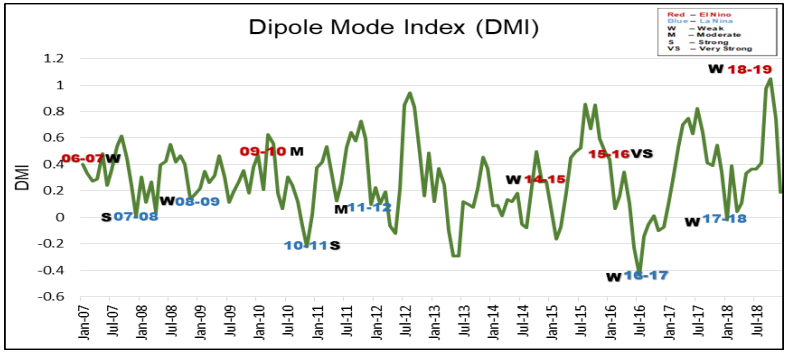

Figure 4.1i: Time series of Dipole Mode Index for 2007-2018

Table 4.1: ENSO events that have occurred during the period of 2007-2018 as identified by the different ENSO indices.

Indices / **Events**	ONI	Nino 3.4	Nino 1.2	Nino 4	TNI	MEI	SOI	EMI	DMI
2006-2007	E	E	E	E	E	E	E	E	E
2009-2010	E	E	E	E	E	E	E	E	E
2014-2015	E	E	E	E	E	_	E	E	E
2015-2016	E	E	E	E	E	E	E	E	E
2018-2019	E	E	E	E	E	E	E	E	E
2007-2008	L	L	L	L	L	L	L	L	L
2008-2009	L	L	L	L	L	L	L	L	L
2010-2011	L	L	L	L	L	L	L	L	L
2011-2012	L	L	L	L	L	L	L	L	L
2016-2017	L	L	_	_	L	_	L	L	L
2017-2018	L	L	L	L	_	L	L	_	L

'E' stands for El Nino and 'L' stands for La Nina

Correlation analysis

ONI is highly positively correlated (0.92) with MEI ($p<0.001$), highly positively correlated (0.99) with Nino 3.4 ($P< 0.001$). Both SOI and TNI were negatively correlated with all other Indices such as DMI, EMI, MEI, Nino 3.4, Nino4, and ONI. The SOI was positively correlated (0.46) with TNI ($p<0.001$) (Table 4.1a). In order to avoid the multi-collinearity problem, out of the three highly correlated indices, ONI and Nino 3.4 were discarded and MEI was kept for further Model construction.

Table4.2- Correlation coefficient matrix of different ENSO indices.

	DMI	EMI	MEI	Nino3.4	Nino4	ONI	SOI	TNI
DMI								
EMI	0.16							
MEI	0.23**	0.67****						
Nino3.4	0.29***	0.70****	0.91****					
Nino4	0.23**	0.82****	0.82****	0.89****				
ONI	0.29***	0.69****	0.92****	0.99****	0.87****			
SOI	-0.20*	-0.67****	-0.79****	-0.76****	-0.73****	-0.76****		
TNI	-0.06	-0.88****	-0.44****	-0.46****	-0.67****	-0.44****	0.46****	
Nino1.2	0.25**	0.14	0.70****	0.73****	0.55****	0.74****	-0.50****	0.15

4.1.2 Influence of ENSO phenomenon on various Ocean-atmospheric parameters

GAM modelling was used to study the influence of ENSO phenomenon on different ocean-atmospheric parameters by considering ocean-atmospheric parameters as the response variable and the different ENSO indices as the predictors. GAM models were developed for the ocean-atmospheric parameters such as Chlorophyll a (CHL_A), Local Temperature Anomaly (LTA), Sea surface Temperature (SST), Sea Surface Height Anomaly (SSHA), Sea Surface Salinity (SALT), Rainfall (RF), Ocean Current velocity (OCV), and Ocean Current Direction (OCD). The best fit model was selected on the basis of AIC value (model with lowest AIC value) (table 4.3a). Out of the best fit model for each response variable, the models with an adjusted R^2 value above 0.25 were selected for further analysis and are discussed below.

Chlorophyll a

The GAM model, where chlorophyll a concentration was taken as response variable and DMI, EMI, MEI, TNI and Nino4 were considered as the predictors, returned an adjusted R^2 value of 0.45 and the percentage deviance explained was 52.9% (Table 4.3[a,b]). The parameters such as SOI and Nino 1+2 had no significant influence in the model and were removed from the final model. The MEI (edf=7.16, $p<0.05$) and TNI (edf=7.53, $p<0.001$) had high edf values meaning that the curves were complex and wiggly which could be seen from the plots. The curve for the partial effect of MEI suggest that chlorophyll concentration had a decreasing trend but they had an increasing trend between -1.5 to -1 and 0 to 0.5 values (Figure4.2b). The curve for the partial effect of TNI showed a strong positive effect between -1.5 to -0.5 values (Figure 4.2e). The curve for the partial effect of EMI (edf=1.00, $p<0.001$) showed that, it had a negative effect on chlorophyll concentration (Figure 4.2c). The Nino 4

index (edf=2.55, p<0.001) showed a positive relation with chlorophyll value up to a value of 29°C later the curve is nearly flat (Figure 4.2d). The curve for the partial effect of DMI (edf=2.03, p<0.1) suggest that the DMI had a negative effect on chlorophyll concentration up to 0, had a positive effect from the value 0.5 and the curve is almost flat between 0 and 0.5 (Figure 4.2a).

Local Temperature Anomaly

The adjusted R^2 value of GAM taking LTA as response variable was 0.56 and the percentage deviance explained was 62.2%. The GAM model results revealed that DMI, EMI, MEI, SOI, TNI, and Nino 4 had strong influence on LTA. The Nino 1+2 had no effect on the LTA and was removed from the final model (Table 4.4[a,b]). The curve for the partial effect of TNI (edf=8.34, p<0.001) showed a strong influence on LTA. There was a strong decrease in LTA between -2.5 and -1.5, continuing its decreasing trend and the curve between -1.5 to 0 is almost flat (Figure 4.3f). The curve for the partial effects of EMI (edf=5.66, p< 0.001), MEI (edf=1.00, p<0.01) and SOI (edf=1.00, p<0.1) had shown a negative effect on LTA (Figure 4.3[b,c,e]). The curve for the partial effect of Nino 4 index (edf=1.00, p<0.001) suggest that it had a positive relation with LTA (Figure 4.3d). The curve for the partial effect of DMI (edf=2.073, p<1) was flat in the range of 0 to 0.5, and it had a decreasing trend up to zero and increasing trend after a value of 0.5 (Figure 4.3a).

Sea Surface Temperature

The GAM model where monthly mean SST was taken as response variable and the DMI, EMI, MEI, SOI, Nino 1+2 index and TNI were considered as predictors returned an adjusted R^2 value of 0.303 and the model explained 36.9% of deviance (Table 4.5[a,b]). The Nino4 index had no significant influence in the model and were discarded from the final model. Model result indicated that TNI (edf=7.3, p<0.001) had strong influence on SST and gives a complex curve, which demonstrated the complicated relationship of changes in SST to TNI (Figure 4.4e). The curve for the partial effect of EMI (edf=1.39, p<0.001), MEI (edf=1.00, p<0.05) and SOI (edf= 1.00, p<0.05) revealed that they had a positive effect on SST (Figure4.4 [b,a,c]), EMI had greater influence than MEI and SOI. The curve for the partial effect of DMI is flat from 0 to 0.5 value and showed an increasing trend before zero and decreasing trend after a value of 0.5 (Figure 4.4a). The curve for the partial effect of Nino 1+2 (edf=1.00, p<1) had revealed a negative effect on SST (figure 4.4f).

Sea Surface Height Anomaly

The percentage deviance explained by the GAM taking monthly mean SSHA as response variable was 55.9% and returned an adjusted R^2 value of 0.52. The model result indicated that parameters such as DMI, EMI, MEI, SOI, Nino4, Nino1+2 and TNI had strong influence on SSHA (Table 4.6[a,b]). The curve for the partial effect of DMI (edf=1, $p<0.01$) and Nino 4 index (edf=2.39, $p<0.001$) revealed that they had a negative effect on SSHA. The SSHA had a very strong decreasing trend up to a value of 29°C with Nino4 (Figure 4.5[a,f]). The curve for the partial effect of EMI (edf=1.00, $p<0.001$), MEI (edf=1, $p<0.05$), SOI (edf=0.1, $p<0.1$) and Nino1+2 index (edf=1.00, $p<0.001$) showed that they had a positive effect on SSHA (Figure 4.5[b,c,d,g]). The edf value for the TNI curve was 5.43 ($p<0.01$), meaning that the curve is complex and it is evident from the plots. The TNI showed a negative effect between -1 to -0.5 and again showed a decreasing trend after the value 1.5 (Figure 4.5e).

Sea Surface Salinity

The GAM model where the monthly mean salinity of Kerala coast was taken as the response variable and DMI, EMI, MEI, Nino4 and Nino1+2 were considered as predictors returned an adjusted R^2 value of 0.27 and the percentage deviance explained was 34% (Table 4.7[a,b]). The parameters such as SOI, and TNI had no remarkable influence on salinity and was discarded from the final model. The curve for the partial effect of Nino 1+2 (edf=6.44, $p<0.1$) had high edf value suggesting that the curve was complex and the relation between salinity and Nino 1+2 was wiggly, which could be seen from the plots. The curve showed a decreasing trend up to a value of -1, further increase in the value had strong positive effect on salinity except that Nino1+2 had a slight negative effect between 0.5 -1.0 value (Figure 4.6e). The curve for the partial effect of EMI (edf=1.00, $p<0.05$) had a positive effect on salinity (Figure 4.6b). The curve for the partial effect of DMI (edf=1, $p<0.001$) and Nino 4 (edf=3.02, $p<0.001$) had a negative effect on salinity, the curve for the partial effect of Nino 4 showed a strong decreasing trend above the value 28.5 (Figure 4.6[a, d]). The curve for the partial effect of MEI (edf=2.94, $p<1$) had a positive effect on salinity up to -0.5 and further increase in the value led to the flattening of curve (Figure 4.6c).

Rainfall

The GAM model were monthly mean Rainfall along the Kerala coast was taken as response variable and EMI, MEI, SOI, TNI, and Nino 4 were taken as predictors, returned an adjusted R^2 value

of 0.53 and the percentage deviance explained was 59.9% (Table 4.8 [a,b]). The model result revealed that EMI, MEI, TNI, SOI and Nino4 had great influence on monthly rainfall. Other parameters such as DMI, and Nino 1+2 were insignificant and removed from the final model. The edf was high for TNI (edf=7.39, $p<0.001$) and the curve was complex. The rainfall shows a decreasing trend up to the TNI value -1.5, further increase in TNI value shows slight increasing trend (Figure 4.7d). The curve for the partial effect of MEI also had a complex nature (edf=6.68, $p<0.001$). The curve indicate that MEI had a negative effect on rainfall. Between -1.5 to-1 and 0 to 0.5 there is an increasing trend of rainfall with MEI (Figure4.7b). The curve for the partial effect of EMI (edf=4.29, $p<0.001$) suggest that there was a positive effect between -0.5 to 0 (Figure 4.7a). The curve for the partial effect of Nino 4.1index (edf=1.0, $p<0.001$) showed a positive relation with Rainfall (Figure 4.7e). The curve for the partial effect of SOI was flat up to the value 1, a further increase in the value showed a negative effect on rainfall (Figure 4.7c).

Table 4.3a: Details of AIC, Adjusted R-square, and Deviance explained for the Chlorophyll a models (obtained by stepwise fitting procedure).

Model	AIC	R-sq. (adj)	Deviance explained (%)
CHL_A ~ s(DMI) + s(EMI) + s(MEI) + s(SOI)+ s(TNI) + s(Nino4)+ s(Nino1.2)	545.0579	0.441	52.8
CHL_A ~ s(DMI) + s(EMI) + s(MEI) + s(SOI)+ s(TNI) + s(Nino4)	543.1221	0.446	52.8
*CHL_A ~ s(DMI) + s(EMI) + s(MEI) + s(TNI) + s(Nino4)	541.2957	0.45	52.9
CHL_A ~ s(EMI) + s(MEI) + s(TNI) + s(Nino4)	543.6029	0.435	50.8
CHL_A ~ s(EMI) + s(TNI) + s(Nino4)	553.3587	0.364	41
CHL_A ~ s(EMI) + s(TNI)	562.4729	0.315	36.1
CHL_A ~ s(TNI)	586.0329	0.184	22.2

* Best fit model based on lowest AIC value

Table4.3b: Details of deviance explained & adjusted R-square value for Chlorophyll a model and the effective degrees of freedom & significance of the explanatory variables of the model

CHL_A ~ s(DMI) + s(EMI) + s(MEI) + s(TNI) + s(Nino4) R-sq.(adj) = 0.45 Deviance explained = 52.9%					
	edf	Ref.df	F	Deviance explained (%)	p-value
s(DMI)	2.031	2.576	1.602	6.08	0.181936
s(EMI)	1.285	1.515	16.039	6.16	0.000170 ***
s(MEI)	7.158	8.188	2.085	14.8	0.035005 *
s(TNI)	7.526	8.428	5.229	22.2	1.82e-05 ***
s(Nino4)	2.384	3.072	5.827	6.06	0.000892 ***

Signif. codes: 0 '***' 0.001 '**' 0.01 '*' 0.05 '.' 0.1 ' ' 1

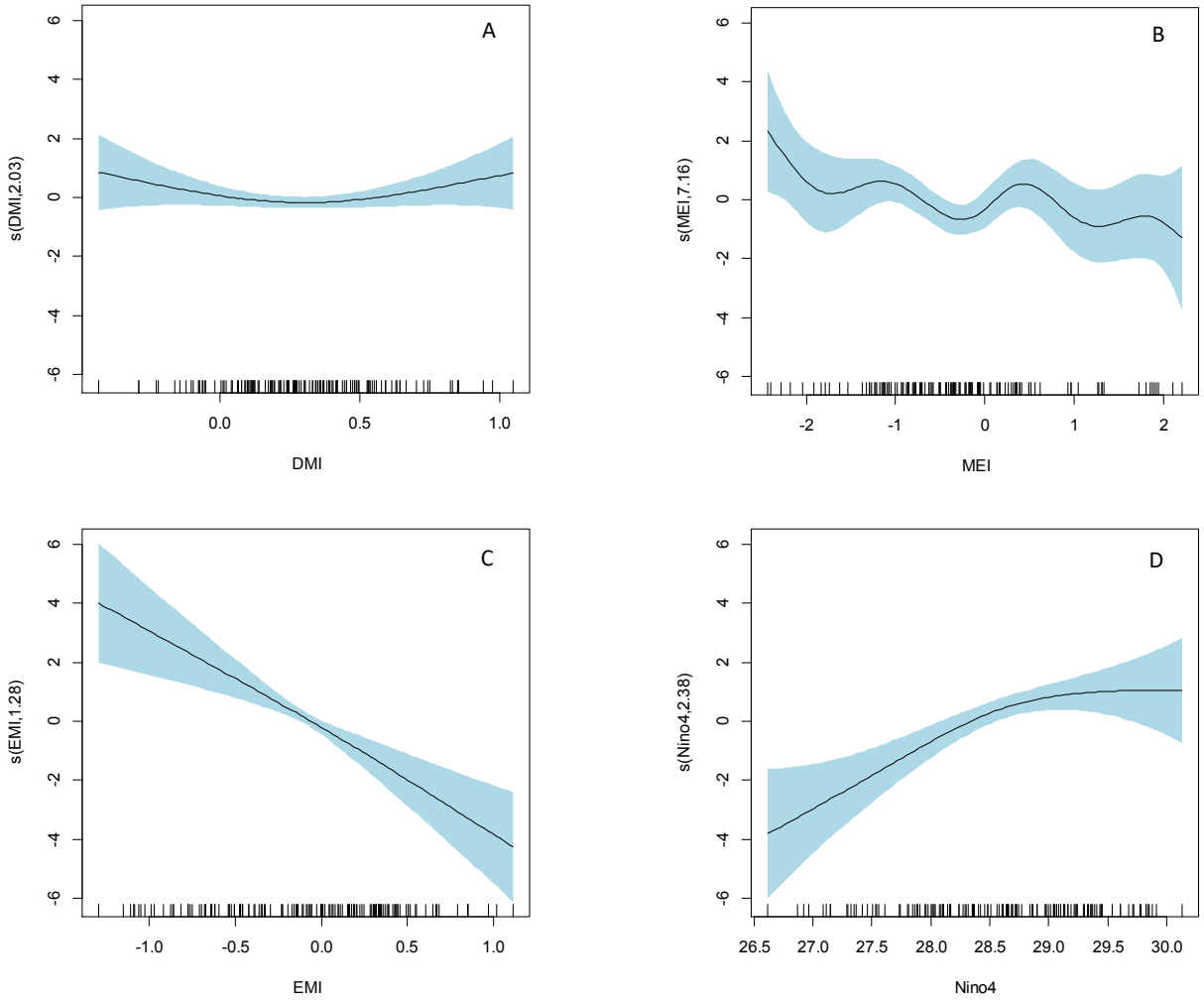

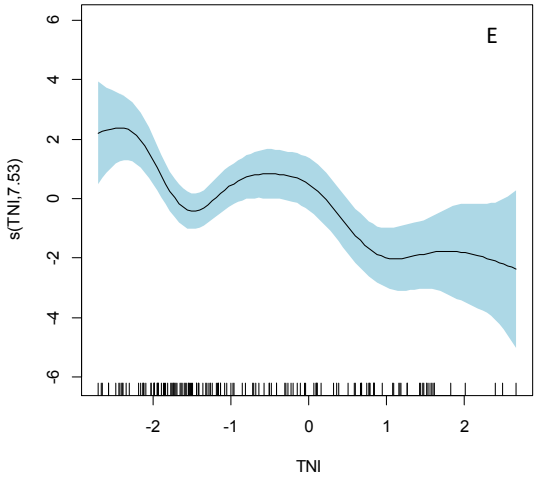

Figure 4.2: GAM model for CHL_A showing effects of explanatory variables ; DMI (A), MEI (B), EMI (C), Nino4 (D), and TNI (E)

Table 4.4: Details of deviance explained & adjusted R-square value for LTA model and the effective degrees of freedom & significance of the explanatory variables of the model

LTA ~ s(DMI) + s(EMI) + s(MEI) + s(SOI) + s(TNI) + s(Nino4) R-sq.(adj) = **0.57**; Deviance explained = **62.2%**					
	edf	Ref.df	F	Deviance explained (%)	p-value
s(DMI)	2.073	2.633	1.710	6.88	0.15522
s(EMI)	5.661	6.81	11.317	9.48	1.97e-11 ***
s(MEI)	1.000	1.000	9.716	13.6	0.00226**
s(SOI)	1.000	1.000	2.365	2.93	0.12661
s(TNI)	8.341	8.872	8.964	20.5	5.73e-11 ***
s(Nino4)	1.000	1.000	39.663	8.79	3.72e-09 ***

Signif. codes: 0 '***' 0.001 '**' 0.01 '*' 0.05 '.' 0.1 ' ' 1

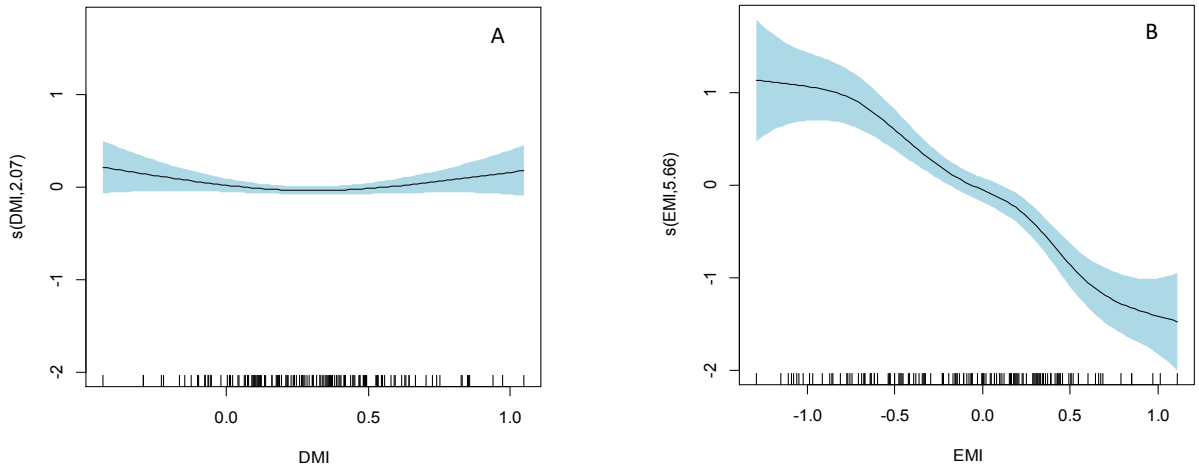

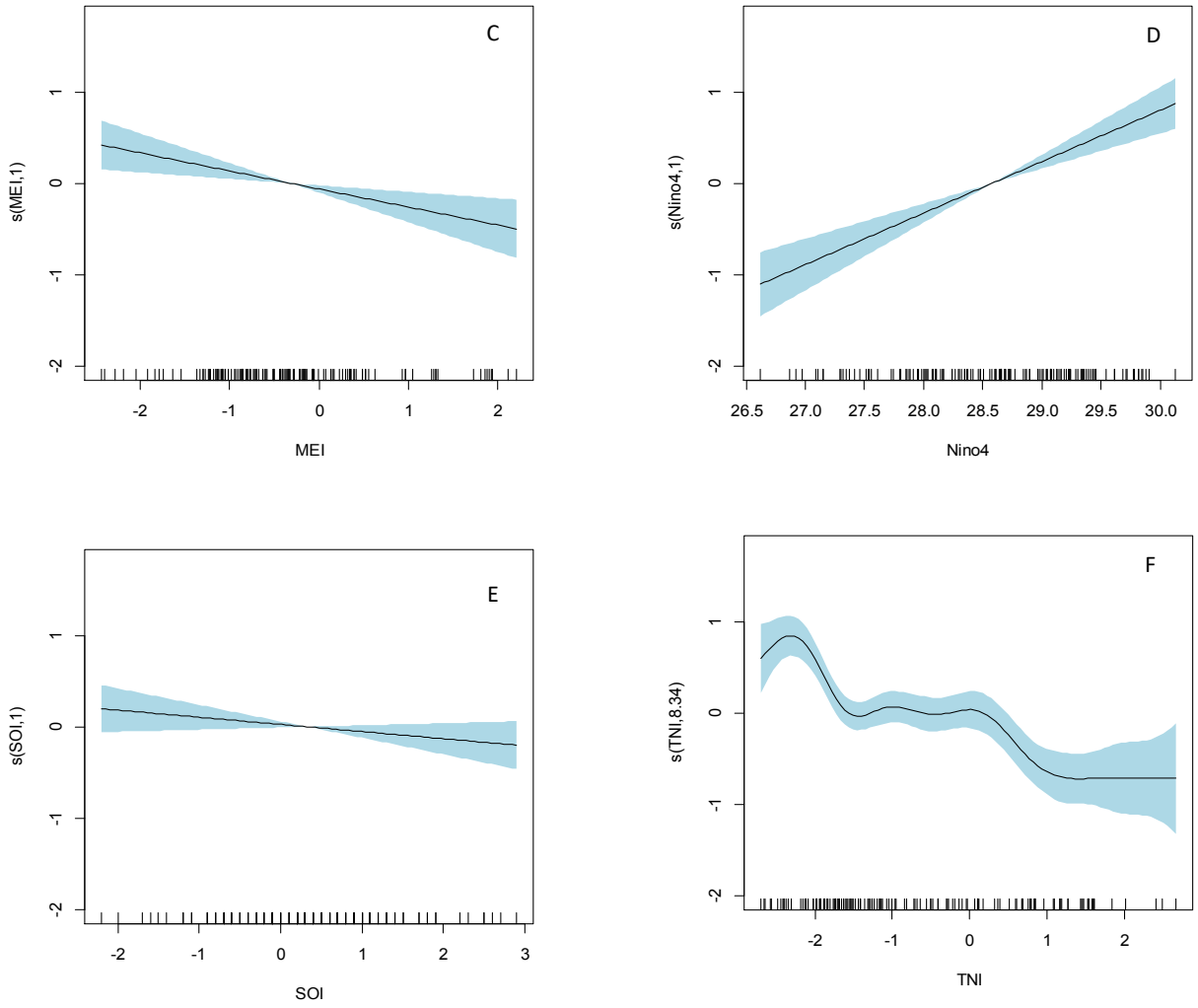

Figure 4.3: GAM model for LTA showing effects of explanatory variables ; DMI (A), EMI (B), MEI (C), Nino4 (D), SOI (E) and TNI (F)

Table4.5: Details of deviance explained & adjusted R-square value for SST model and the effective degrees of freedom & significance of the explanatory variables of the model

SST ~ s(DMI) + s(EMI) + s(MEI) + s(SOI) + s(TNI) + s(Nino1.2) R-sq.(adj) = 0.30; Deviance explained = 36.9%					
	edf	Ref.df	F	Deviance explained (%)	p-value
s(DMI)	1.841	2.335	1.042	1.8	0.3210
s(EMI)	1.389	1.697	17.204	8.53	2.99e-05 ***
s(MEI)	1.000	1.000	4.200	17.3	0.0424 *
s(SOI)	1.000	1.000	6.043	0.84	0.0153 *
s(TNI)	7.305	8.288	5.382	11.8	4.18e-06 ***
s(Nino1.2)	1.000	1.000	2.687	1.65	0.1036

Signif. codes: 0 '***' 0.001 '**' 0.01 '*' 0.05 '.' 0.1 ' ' 1

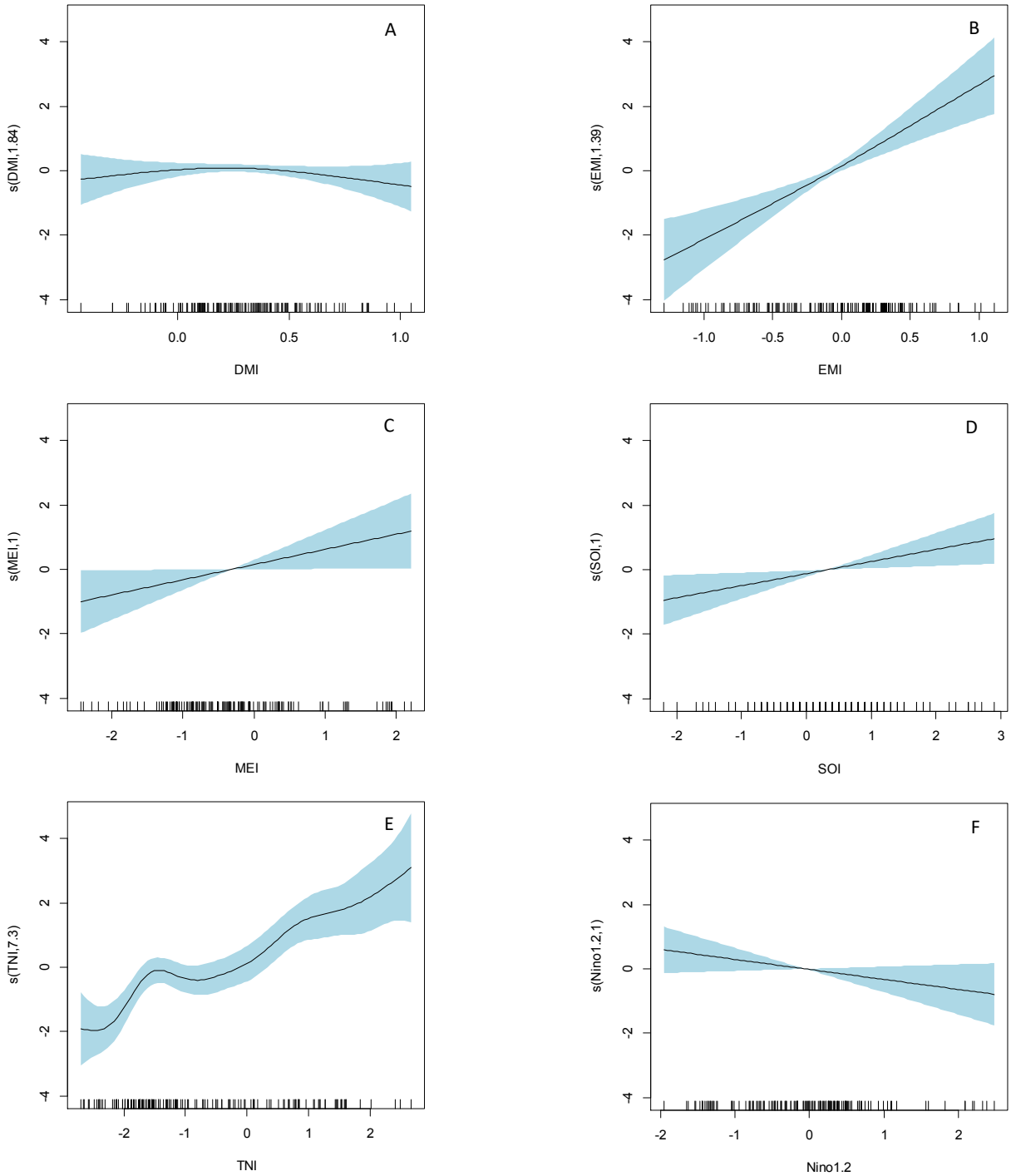

Figure 4.4: GAM model for SST showing effects of explanatory variables; DMI (A), EMI (B), MEI (C), SOI (D), TNI (E) and Nino1+2 (F)

Table4.6: Details of deviance explained & adjusted R-square value for SSHA model and the effective degrees of freedom & significance of the explanatory variables of the model

SSHA ~ s(DMI) + s(EMI) + s(MEI) + s(SOI) + s(TNI) + s(Nino4) + s(Nino1.2) R-sq.(adj) = **0.54**; Deviance explained = **57.6%**					
	edf	Ref.df	F	Deviance explained (%)	p-value
s(DMI)	1.000	1.000	10.441	4.77	0.00155 **
s(EMI)	1.000	1.000	53.545	13.2	1.27e-11 ***
s(MEI)	1.000	1.000	6.075	14.9	0.01498 *
s(SOI)	1.000	1.000	3.757	8.62	0.05471 .
s(TNI)	5.432	6.548	2.885	15.5	0.00968 **
s(Nino4)	2.390	3.058	19.587	13.6	6.65e-11 ***
s(Nino1.2)	1.000	1.000	5.564	8.11	0.01979 *

Signif. codes: 0 '***' 0.001 '**' 0.01 '*' 0.05 '.' 0.1 ' ' 1

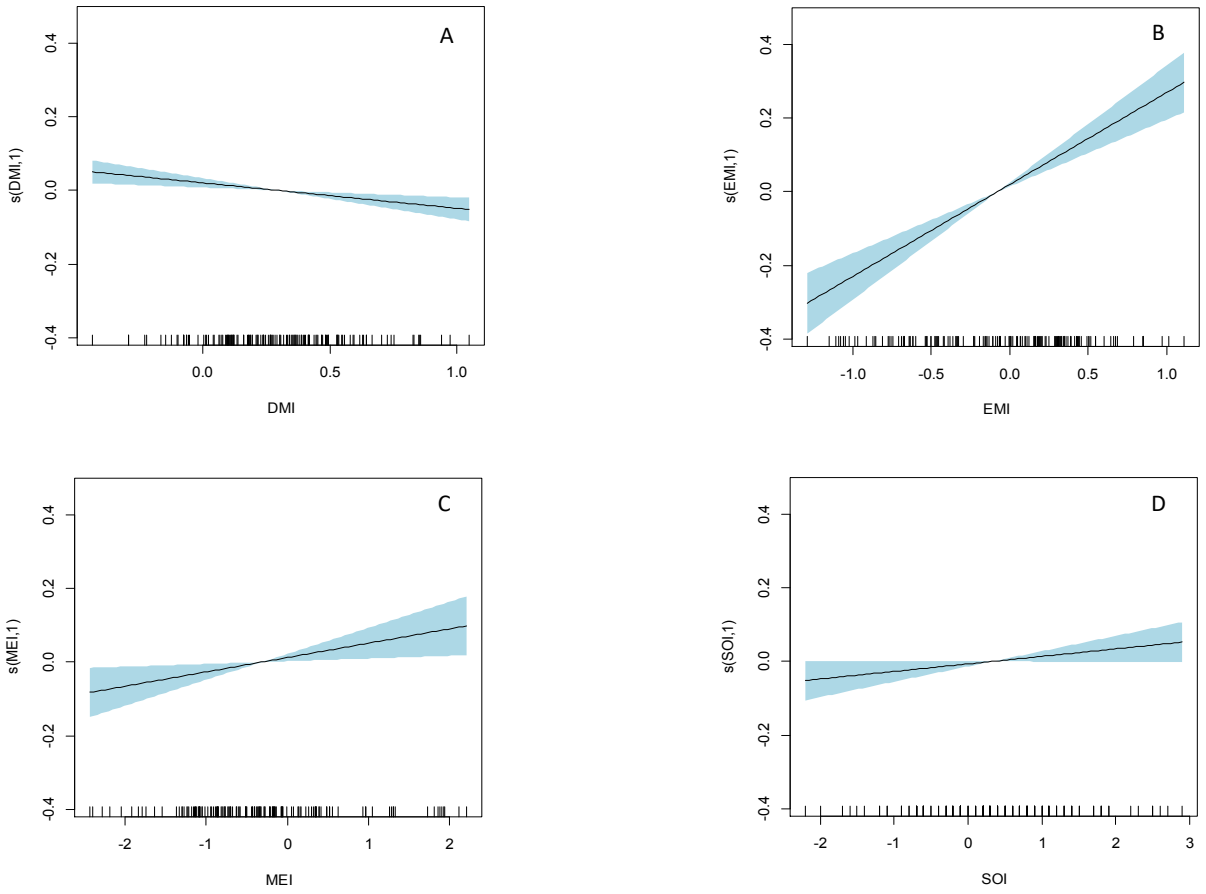

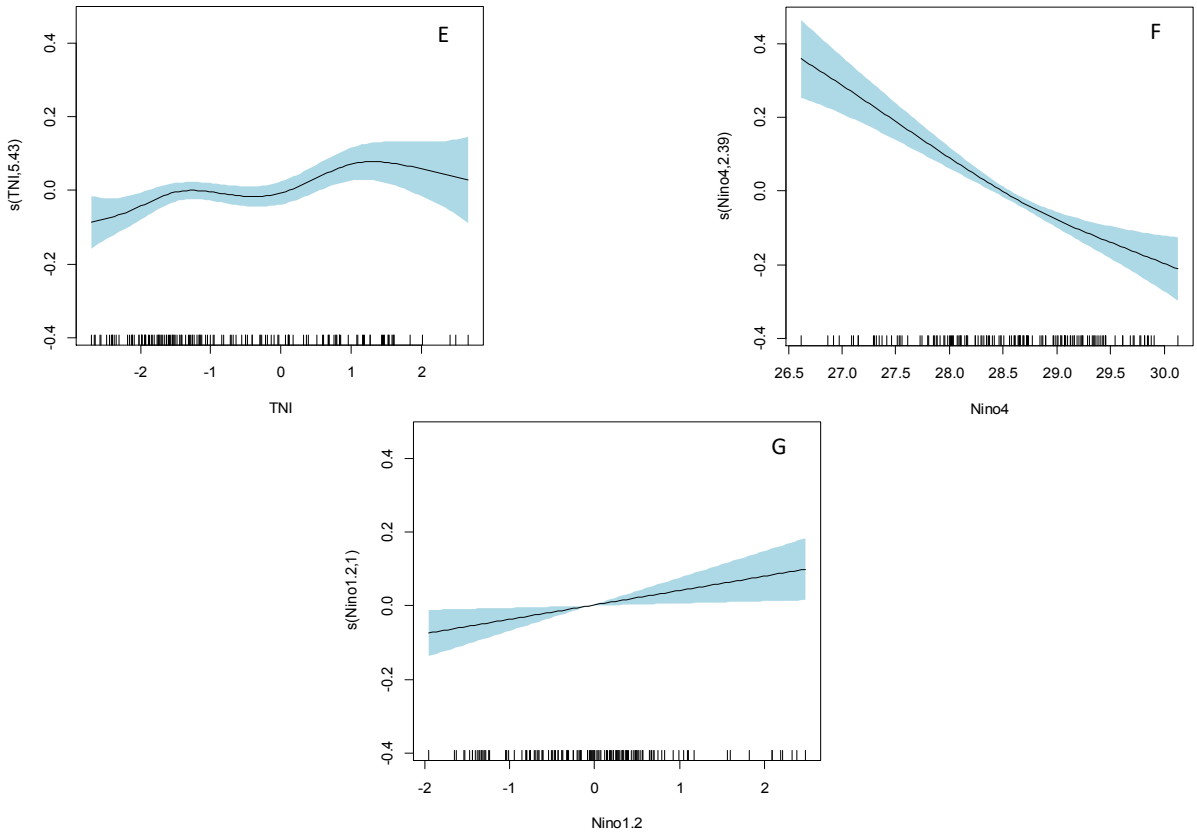

Figure 4.5: GAM model for SSHA showing effects of explanatory variables; DMI (A), EMI (B), MEI (C), SOI (D), TNI (E), Nino4 (F) and Nino1+2 (G)

Table4.7: Details of deviance explained & adjusted R-square value for SALT model and the effective degrees of freedom & significance of the explanatory variables of the model

SALT ~ s(DMI) + s(EMI) + s(MEI) + s(Nino4) + s(Nino1.2) R-sq.(adj) = 0.27 Deviance explained = 34%					
	edf	Ref.df	F	Deviance explained (%)	p-value
s(DMI)	1.000	1.000	11.405	7.21	0.000961 ***
s(EMI)	1.000	1.000	5.101	0.675	0.025561 *
s(MEI)	2.942	3.712	1.987	15.7	0.147479
s(Nino4)	2.399	3.054	6.789	5.64	0.000248 ***
s(Nino1.2)	6.445	7.612	1.877	8.86	0.072775

Signif. codes: 0 '***' 0.001 '**' 0.01 '*' 0.05 '.' 0.1 ' ' 1

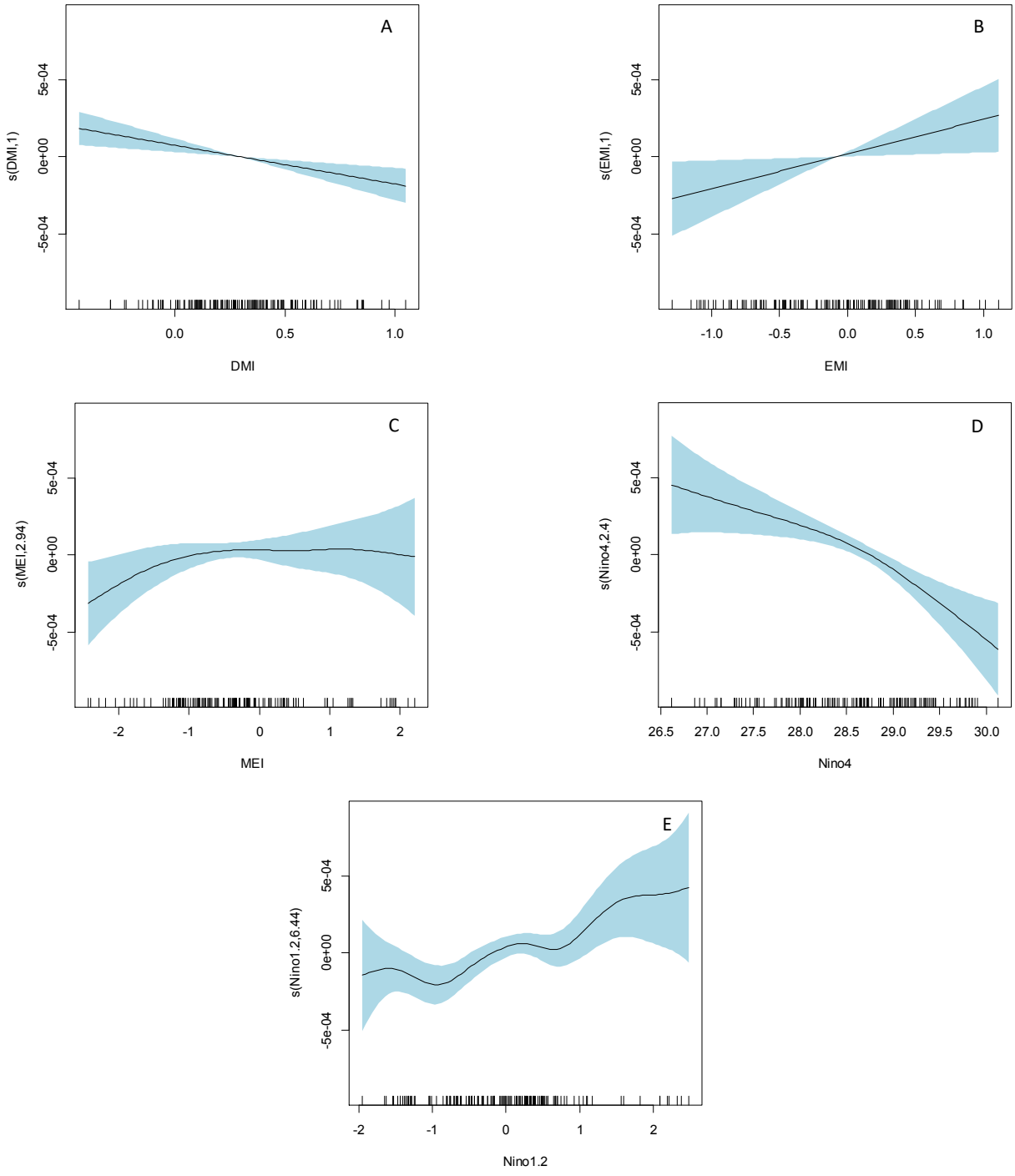

Figure 4.6: GAM model for SALT showing effects of explanatory variables ; DMI (A), EMI (B), MEI (C), Nino4 (D) and Nino1+2 (E)

Table4.8: Details of deviance explained & adjusted R-square value for Rain fall model and the effective degrees of freedom & significance of the explanatory variables of the model

RF ~ s(EMI) + s(MEI) + s(SOI) + s(TNI) + s(Nino4) R-sq.(adj) = **0.53** Deviance explained = **59.9%**					
	edf	Ref.df	F	Deviance explained (%)	p-value
s(EMI)	4.285	5.368	7.764	10.3	1.16e-06 ***
s(MEI)	6.670	7.782	5.049	0.73	1.99e-05 ***
s(SOI)	1.812	2.324	1.214	6	0.317
s(TNI)	7.391	8.332	4.698	15.7	4.30e-05 ***
s(Nino4)	1.000	1.000	46.456	8.52	2.51e-10 ***

Signif. codes: 0 '***' 0.001 '**' 0.01 '*' 0.05 '.' 0.1 ' ' 1

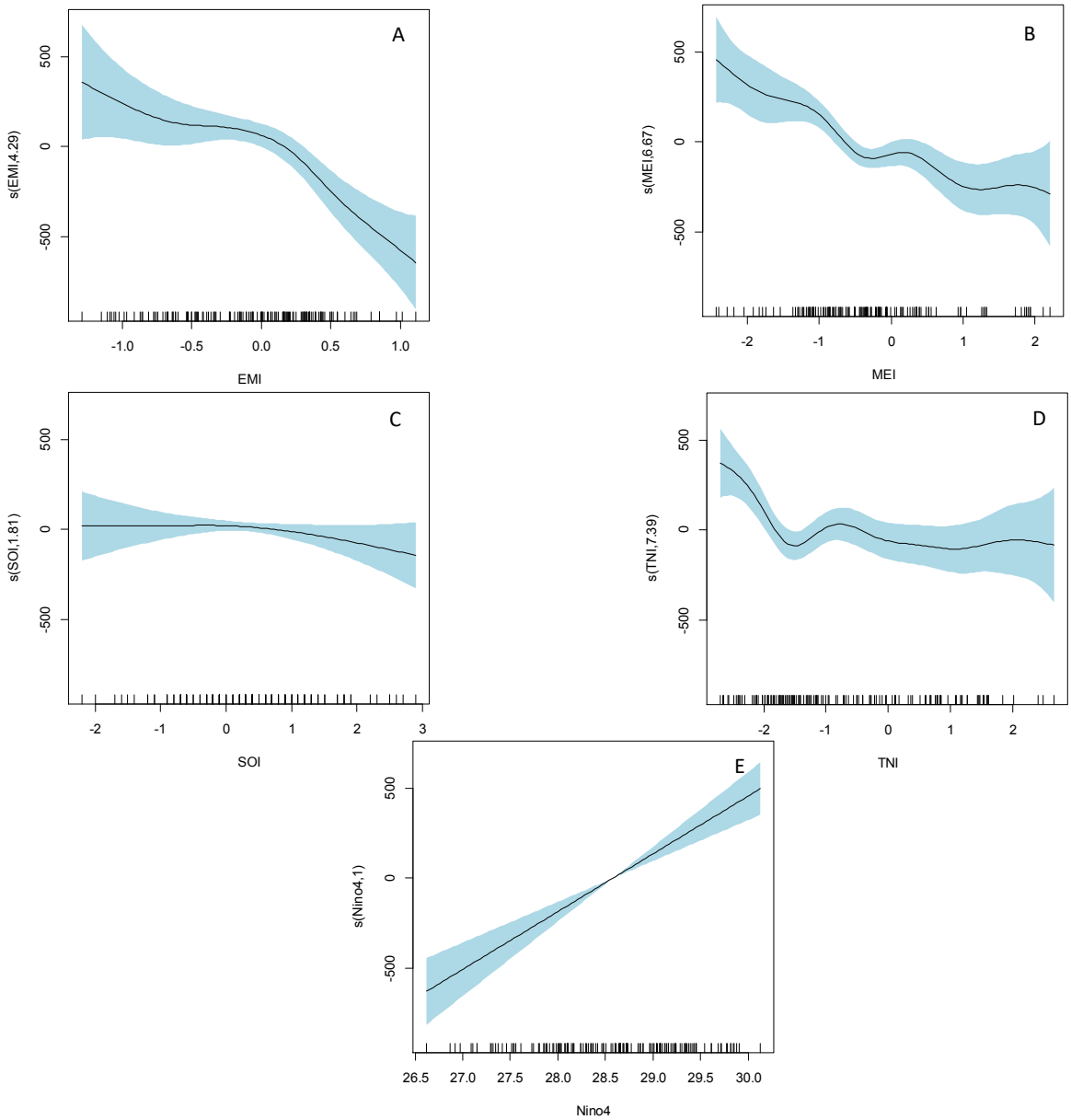

Figure 4.7: GAM model for RF showing effect of ; EMI (A), MEI (B), SOI (C), TNI (D) and Nino4 (E)

4.2 Impact of El Nino and La Nina on major pelagic and demersal resources of Kerala

4.2.1 Variations in Oil sardine Fishery

The total (Figure 4.8) and gear-wise (Figure 4.14) catch per unit effort (CPUE) data of Oil sardine during 2007-2018 along the Kerala coast and the warm and cold events of El Nino Southern Oscillation inferred from Oceanic Nino Index (ONI) are illustrated here. Total CPUE of Oil sardine were shown a decrease during October, November and December months of 2009, 2015, and 2018 but weak El Nino in the year 2014 had not affected the oil sardine abundance, but the CPUE of oil sardine had a severe decline during 2015-2016. The years 2007-2008, 2008-2009, 2010-2011, 2011-2012, 2016-2017, 2017-2018 were La Nina periods and the CPUE was increased during these periods. MRS (Mechanized Ring Seines), OBRS (Outboard Ring Seines), OBGN (Outboard Gill Nets), and other non-mechanized (NM) fishing gears are important for oil sardine landings. In very strong El Nino years (2015-2016) CPUE of MRS, OBRS, OBGN, NM, and all other gears such as MDTN (Multiday Trawl Net), MPS (Mechanized Purse Seines), MTN (Mechanized Trawl Net), and OBBS (Outboard Boat Seine) were decreased. CPUE of MRS, OBRS, and NM were increased in the years 2011, 2012, and 2013. A strong and moderate La Nina years were reported during 2010-2013. There was a strong La Nina event just after the occurrence of 2006-2007 El Nino, the reduced CPUE of MRS, NM, OBGN, and OBRS had reported an increase during the years 2007-2008. During 2009-2010 El Nino years, the CPUE of MRS, OBGN, and NM had declined during the peak El Nino period, CPUE returned to normal during the following La Nina period. CPUE also increased in the 2017-2018 weak La Nina year, but there was no such increase in the 2016-2017 La Nina period. The MRS CPUE increased during the post-La Nina period. CPUE of MRS, OBRS, and OBGN didn't show any decrease during the weak El Nino of 2014-2015, but there was a slight decrease for the NM.

4.2.2 Variations in Indian Mackerel Fishery

The total (Figure 4.9)and gear-wise (Figure 4.15) catch per unit effort (CPUE) data of Indian Mackerel during 2007-2018 and the El Nino and La Nina events of El Nino Southern Oscillation inferred from Oceanic Nino Index (ONI) are discussed here. Total CPUE of Indian mackerel didn't show severe decrease during El Nino periods, but there was as strong increase in the September 2015 and 2016. The CPUE were increased during August 2007 and 2010 and June 2011 which was prior to Strong La Nina. MRS, OBGN, and OBRS are important for Indian mackerel landings. MRS CPUE was very high during June 2011, September 2015, August 2018 and September 2018. These all peaks

were prior to La Nina episodes except for the 2015 September, where it was before a very strong El Nino episode. CPUE of MDTN, MTN, and OBGN were also shown a hike during 2015 September (Figure 4.15[A, D, H]). OBBS, OBHL, and MOTHS (mechanized other gears) CPUE showed a decrease during the peak of 2015-2016 El Nino. CPUE of all the gears showed an increase during La Nina years.

4.2.3 Variations in Anchovy Fishery

The total (Figure 4.10)and gear-wise (Figure 4.16) catch per unit effort (CPUE) data of anchovy during 2007-2018 and the El Nino and La Nina events of El Nino Southern Oscillation inferred from Oceanic Nino Index (ONI) are illustrated here. Total CPUE of anchovy had increased before all La Nina peaks. Total CPUE were decreased during 2009-2010 moderate El Nino period, but very strong El Nino in 2015-2016, weak El Nino episodes in 2014-2015 and 2017-2018 didn't show any decrease in CPUE. OBRS, MRS, MDTN, OBBS, MTN and NM are important gears for anchovy landings in Kerala. In pre and post La Nina months OBRS CPUE was peaked, but the CPUE decreased during 2009-2010 and 2014-2015 El Nino years. It was seen that OBRS CPUE was not much affected by the very strong El Nino during 2015-2016 (Figure 4.16G). OBGN CPUE showed an increase for all La Nina Events, except for the 2010-2011 strong La Nina peak time and 2011-2012 moderate La Nina peak. CPUE of OBGN also showed an increase in the peak month of 2009-2010 and 2015-2019 El Nino episodes (Figue 4.16H). NM CPUE increased during 2015-16 El Nino period and prior to all La Nina events. During the La Nina peak there was no hike in CPUE. CPUE of non-mechanized gears showed decline during 2014-15 and 2018-19 El Nino years (Figure 4.16E). MDTN CPUE had a hike during the post El Nino period in the year 2015-2016, there was an increase during the peak period of moderate El Nino episode in 2009-2010 and 2018-2019 El Nino (Figure 4.16A).

4.2.4 Variations in Penaeid Prawn Fishery

The total (Figure 4.11) and gear-wise (Figure 4.17) catch per unit effort (CPUE) data of Penaeid prawn during 2007-2018 along the Kerala coast and the warm and cold events of El Nino Southern Oscillation are discussed here. CPUE of Penaeid prawns peaked during June, it was above normal during La Nina episodes in 2008, 2010, & 2017 and also during El Nino episodes in 2018 & 2015. The La Nina events in 2016-2017 and 2017-2018 showed an increased CPUE of total PP landings. Total CPUE was decreased during the moderate (2009-2010) and very strong El Nino episodes (2015-2016, except for July and August). Trawl nets are important for Penaeid prawn

landings. The highest peak in MDTN CPUE was recorded in August 2015 (before 2015-16 El Nino), MDTN CPUE was also above normal in December 2015, but MDTN CPUE was lower than the normal CPUE during three months after December 2015. MDTN CPUE showed a decrease in 2009-2010 moderate El Nino year, the years 2014-2015 and 2018 didn't show much decline in MDTN CPUE. The MDTN CPUE showed an increase during the post-La Nina period except for the 2007-2008 strong La Nina (Figure 4.17A). MTN CPUE was increased in August months and during all post-La Nina periods and was decreased during all El Nino periods (Figure 4.17B). OBTN CPUE hiked during June months of La Nina years and OBTN CPUE was below normal during the 2009-2010 and 2015-2016 El Nino years (Figure 4.17G). OBRS CPUE was high for June-July months and 2016-2017, 2017-2018 weak La Nina periods (Figure 4.17 F).

4.2.5 Variations in Threadfin breams catch per unit effort

The total (Figure 4.12) and gear-wise (Figure 4.18) catch per unit effort (CPUE) data of threadfin breams during 2007-2018 along the Kerala coast and the warm and cold events of El Nino Southern Oscillation are illustrated here. Trawl nets are important for Threadfin bream landings. The total CPUE were higher in August months, it was above normal for 2011, 2018, (after strong and weak La Nina episode) and 2015(very strong El Nino). Total CPUE was increased during 2017-2018 La Nina period, 2016-2017, 2010-2011, and 2011-2012 post La Nina periods. Total CPUE was decreased during 2009-2010 moderate El Nino episode. The CPUE was very less for the years 2007 and 2008 even though it was a strong La Nina episode. The CPUE of MTN, OBGN, OBHL were increased during August 2015, CPUE of NM and MOTHS were decreased during 2015. NM CPUE increased before La Nina episodes in 2010, 2011, 2016 and 2017 and CPUE of MOTHS increased during post La Nina periods of 2008, 2009, 2011, 2012 and 2017.

4.2.6 Variations in catch per unit effort of total fish landings

The catch per unit effort of total fish landings (Figure 4.13) and gear wise CPUE (Figure 4.19) of total fish landings by different gears along the Kerala coast during 2007-2018 is illustrated along with the El Nino and La Nina events in the figures. The total CPUE was decreased during very strong El Nino episode in 2015-2016 and moderate El Nino event in 2009-2010. The total CPUE was increased in 2016, 2017, and 2018 and CPUE was higher for post La Nina events in 2008, and 2011. The CPUE of MDTN had a decline during the years of very strong, moderate and weak El Nino years, but increased during the post-La Nina periods in the years 2007-2008, 2010-2011, and

2011-2012. The MDTN CPUE was higher for 2016-2018 when we experienced two consecutive weak La Nina events (Figure 4.19A). The CPUE during 2008-2009 and 2016-2018 was high for all the gears. CPUE of MOTHS, MGN, MHL, OBHL, and OBOTHS didn't show any decrease during the peak month of 2015-16 El Nino, but CPUE of MPS, MRS, MTN, NM, OBBS, OBGN, OBRS, and OBTN was low. During moderate El Nino in the 2009-10 CPUE of MRS, MTN, NM, OBBS, OBGN, and OBRS had the same changes as in the year 2015-2016. CPUE OF MHL increased in December 2009, but CPUE was less during November and January. MGN CPUE decreased during December 2009. CPUE of OBBS, NM, MPS, and MGN decreased during 2014-2015 El Nino, CPUE of other gears not much affected by 2014-2015 El Nino. CPUE of MRS, MPS, OBRS, and NM was increased during 2007-2008 (strong), 2010-2011 (strong) and 2011-12 (moderate) La Nina years. MTN CPUE had hiked before La Nina peak month, CPUE of other gears such as OBGN, OBTN, MGN, MHL, MOTHS, was also hiked during post-La Nina periods.

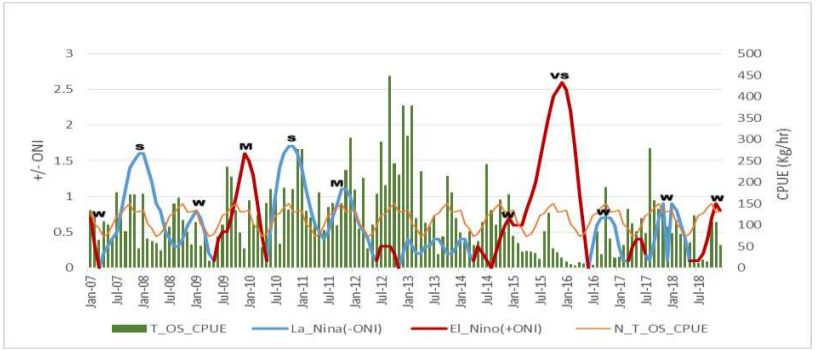

Figure 4.8: Monthly Oil sardine fishery from 2007 to 2018; T_OS_CPUE: Monthly Oil sardine CPUE, N_T_OS_CPUE: Month wise 12 year average Oil sardine CPUE

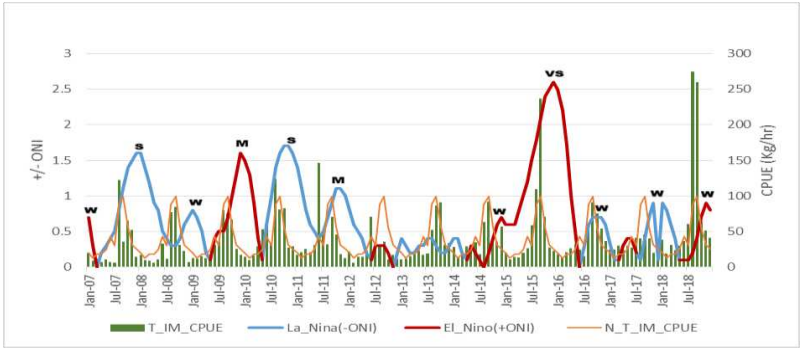

Figure 4.9: Monthly Indian mackerel fishery from 2007 to 2018; T_IM_CPUE: Monthly Indian mackerel CPUE, N_T_IM_CPUE: Month wise 12 year average IM CPUE

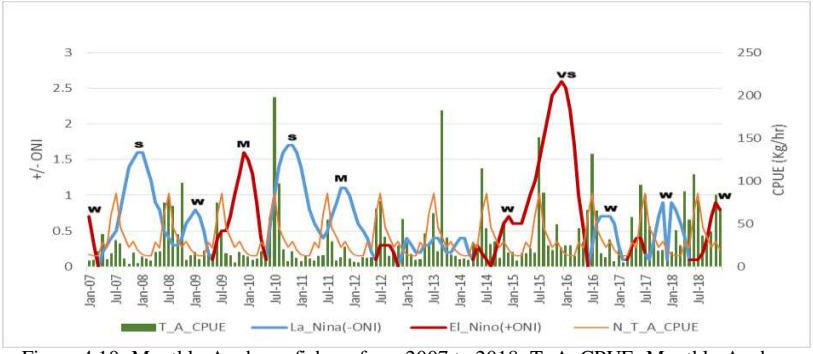

Figure 4.10: Monthly Anchovy fishery from 2007 to 2018; T_A_CPUE: Monthly Anchovy CPUE, N_T_A_CPUE: Month wise 12 year average Anchovy CPUE

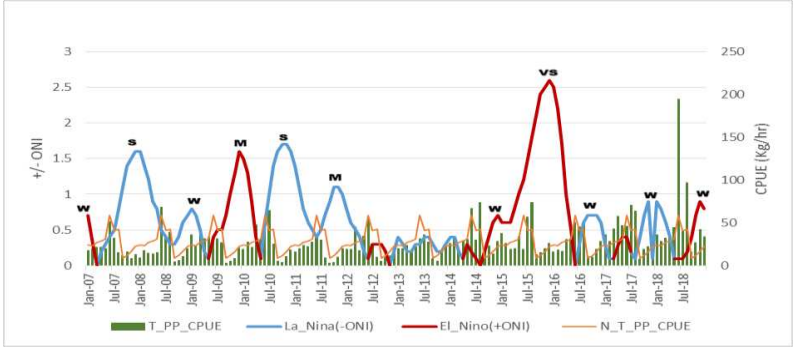

Figure 4.11: Monthly Penaeid prawn fishery from 2007 to 2018; T_PP_CPUE: Monthly Penaeid prawn CPUE, N_T_PP_CPUE: Month wise 12 year average Penaeid prawn CPUE

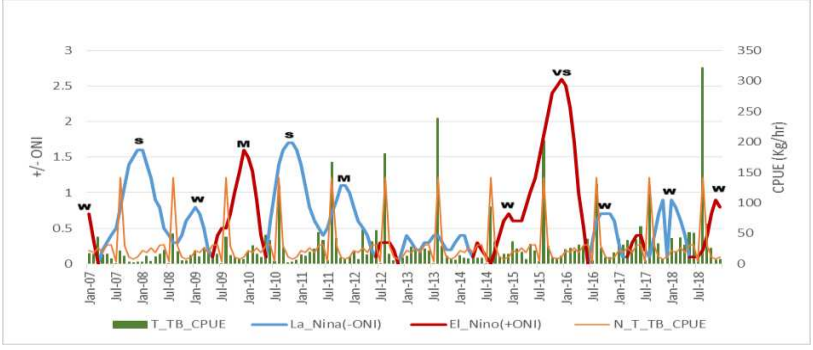

Figure 4.12: Monthly Threadfin breams fishery from 2007 to 2018; T_TB_CPUE: Monthly Threadfin breams CPUE, N_T_TB_CPUE: Month wise 12 year average Threadfin breams CPUE

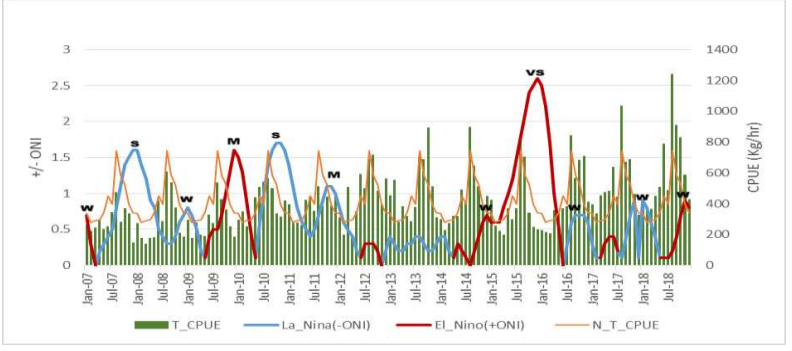

Figure 4.13: Monthly total fishery of Kerala from 2007 to 2018; T_ CPUE: Monthly total CPUE, N_T _CPUE: Month wise 12 year average total CPUE

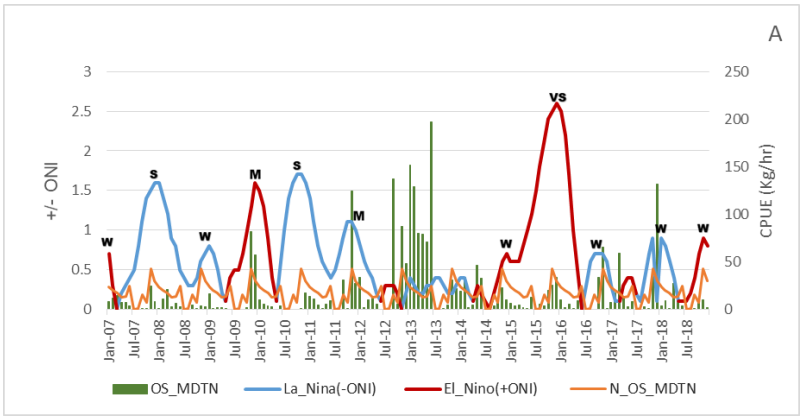
A
+/- ONI
CPUE (Kg/hr)
OS_MDTN
La_Nina(-ONI)
El_Nino(+ONI)
N_OS_MDTN

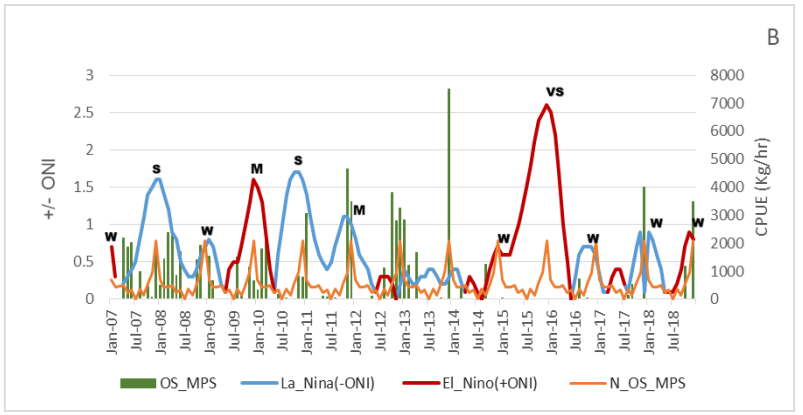
B
+/- ONI
CPUE (Kg/hr)
OS_MPS
La_Nina(-ONI)
El_Nino(+ONI)
N_OS_MPS

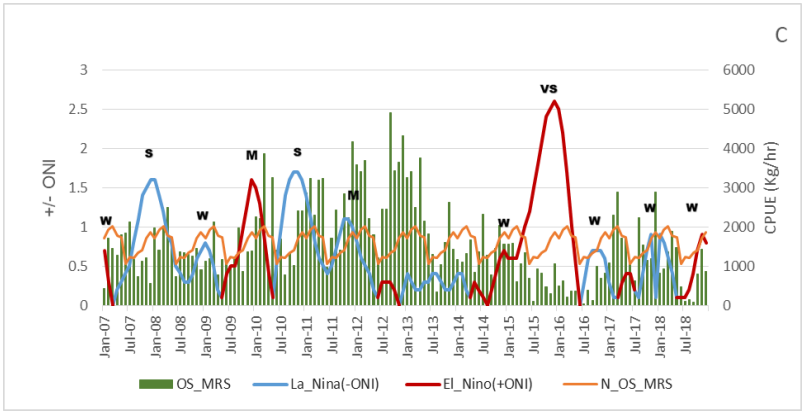
C
+/- ONI
CPUE (Kg/hr)
OS_MRS
La_Nina(-ONI)
El_Nino(+ONI)
N_OS_MRS

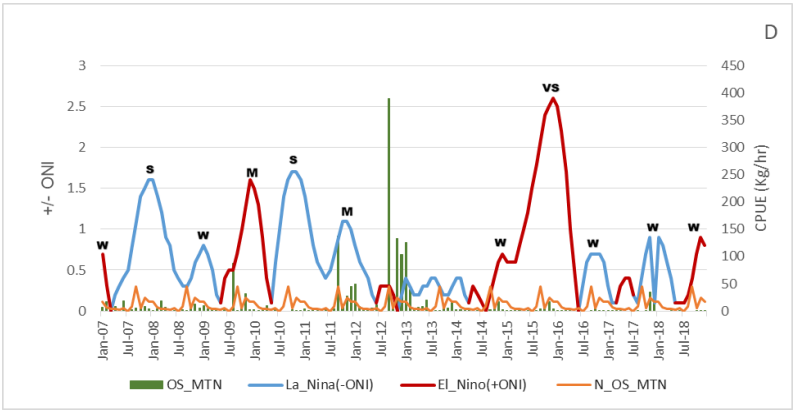
D
+/- ONI
CPUE (Kg/hr)
OS_MTN
La_Nina(-ONI)
El_Nino(+ONI)
N_OS_MTN

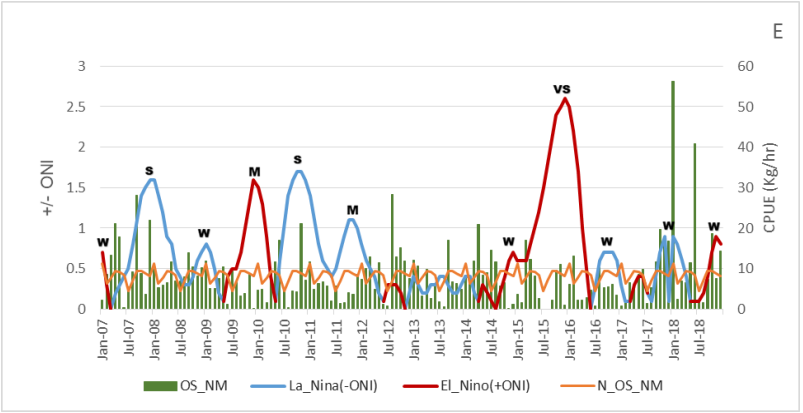
E
+/- ONI
CPUE (Kg/hr)
OS_NM
La_Nina(-ONI)
El_Nino(+ONI)
N_OS_NM

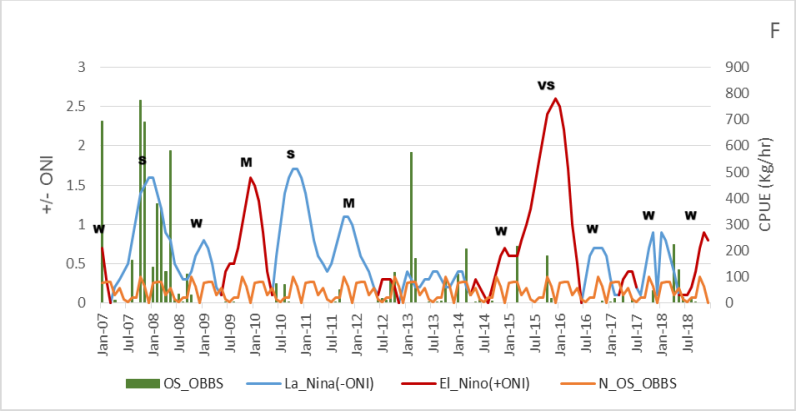
F
+/- ONI
CPUE (Kg/hr)
OS_OBBS
La_Nina(-ONI)
El_Nino(+ONI)
N_OS_OBBS

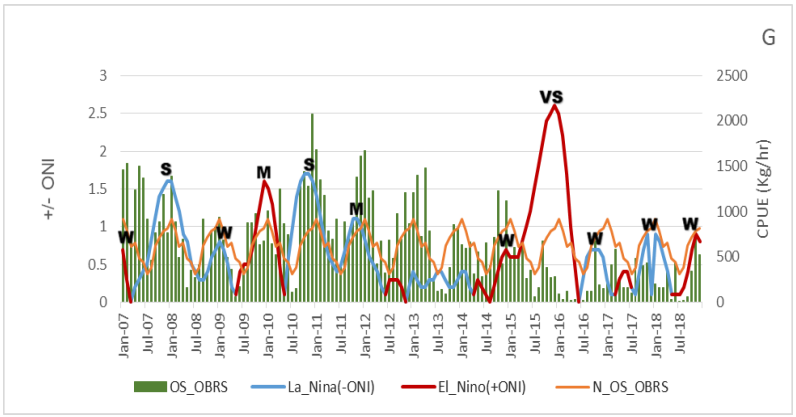

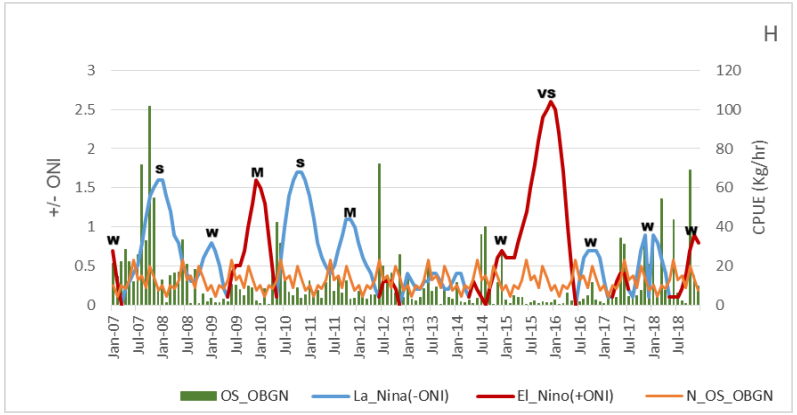

Figure 4.14: Monthly CPUE (Catch per unit effort) of Oil sardine for different crafts and gears from 2007-2018; A) MDTN, B) MPS, C) MRS, D) MTN, E) NM, F) OBBS, G) OBRS, H) OBGN

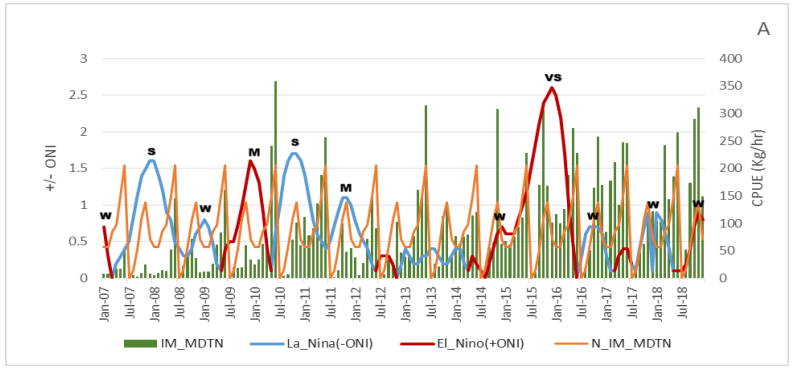

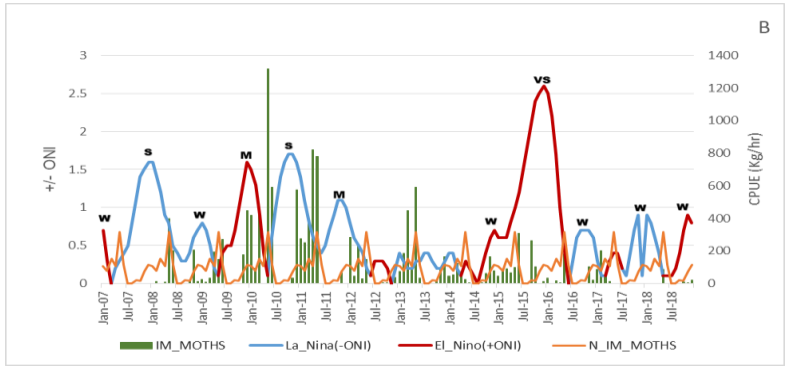

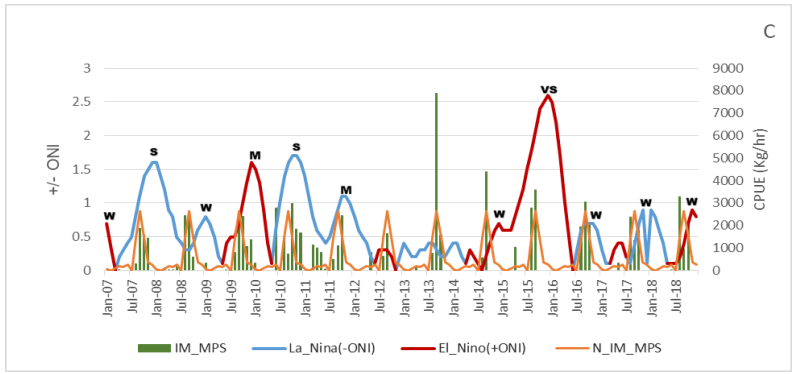

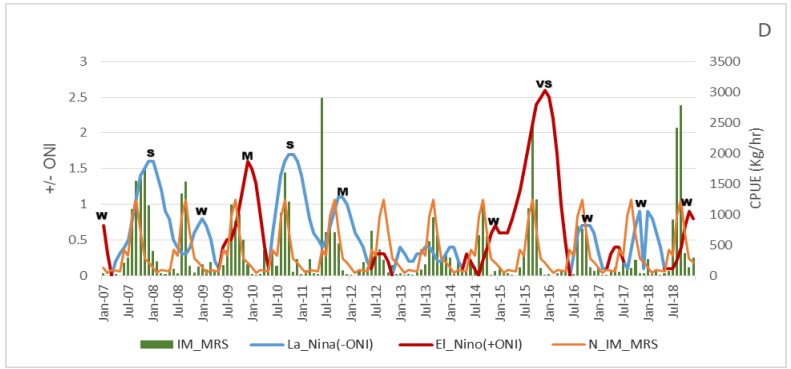

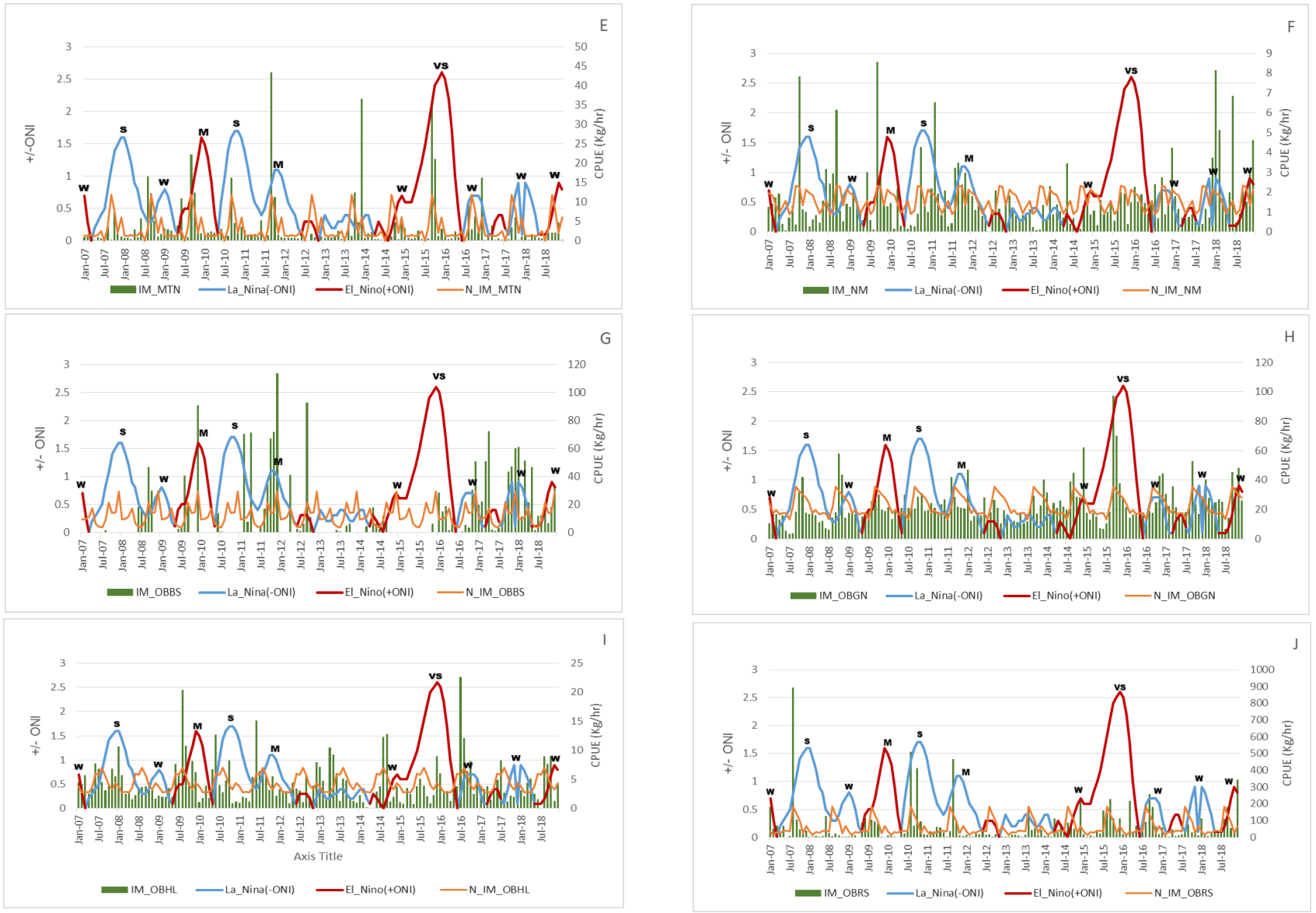

Figure 4.15: Monthly CPUE (Catch per unit effort) of Indian mackerel for different crafts and gears from 2007-2018; A) MDTN B) MOTHS, C) MPS, D) MTN, E) MRS, F) NM, G) OBBS, H) OBGN, I) OBHL, J)OBRS

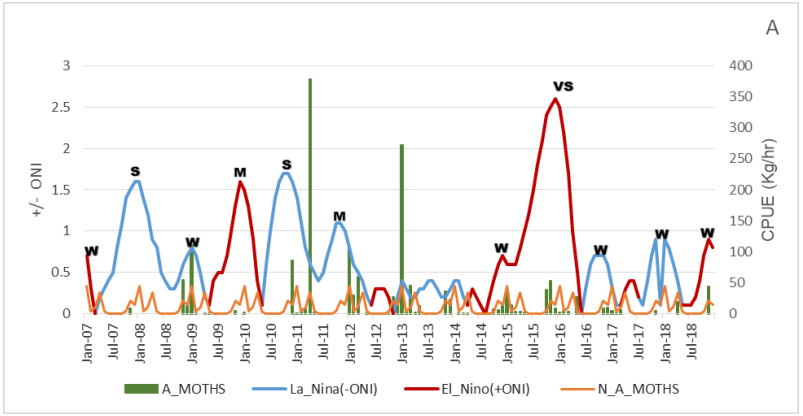
A
+/- ONI
CPUE (Kg/hr)
A_MOTHS
La_Nina(-ONI)
El_Nino(+ONI)
N_A_MOTHS

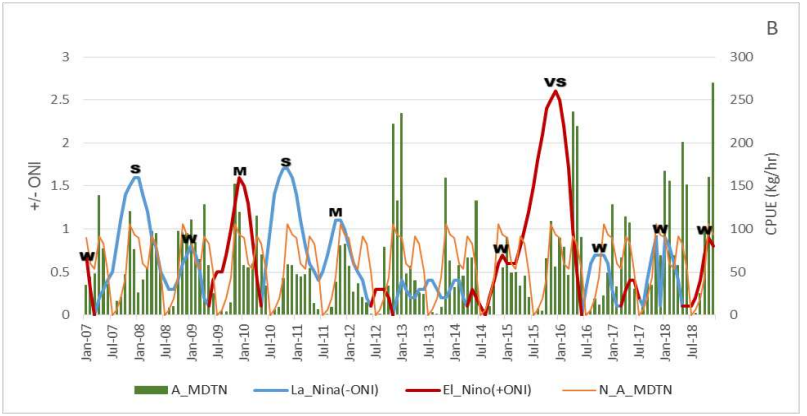
B
+/- ONI
CPUE (Kg/hr)
A_MDTN
La_Nina(-ONI)
El_Nino(+ONI)
N_A_MDTN

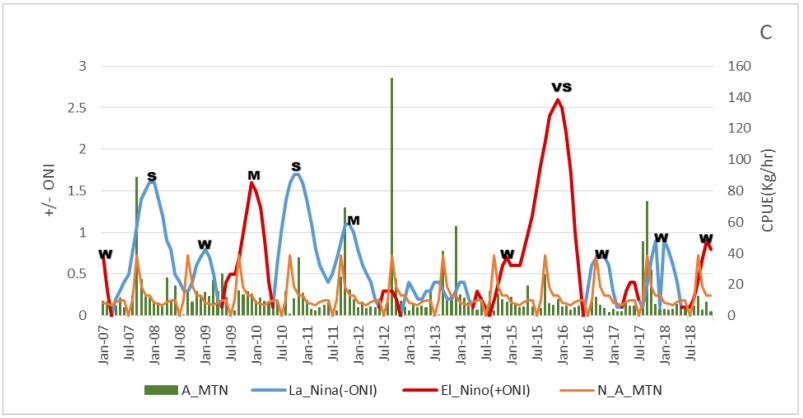
C
+/- ONI
CPUE(Kg/hr)
A_MTN
La_Nina(-ONI)
El_Nino(+ONI)
N_A_MTN

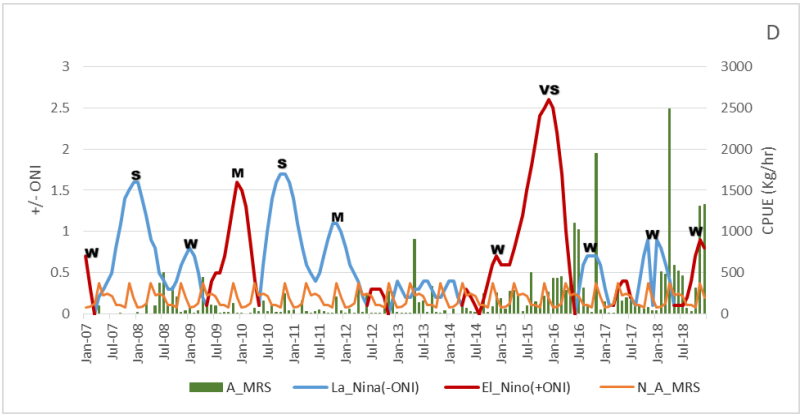
D
+/- ONI
CPUE (Kg/hr)
A_MRS
La_Nina(-ONI)
El_Nino(+ONI)
N_A_MRS

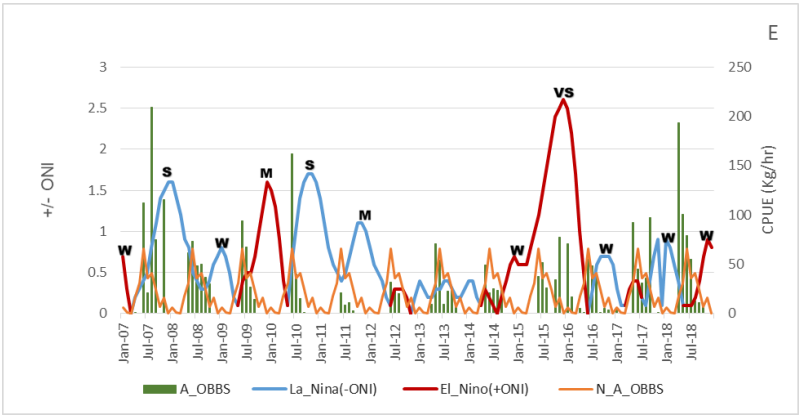
E
+/- ONI
CPUE (Kg/hr)
A_OBBS
La_Nina(-ONI)
El_Nino(+ONI)
N_A_OBBS

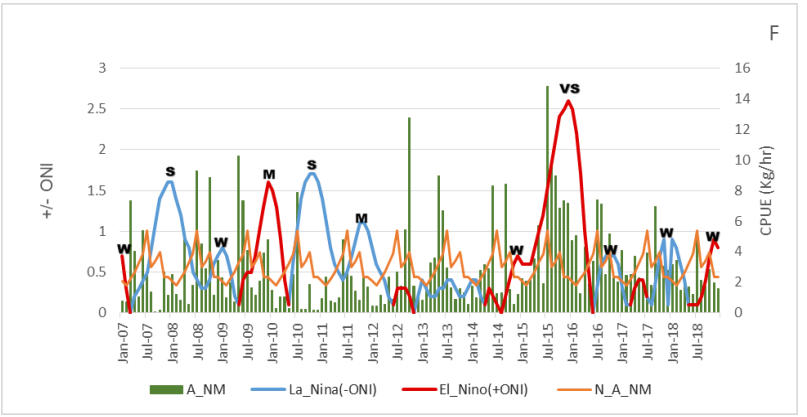
F
+/- ONI
CPUE (Kg/hr)
A_NM
La_Nina(-ONI)
El_Nino(+ONI)
N_A_NM

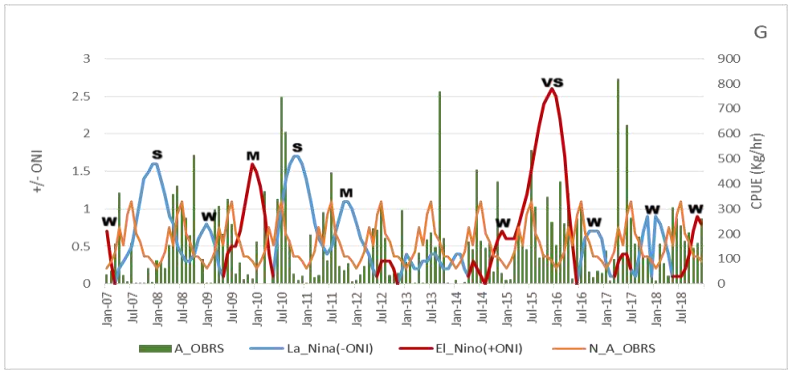

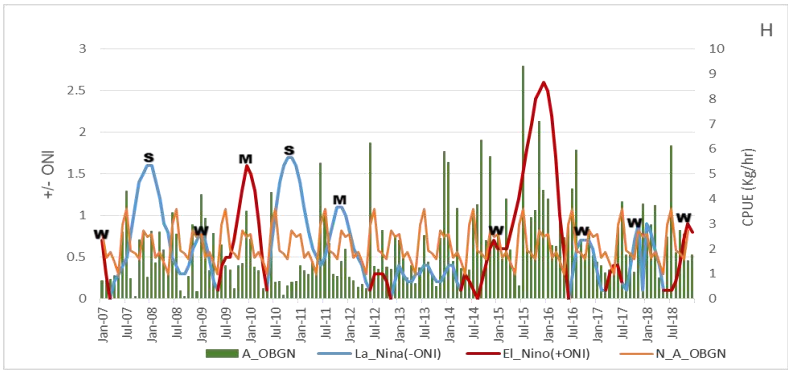

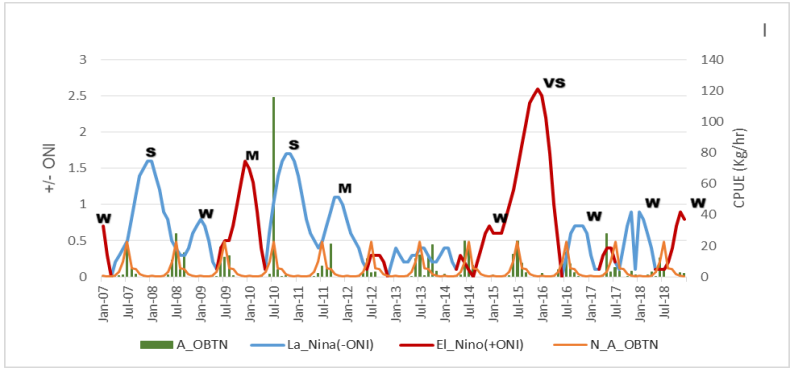

Figure 4.16: Monthly CPUE (Catch per unit effort) of Anchovy for different crafts and gears from 2007-2018; A) MDTN, B) MOTHS, C) MTN, D)MRS, E) OBRS, F) OBGN, G) NM, H) OBBS, I) OBTN

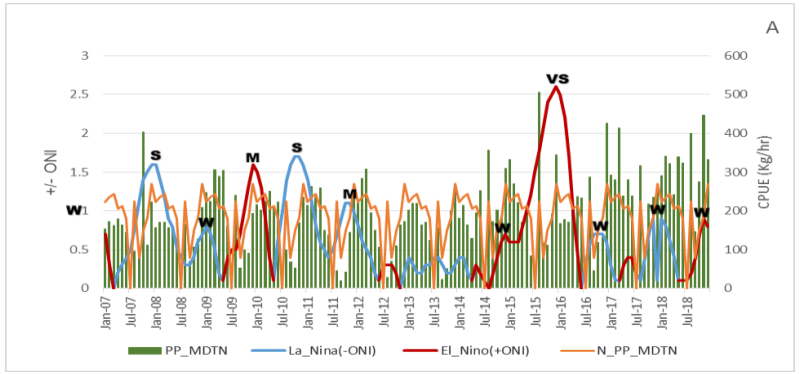

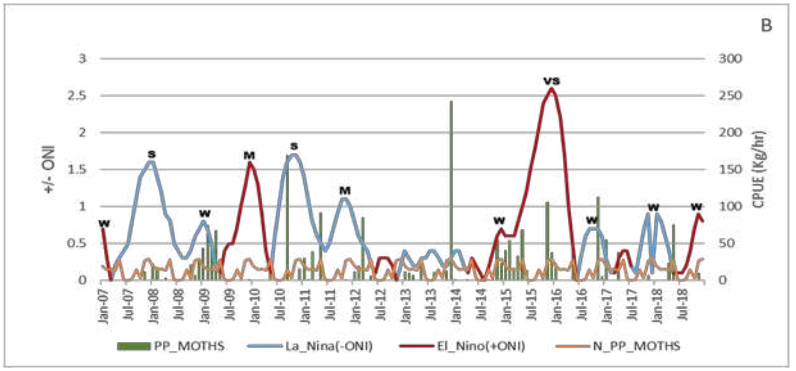

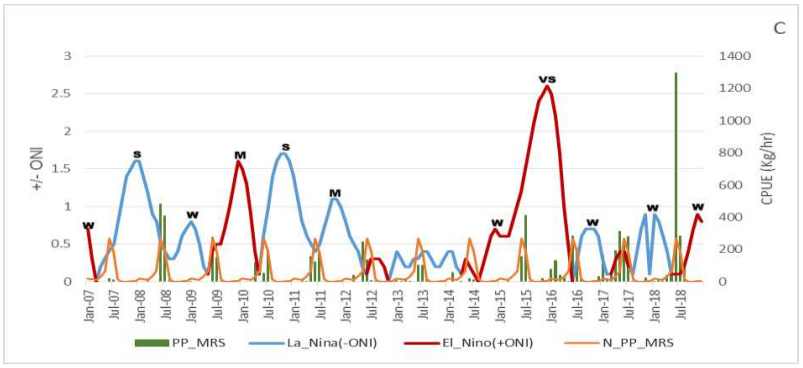
C
+/- ONI
CPUE (kg/hr)
PP_MRS
La_Nina(-ONI)
El_Nino(+ONI)
N_PP_MRS

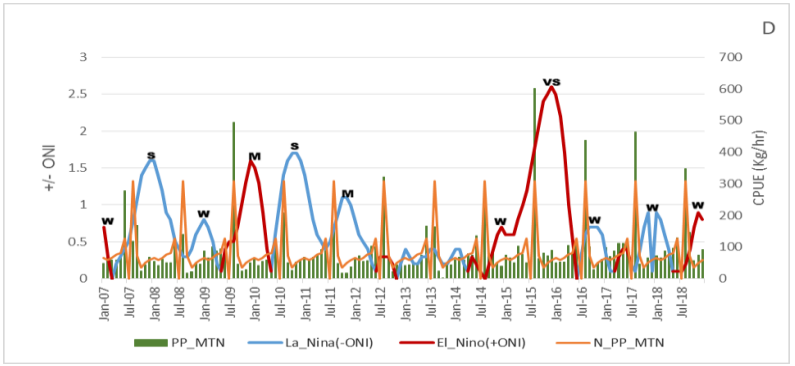
D
+/- ONI
CPUE (kg/hr)
PP_MTN
La_Nina(-ONI)
El_Nino(+ONI)
N_PP_MTN

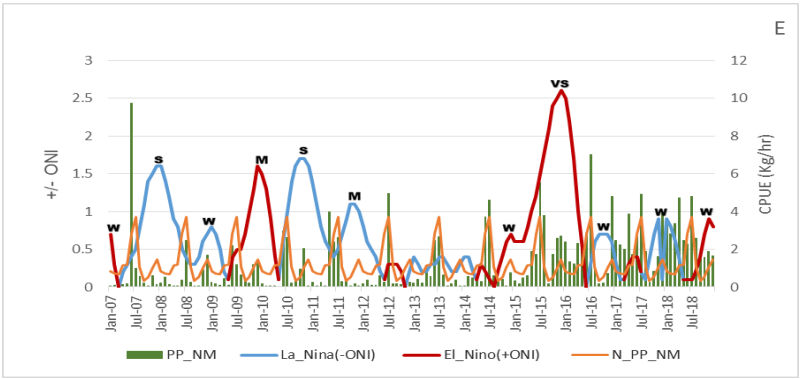
E
+/- ONI
CPUE (Kg/hr)
PP_NM
La_Nina(-ONI)
El_Nino(+ONI)
N_PP_NM

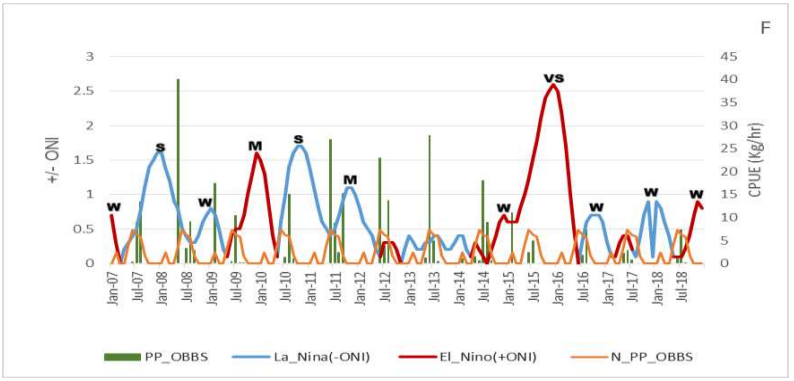
F
+/- ONI
CPUE (Kg/hr)
PP_OBBS
La_Nina(-ONI)
El_Nino(+ONI)
N_PP_OBBS

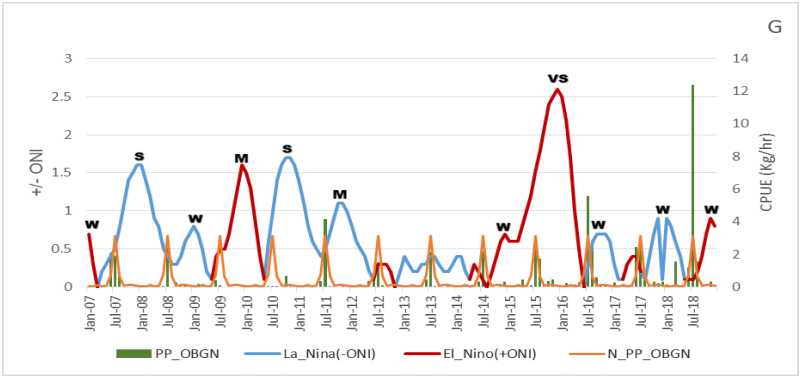
G
+/- ONI
CPUE (Kg/hr)
PP_OBGN
La_Nina(-ONI)
El_Nino(+ONI)
N_PP_OBGN

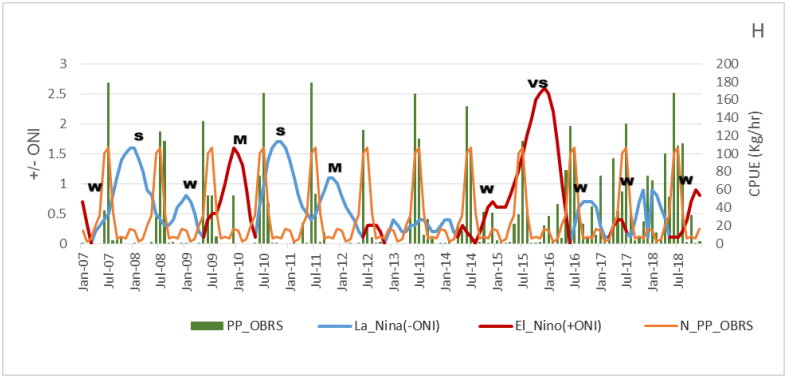
H
+/- ONI
CPUE (Kg/hr)
PP_OBRS
La_Nina(-ONI)
El_Nino(+ONI)
N_PP_OBRS

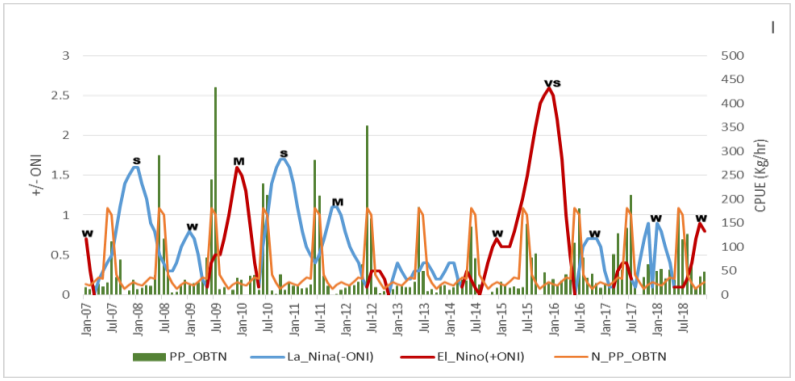

Figure 4.17: Monthly CPUE (Catch per unit effort) of Penaeid prawn for different crafts and gears from 2007-2018; A) MDTN, B) MOTHS, C) MRS, D) MTN, E) NM, F) OBBS, G) OBGN, H) OBRS I)OBTN

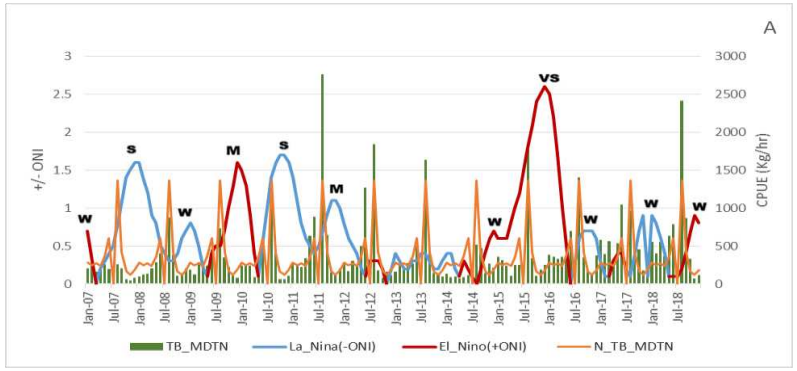

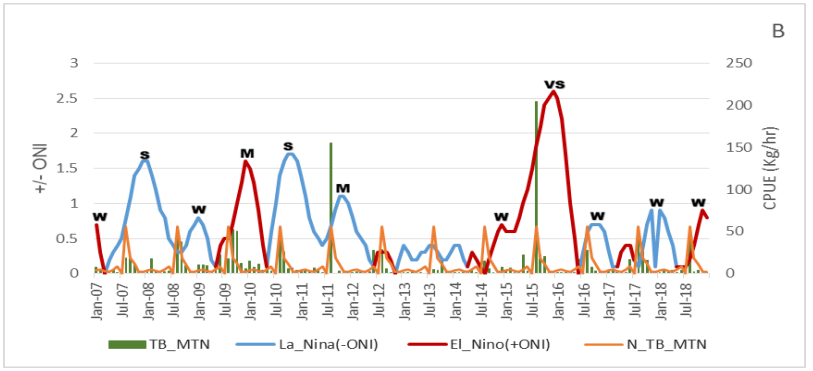

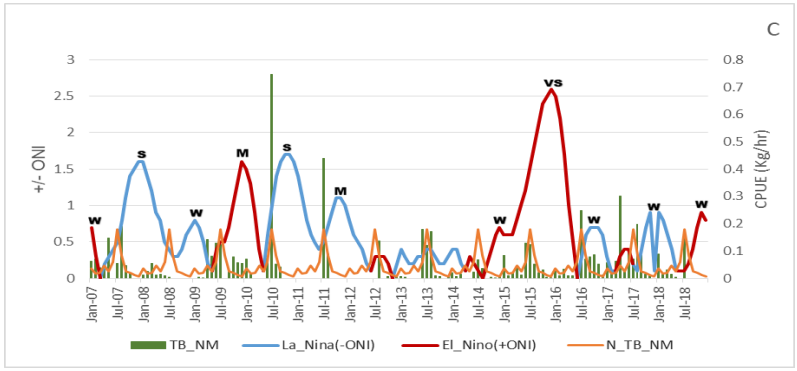

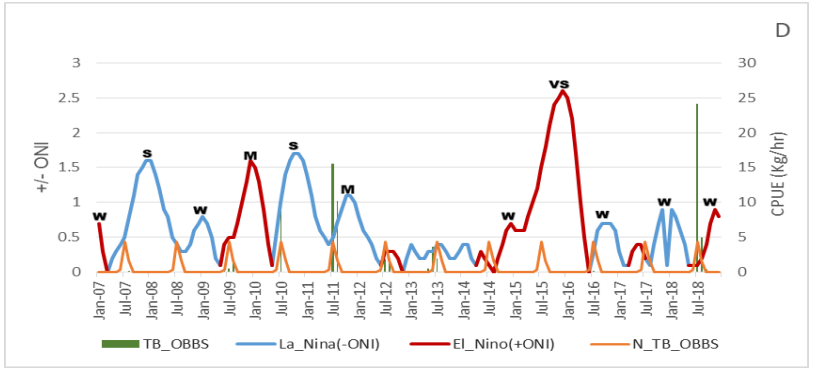

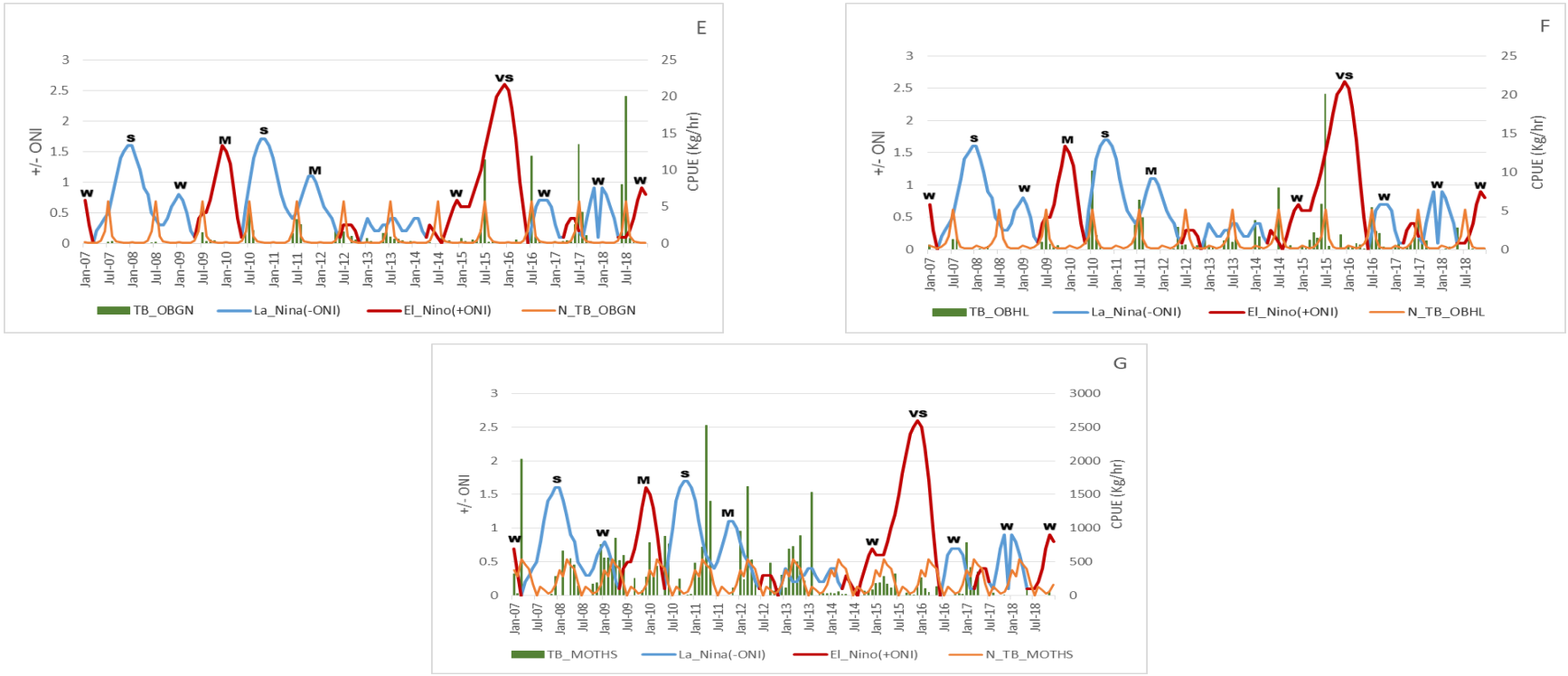

Figure 4.18: Monthly CPUE (Catch per unit effort) of Threadfin breams for different crafts and gears from 2007-2018; A) MDTN, B) MTN, C) NM, D) OBBS, E) OBGN, F) OBHL, G) MOTHS

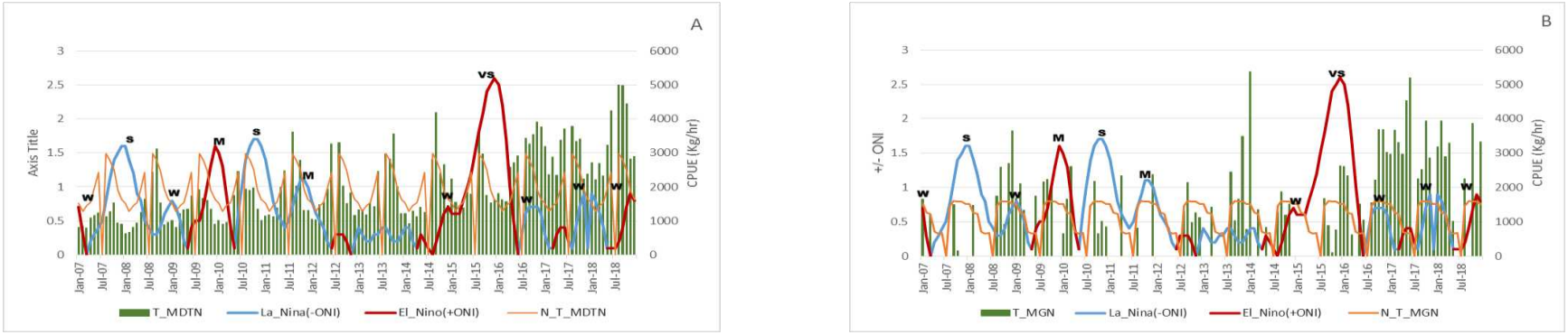

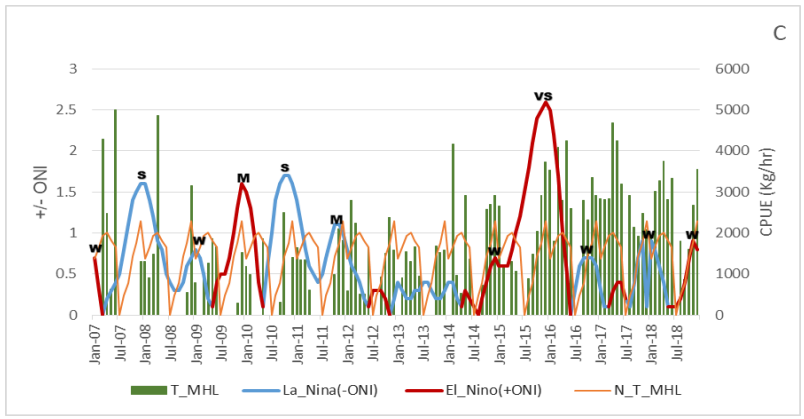
C
+/- ONI
CPUE (Kg/hr)
T_MHL
La_Nina(-ONI)
El_Nino(+ONI)
N_T_MHL

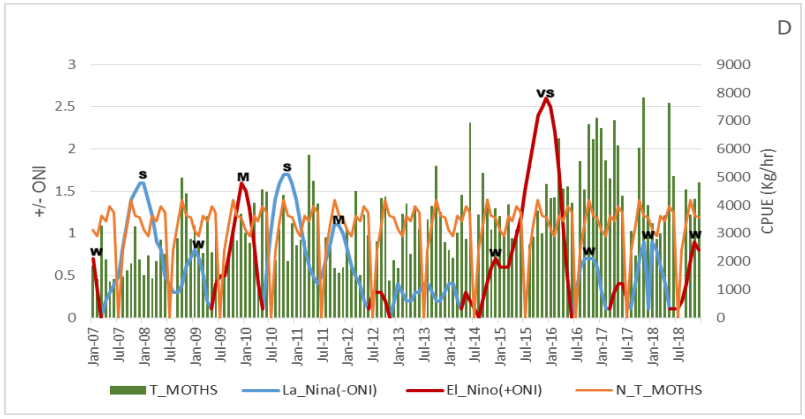
D
+/- ONI
CPUE (Kg/hr)
T_MOTHS
La_Nina(-ONI)
El_Nino(+ONI)
N_T_MOTHS

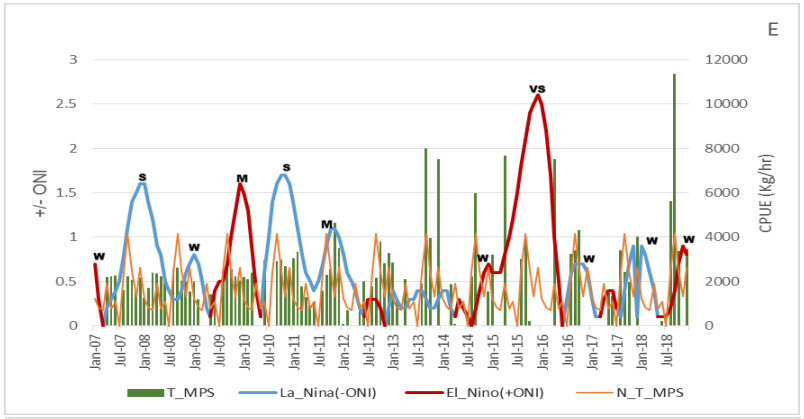
E
+/- ONI
CPUE (Kg/hr)
T_MPS
La_Nina(-ONI)
El_Nino(+ONI)
N_T_MPS

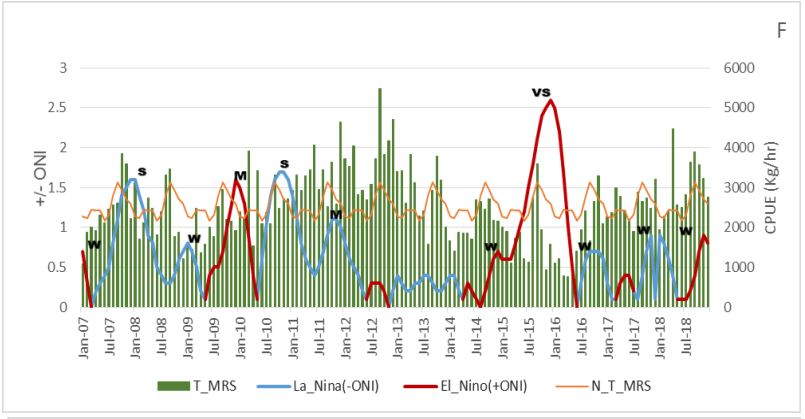
F
+/- ONI
CPUE (Kg/hr)
T_MRS
La_Nina(-ONI)
El_Nino(+ONI)
N_T_MRS

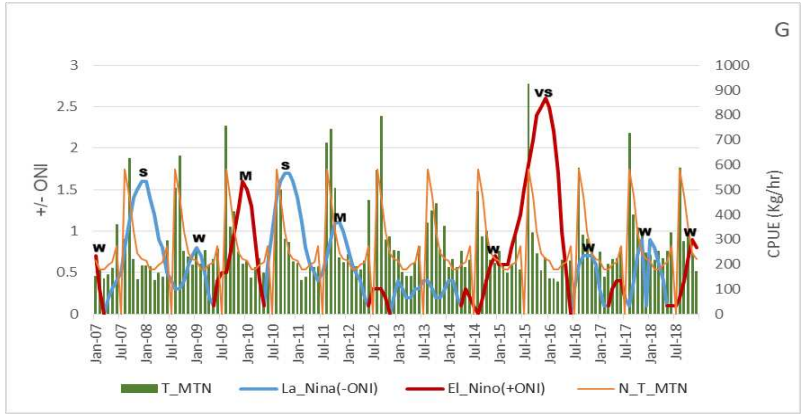
G
+/- ONI
CPUE (Kg/hr)
T_MTN
La_Nina(-ONI)
El_Nino(+ONI)
N_T_MTN

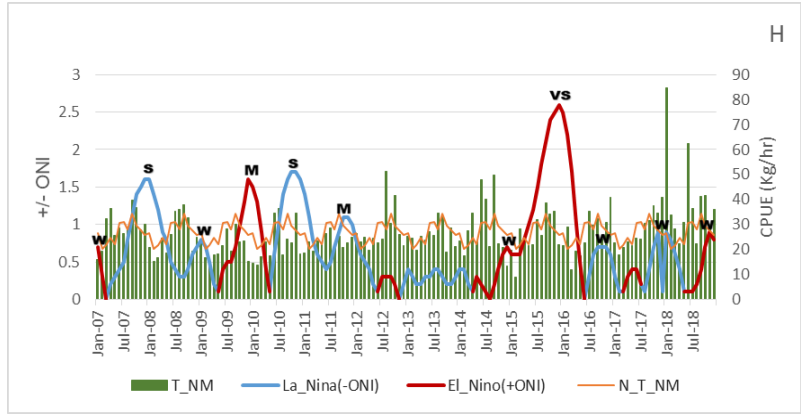
H
+/- ONI
CPUE (Kg/hr)
T_NM
La_Nina(-ONI)
El_Nino(+ONI)
N_T_NM

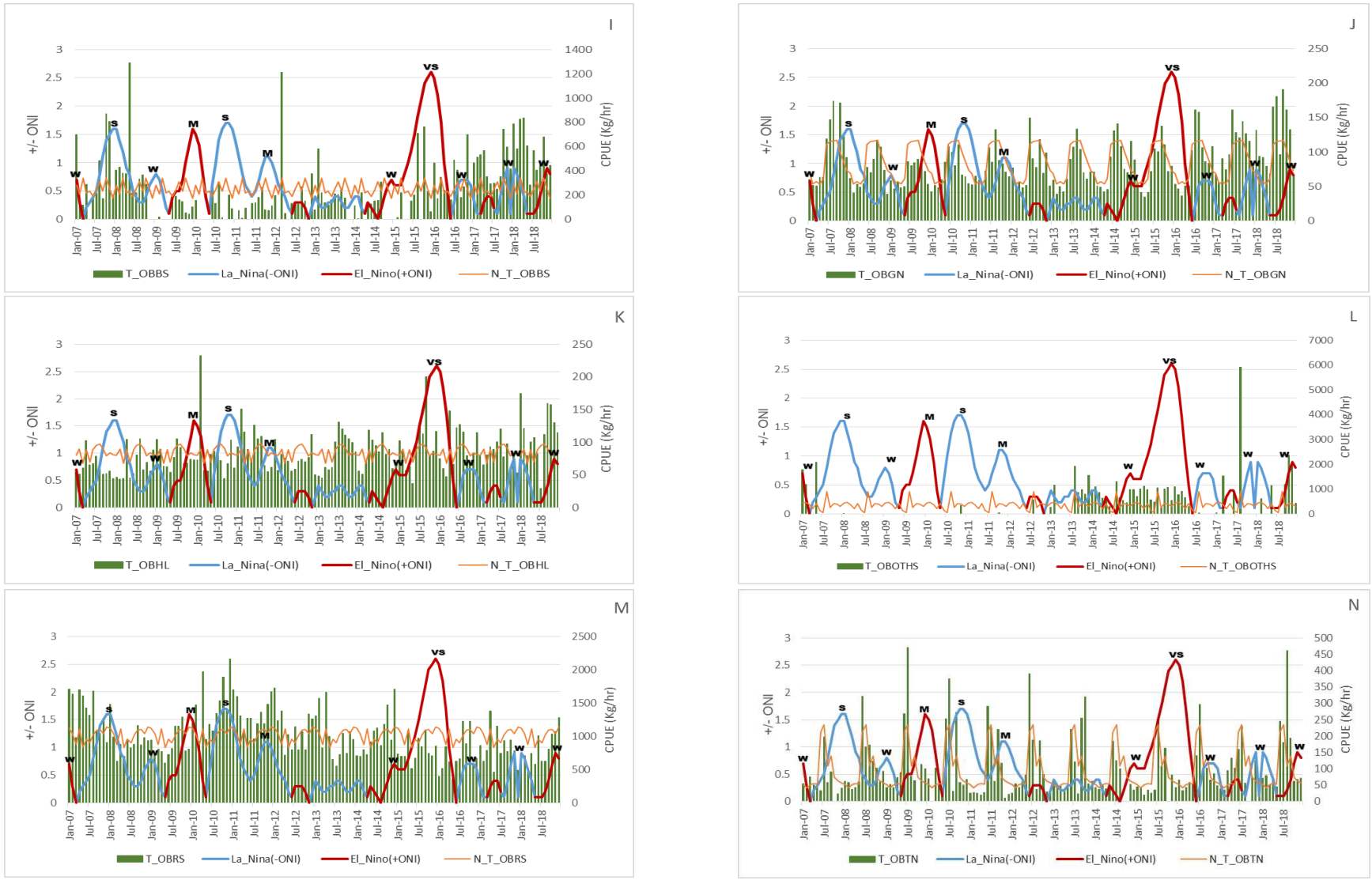

Figure 4.19: Monthly CPUE (Catch per unit effort) of Total fish resources for different crafts and gears from 2007-2018; A) MDTN B) MGN C) MHL, D) MOTHS, E) MPS, F) MRS, G)MTN, H)NM, I)OBBS, J) OBGN, K) OBHL, L) OBOTHS, M) OBRS, N) OBTN

4.2.7 Impacts of ENSO events on Oil Sardine

The GAM model, where CPUE of oil sardine was taken as response variable and DMI, EMI, MEI, SOI, TNI and Nino4 were considered as the predictors, returned an adjusted R^2 value of 0.25 and the percentage deviance explained was 31.4% (Table 4.9). The Nino 1+2 had no significant influence in the model and was removed from the final model. The curve for the partial effect of DMI (edf=1, $p<0.001$) had a positive effect (Figure 4.20E) and EMI (edf=1, $p<0.05$), TNI (edf-2.06, $p< 0.01$) and Nino4 (edf=1, $p<0.05$) had a decreasing effect (Figure 4.26[F, C, D]). The curve for the partial effect of MEI (edf=5.66, $p<0.1$) showed an increasing trend up to -2 and between -1 to 0, but showed a strong decreasing trend between 0 to 2 (Figure 4.20A). The curve for the partial effect of SOI (edf=2.57, $p<0.05$) suggest that the SOI had a negative effect on OS CPUE between -2 to 2 and a small positive effect above the value 2(Figure 4.20B).

The deviance explained and adjusted R^2 value for oil sardine CPUE model of different gears are given in the table 4.10. The gears contribute to total oil sardine landing of Kerala in the order of MRS> OBRS> OBGN> NM> MDTN> MTN> OBBS> MPS. The GAM model, where MDTN CPUE of Oil sardine landings was taken as response variable and, DMI, MEI, TNI, and Nino4 were considered as the predictors, returned an adjusted R^2 value of 0.09 and the percentage deviance explained was 14.9%. The Adjusted R^2 value of the GAM taking MPS CPUE of oil sardine landings as response variable was 0.11 and the percentage deviance explained was 17.2%. The GAM results revealed that DMI, MEI, TNI, and Nino 1+2 strongly influence the CPUE of MPS. The parameters such as EMI and SOI had no significant influence and were removed from the final model. The GAM model where MRS CPUE of oil sardine landings was taken as response variable and DMI, EMI, TNI, and Nino4 were considered as explanatory variables, returned an adjusted R^2 value of 0.24 and the percentage deviance explained was 31.3%. The GAM model where NM CPUE of oil sardine landings was taken as response variable and DMI, EMI, MEI, SOI, TNI and Nino 4 were taken as the predictors, returned an adjusted R^2 value of 0.26 and the percentage deviance explained was 38.9%.The adjusted R^2 value of the GAM model taking OBBS CPUE of oil sardine landings as response variable was 0.38 and the percentage deviance explained was 44.4%. The GAM results revealed that DMI, SOI, TNI, Nino 4, and Nino 1+2 had strong influence on the OBBS CPUE. The GAM model, where OBGN CPUE of oil sardine landings was taken as response variable and DMI, EMI, MEI and Nino1+2 were considered as the predictors, returned an adjusted R^2 value of 0.26 and the percentage deviance explained was 30%. The GAM model where OBRS CPUE of oil sardine landings was taken as response variable and DMI, MEI, TNI and Nino 4 were taken as predictors, returned an R^2 value of

0.48 and the percentage deviance explained was 55.9%. The GAM model were MTN CPUE of oil sardine was taken as response variable and DMI were taken as explanatory variable returned an adjusted R^2 value of 0.01, percentage deviance explained was 2.05%.

Table4.9: Details of deviance explained & adjusted R-square value for OS CPUE model and the effective degrees of freedom & significance of the explanatory variables of the model

T_OS_CPUE ~ s(DMI) + s(EMI) + s(MEI) + s(SOI) + s(TNI) + s(Nino4) R-sq.(adj) = 0.25 Deviance explained = 31.4%					
	edf	Ref.df	F	Deviance explained (%)	p-value
s(DMI)	1.000	1.000	13.413	2.49	0.000359 ***
s(EMI)	1.000	1.000	4.012	3.33	0.047228 *
s(MEI)	5.563	6.709	1.851	12.4	0.083337 .
s(SOI)	2.572	3.322	1.284	6.84	0.335045
s(TNI)	2.053	2.611	4.594	1.47	0.006430 **
s(Nino4)	1.000	1.000	6.548	9.49	0.011625 *

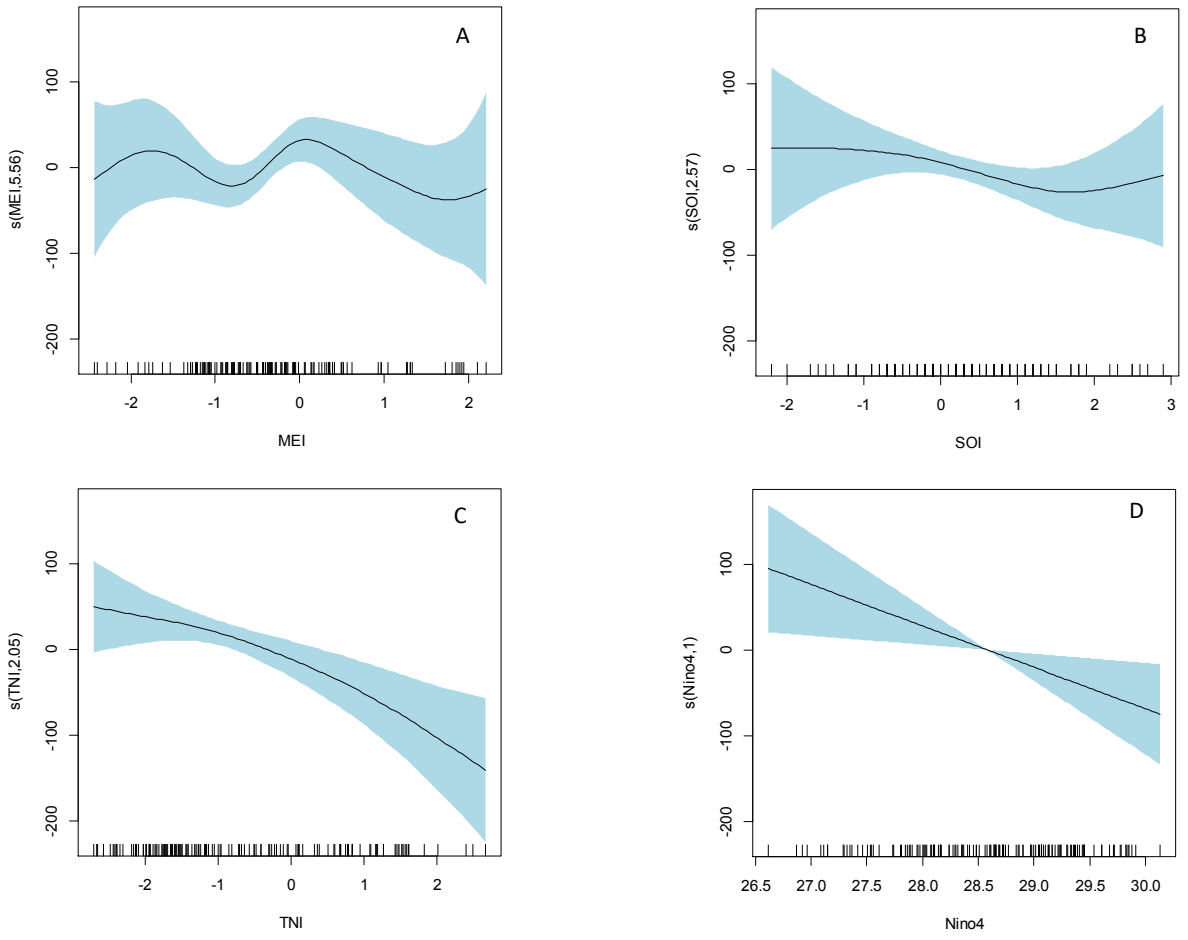

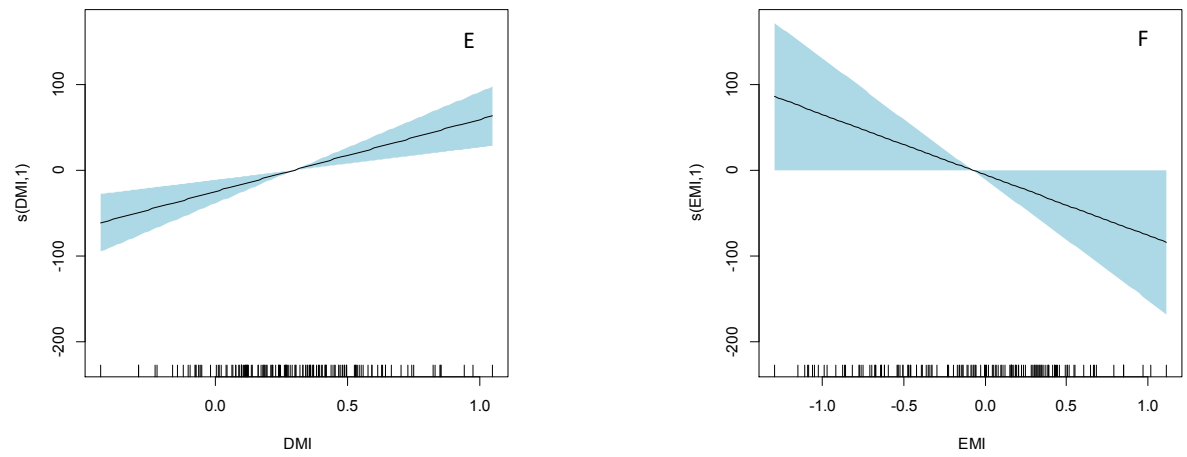

Figure 4.20: GAM model for OS CPUE showing effects of explanatory variables; MEI (A), SOI (B), TNI (C), Nino4 (D), DMI (E), and EMI (F)

Table 4.10: AIC, Adjusted R-square, and Deviance explained for the gear wise models of oil sardine

Model	AIC	R-sq. (adj)	Deviance explained (%)
OS_MDTN ~ s(DMI) + s(MEI) + s(TNI) + s(Nino4)	1410.681	0.09	14.9
OS_MPS ~ s(DMI) + s(MEI) + s(TNI) + s(Nino1.2)	2432.896	0.11	17.2
OS_MRS ~ s(DMI) + s(EMI) + s(TNI) + s(Nino4)	2372.474	0.24	31
OS_NM ~ s(DMI) + s(EMI) + s(MEI) + s(SOI) + s(TNI) + s(Nino4)	969.5457	0.26	38.9
OS_OBBS ~ s(DMI) + s(SOI) + s(TNI) + s(Nino4) + s(Nino1.2)	1765.597	0.38	44.4
OS_OBGN ~ s(DMI) + s(EMI) + s(MEI) + s(Nino1.2)	1176.271	0.26	30
OS_OBRS ~ s(DMI) + s(MEI) + s(TNI) + s(Nino4)	2097.203	0.48	55.9
OS_MTN ~ s(DMI)	1465.619	0.01	2.05

4.2.8 Impacts of ENSO events on Indian Mackerel

The adjusted R^2 value of GAM taking CPUE of Indian mackerel as response variable was 0.25 and the percentage deviance explained was 31.7%. The GAM model results revealed that DMI, EMI, MEI, SOI, Nino 4 and Nino 1+2 had strong influence on CPUE of Indian mackerel. The TNI had no effect on the CPUE of Indian mackerel and was removed from the final model (Table 4.11). The curve for the partial effect of DMI (edf=1, $p<0.05$) and Nino4 (edf=1, $p<0.001$) showed a positive effect and the curve for the partial effect of EMI (edf=1, $p<0.001$), SOI (edf=1, $p<1$), and Nino1+2 (edf=1, $p<0.01$) showed a negative effect on Indian mackerel CPUE (Figure 4.21[A, E, B, D, F]). The edf was high for MEI (edf=7.73, $p<0.01$) and the curve was complex. The curve for the partial effect of MEI showed a decreasing trend from 0.5 to 1.5 and a further increase in the value suggest a very strong increasing trend (Figure4.21C).

The deviance explained and adjusted R^2 value for Indian mackerel CPUE model of different gears are given in the table 4.12. The GAM model, where MDTN CPUE of Indian mackerel was taken as response variable and, DMI, MEI, TNI and Nino4 were considered as the predictors, returned an adjusted R^2 value of 0.19 and the percentage deviance explained was 25.3%. The adjusted R^2 value of the GAM taking MOTHS CPUE of Indian mackerel as response variable was 0.18 and the percentage deviance explained was 25.7%. The GAM results revealed that MEI, Nino 1+2, DMI and EMI strongly influence the CPUE of MOTHS. The parameters such as SOI, TNI and Nino4 have no effect on the CPUE of MOTHS and were removed from the final model. The GAM model where MPS CPUE of Indian mackerel was taken as response variable and DMI, EMI, SOI, Nino 4, and Nino 1+2 were considered as predictors returned an adjusted R^2 value of 0.18 and the percentage deviance explained was 22.9%. The GAM model where the MRS CPUE of Indian mackerel was taken as response variable and DMI, EMI, MEI, SOI, Nino4 and Nino 1+2 were considered as explanatory variables returned an adjusted R^2 value of 0.27 and the percentage deviance explained was 35.4%. TNI had no influence in the MRS model and was discarded from the final model. The GAM model where MTN CPUE of Indian mackerel was taken as response variable and Nino 1+2 as explanatory variable, returned an adjusted R^2 value of 0.10 and the deviance explained was 14.7%. Adjusted R^2 value of the GAM taking NM CPUE of Indian mackerel as response variable was 0.12 and the percentage deviance explained was 16.2%. The GAM model where OBBS CPUE of Indian mackerel was taken as response variable and DMI, MEI, SOI, and Nino 4 were considered as explanatory variables, returned an adjusted R^2 value of 0.15 and the percentage deviance explained was22.7%. The GAM model where the OBGN CPUE of Indian mackerel was taken as response variable and MEI, TNI, and Nino 1+2 were considered

as predictors, returned an adjusted R^2 value of 0.37 and the percentage deviance explained was 46.3%. The parameters such as DMI, EMI, SOI, and Nino 4 had no significant influence in the OBGN model and were removed from the final model. The adjusted R^2 value of the GAM taking OBHL CPUE as response variable was 0.31 and the percentage deviance explained was 41.1%. The GAM results revealed that DMI, EMI, MEI, SOI, Nino4 and Nino 1+2 influence the CPUE of OBHL. The TNI had no effect on the CPUE of OBHL and was removed from the final model.

Table4.11: Details of deviance explained & adjusted R-square value for IM CPUE model and the effective degrees of freedom & significance of the explanatory variables of the model

T_IM_CPUE ~ s(DMI) + s(EMI) + s(MEI) + s(SOI) + s(Nino4) + s(Nino1.2) R-sq.(adj) = 0.25 Deviance explained = 31.7%					
	edf	Ref.df	F	Deviance explained (%)	p-value
s(DMI)	1.000	1.000	4.166	7.57	0.043214 *
s(EMI)	1.000	1.000	12.670	1.97	0.000515 ***
s(MEI)	7.734	8.591	3.176 0	21.3	.002124 **
s(SOI)	1.000	1.000	2.482	2.38	0.117535
s(Nino4)	1.000	1.000	12.651	3.7	0.000519 ***
s(Nino1.2)	1.000	1.000	9.091	10.8	0.003075 **

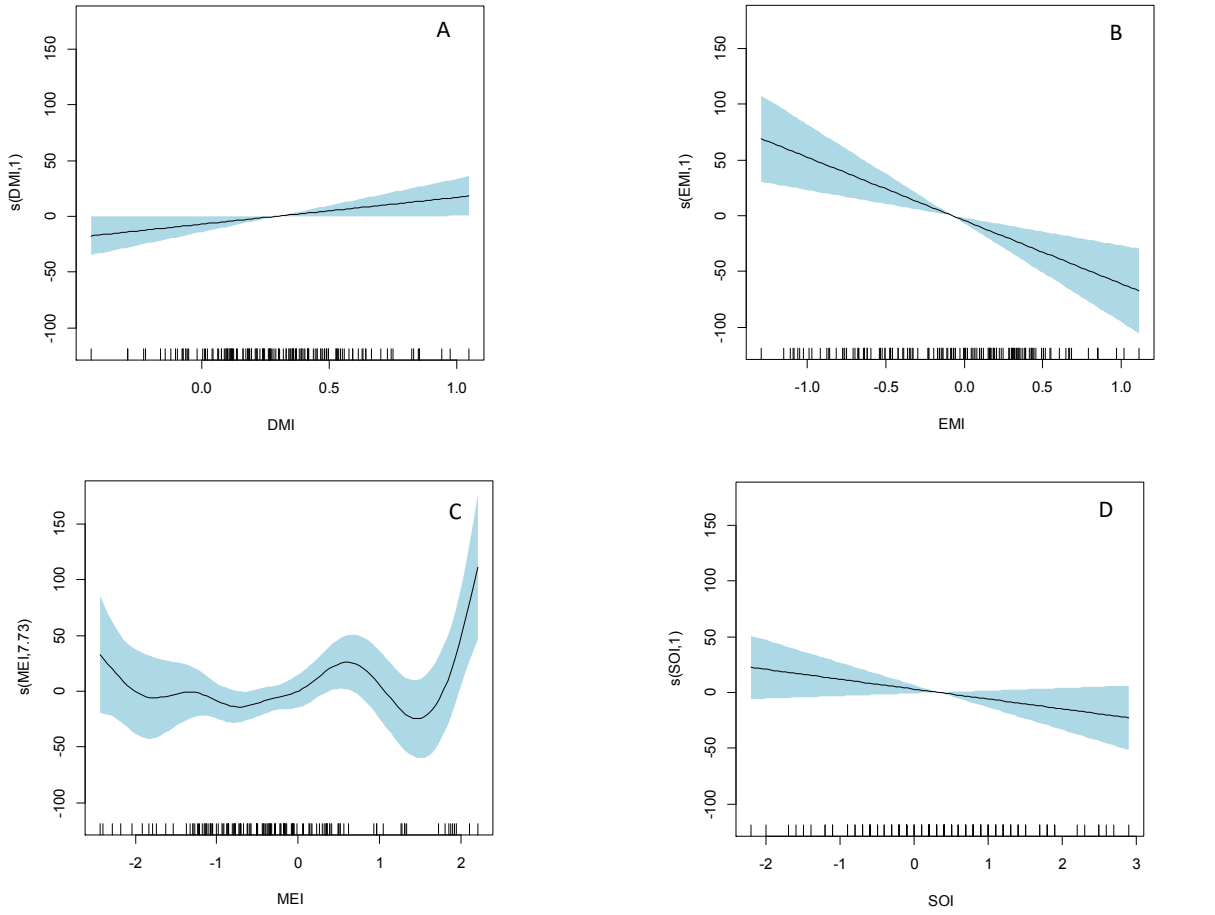

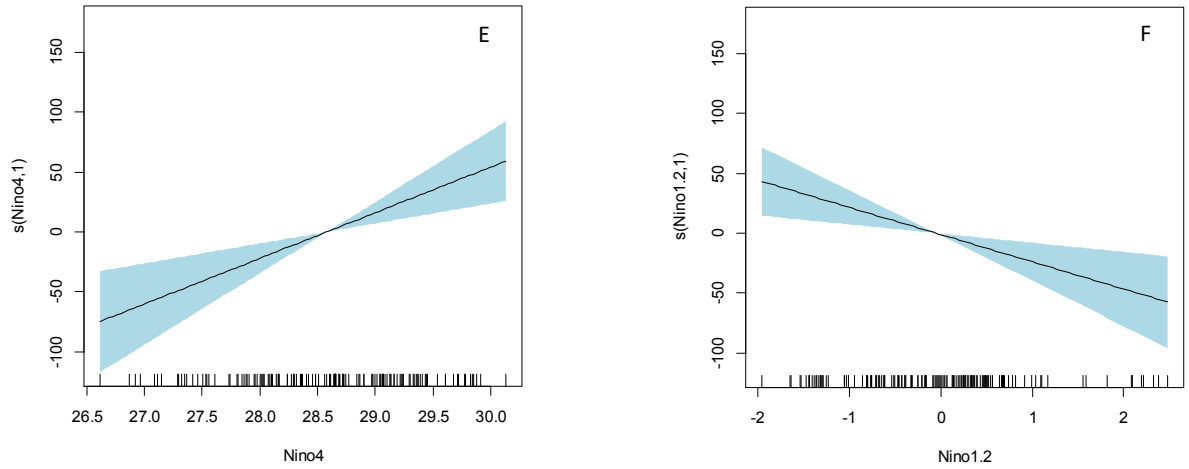

Figure 4.21: GAM model for IM CPUE showing effects of explanatory variables; DMI (A), EMI (B), MEI (C), SOI (D), Nino4 (E), and Nino 1+2 (F)

Table 4.12: AIC, Adjusted R-square, and Deviance explained for the gear wise models of Indian Mackerel

Model	AIC	R-sq. (adj)	Deviance explained (%)
IM_MDTN ~ s(DMI) + s(MEI) + s(TNI) + s(Nino4)	1671.468	0.19	25.3
IM_MOTHS ~ s(DMI) + s(EMI) + s(MEI) + s(Nino1.2)	1900.899	0.18	25.7
IM_MPS ~ s(DMI) + s(EMI) + s(SOI) + s(Nino4) + s(Nino1.2)	2469.315	0.18	22.9
IM_MRS ~ s(DMI) + s(EMI) + s(MEI) + s(SOI) + s(Nino4) + s(Nino1.2)	2205.241	0.27	35.4
IM_MTN ~ s(Nino1.2)	940.9903	0.10	14.7
IM_NM ~ s(Nino4)	528.512	0.12	16.2
IM_OBBS ~ s(DMI) + s(MEI) + s(SOI) + s(Nino4)	1293.262	0.15	22.7
IM_OBGN ~ s(MEI) + s(TNI) + s(Nino1.2)	1103.037	0.37	46.3
IM_OBHL ~ s(DMI) + s(EMI) + s(MEI) + s(SOI) + s(Nino4) + s(Nino1.2)	744.5341	0.31	41.1

4.2.9 Impacts of ENSO events on Anchovy

The GAM model, where CPUE of anchovy was taken as response variable and DMI, EMI, MEI, TNI, Nino1+2 and Nino4 were considered as the predictors, returned an adjusted R^2 value of 0.39 and the percentage deviance explained was 49% (Table 4.13). The SOI had no significant influence in the model and were removed from the final model. The MEI (edf=8.31, $p<0.001$) and Nino1+2 (edf=7.44, $p<0.1$) had high edf values meaning that the curves were complex and wiggly which could be seen from the plots. At around a MEI value of -2, the CPUE value was at the highest point, MEI had negative effect on anchovy CPUE except for the range between -1.5 to -1 and 1 to 1.5 (Figure 4.22C). The curve for the partial effect of Nino 1+2 had strong positive effect from the value 1.5, for other value ranges, it showed weak positive and negative effects (Figure 4.22F). The curve for the partial effects of Nino4 (edf=1, $p<0.001$) had positive effect and TNI (edf=1.81, $p<1$) and EMI (edf=1.46, $p<0.05$) had negative effect on CPUE of anchovy (Figure 4.22 [E, D, B]). The curve for the partial effect of DMI (edf=3.85, 1) had decreasing trend up to 0 and a further increase in the value showed a very slight increasing trend (figure 4.35A).

The deviance explained and adjusted R^2 value for anchovy CPUE model of different gears are given in the table 4.14. The GAM model where MDTN CPUE of anchovy was taken as response variable and, DMI, EMI, MEI, SOI, TNI and Nino1+2 were considered as the predictors , returned an adjusted R^2 value of 0.13 and percentage deviance explained was 17.5%. The GAM model where MOTHS CPUE of anchovy was considered as response variable and SOI were considered as predictor variable, returned an adjusted R^2 value of 0.01, the percentage deviance explained was 1.94%. All other parameters such as DMI, EMI, MEI, and TNI, Nino 4 and Nino 1 + 2 had no significant influence in the MOTHS model, discarded from the final model. The adjusted R^2 value of the GAM taking MRS CPUE of anchovy as response variable was 0.53 and the percentage deviance explained was 60.1%. The GAM results revealed that MEI, SOI, TNI, Nino4 and Nino 1+2 strongly influence the CPUE of MRS. The GAM model where MTN CPUE of anchovy was taken as response variable and DMI and Nino1+2 were considered as the predictors, returned an adjusted R^2 of 0.02 and the percentage deviance explained was 4.01%. The GAM model where NM CPUE of anchovy was taken as response variable and MEI, TNI, and Nino4 were considered as the predictors, returned an adjusted R^2 of 0.02 and the percentage deviance explained was 4.12%. The GAM model where OBBS CPUE of anchovy was taken as response variable and EMI, MEI, SOI, TNI, Nino4 and Nino 1+2 were considered as the predictors, returned an adjusted R^2 of 0.33 and the percentage deviance explained was 41.8%. The adjusted R^2 value of GAM taking OBGN CPUE of anchovy as response variable returned an adjusted

R^2 of 0.22 and the percentage deviance explained was 31.4%. The GAM results revealed that MEI, SOI, TNI, and Nino 1+2 strongly influence the CPUE of OBGN. The parameters such as DMI, Nino4 and EMI had no effect on the CPUE of OBGN and were removed from the final model. The GAM model where OBRS CPUE of anchovy was taken as response variable and DMI, MEI, TNI, and Nino4 were considered as the predictors, returned an adjusted R^2 of 0.36 and the percentage deviance explained was 43.8%. The parameters such as EMI, SOI, and Nino 1+2 had no significant influence in the OBRS model and were removed from the final model. The GAM model where OBTN CPUE of anchovy was taken as response variable and EMI, MEI, TNI, and Nino4 were considered as the predictors, returned an adjusted R^2 of 0.38 and the percentage deviance explained was 45.6%. The parameters such as DMI, SOI and Nino 1+2 had no significant influence in the model and discarded from the final model.

Table4.13: Details of deviance explained & adjusted R-square value for Anchovy CPUE model and the effective degrees of freedom & significance of the explanatory variables of the model

T_A_CPUE ~ s(DMI) + s(EMI) + s(MEI) + s(TNI) + s(Nino4) + s(Nino1.2) R-sq.(adj) = 0.39 Deviance explained = 49.4%					
	edf	Ref.df	F	Deviance explained (%)	p-value
s(DMI)	3.648	4.570	1.390	6.62	0.268928
s(EMI)	1.464	1.791	4.406	6.37	0.049131 *
s(MEI)	8.308	8.842	4.753	17.3	2.36e-05 ***
s(TNI)	1.812	2.286	0.751	5.4	0.422729
s(Nino4)	1.000	1.000	13.390	5.61	0.000374 ***
s(Nino1.2)	7.441	8.369	1.742	4.85	0.075247 .

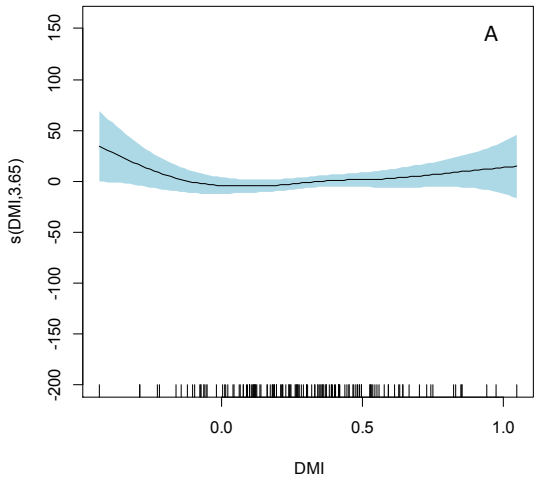

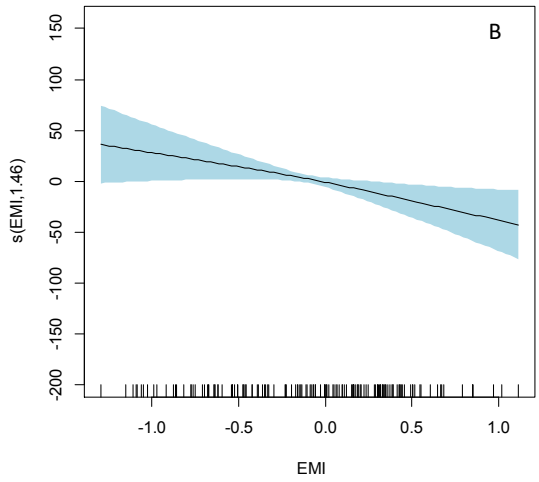

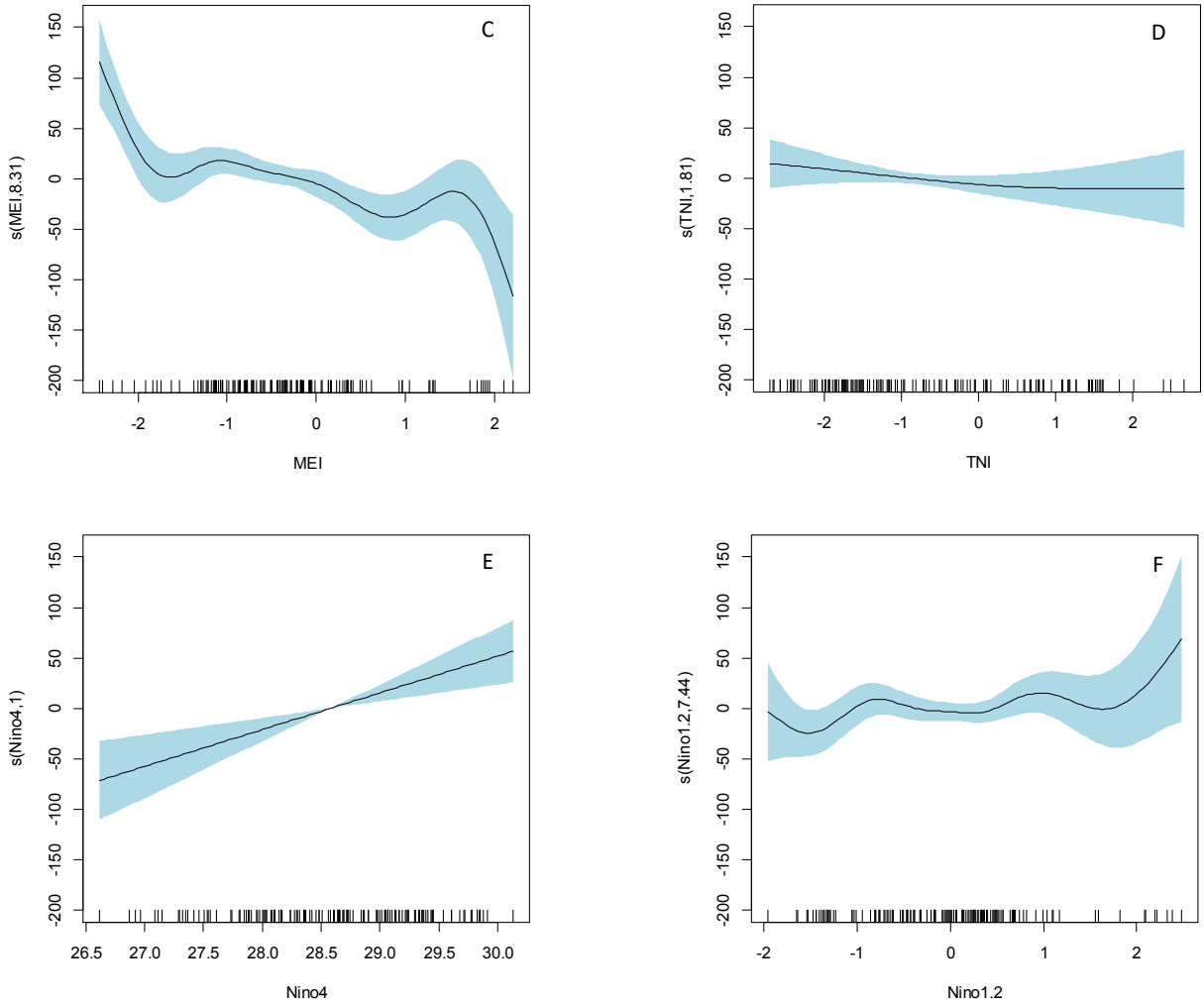

Figure 4.22: GAM model for Anchovy CPUE showing effects of explanatory variables; DMI (A), EMI (B), MEI (C), TNI (D), Nino4 (E), and Nino 1+2 (F)

Table 4.14: AIC, Adjusted R-square, and Deviance explained for the gear wise models of Anchovy

Model	AIC	R-sq. (adj)	Deviance explained (%)
A_MDTN ~ s(DMI) + s(EMI) + s(MEI) + s(SOI) + s(TNI) + s(Nino1.2)	1556.225	0.13	17.5
A_MOTHS ~ s(SOI)	1487.08	0.01	1.94
A_MRS ~ s(MEI) + s(SOI) + s(TNI) + s(Nino4) + s(Nino1.2)	2322.435	0.53	60.1
A_MTN ~ s(DMI) + s(Nino1.2)	1484.912	0.03	4.01
A_NM ~ s(MEI) + s(TNI) + s(Nino4)	1183.667	0.02	4.12
A_OBBS ~ s(EMI) + s(MEI) + s(SOI) + s(TNI) + s(Nino4) + s(Nino1.2)	1561.875	0.32	41.8
A_OBGN ~ s(MEI) + s(SOI) + s(TNI) + s(Nino1.2)	525.9746	0.22	31.4
A_OBRS ~ s(DMI) + s(MEI) + s(TNI) + s(Nino4)	1833.36	0.36	43.8
A_OBTN ~ s(EMI) + s(MEI) + s(TNI) + s(Nino4)	1056.886	0.38	45.6

4.2.10 Impacts of ENSO events on Penaeid prawns

The GAM model, where CPUE of penaeid prawn was taken as response variable and EMI, MEI, TNI, and Nino4 were considered as the predictors, returned an adjusted R^2 value of 0.14 and the percentage deviance explained was 19% (Table 4.15). The parameters such as DMI, SOI and Nino 1+2 had no significant influence in the model and were removed from the final model. The curve for the partial effect of EMI (edf=2.4, $p<1$), MEI (edf=1, $p<0.1$), TNI (edf=2.34, $p<1$), and Nino4 (edf=3.29, $p<0.01$) showed the same trend (Figure 4.23 [A, B, C, D]). The CPUE were increased at values representing La Nina episodes and decreased at values representing El Nino values.

The deviance explained and adjusted R^2 value for penaeid prawn CPUE model of different gears are given in the table 4.16. The GAM model where MDTN CPUE of penaeid prawn landings was taken as response variable and EMI, TNI, and Nino 4 were considered as the predictors, returned an adjusted R^2 of 0.08 and the percentage deviance explained was 12.6%. The GAM model where

MOTHS CPUE of Penaeid prawn landings was taken as response variable, Nino 4 and Nino 1+2 were considered as predictors, returned an R^2 value of 0.12 and the percentage deviance explained was 17.9%. The adjusted R^2 value of the GAM taking MRS CPUE of Penaeid prawn landings as response variable was 0.07 and the percentage deviance explained was 8.75%. The GAM model where CPUE of MTN penaeid prawn landings were taken as response variable and EMI and Nino 4 were considered ad predictors, returned an adjusted R2 value of 0.03 and the percentage deviance explained was 4.37%. The parameters such as DMI, MEI, SOI, TNI, and Nino 1+2 had no significant influence in the MTN model and were removed from the final model. The GAM model, where NM CPUE of Penaeid prawn landings were taken as response variable and DMI, EMI, MEI, and Nino4 were taken as explanatory variables, returned an R^2 value of 0.22 and the percentage deviance explained was 28.5% .The parameters such as SOI, TNI and Nino 1+2 had no significant effect in the NM model, and were removed from the final model. The adjusted R^2 value of the GAM taking OBRS CPUE of penaeid prawn landings as response variable was 0.27 and the percentage deviance explained was 32%. The GAM results revealed DMI, EMI, MEI, and Nino4 strongly influence the CPUE of OBRS. The parameters such as SOI, TNI and Nino1+2 have no effect on the CPUE of OBRS and were removed from the final model. The adjusted R^2 value of the GAM taking OBGN CPUE of penaeid prawns as response variable was 0.09 and the percentage deviance explained was 13.3%. The GAM results revealed that DMI, EMI, TNI, and Nino4 influence the CPUE of OBGN. The GAM model, where CPUE of OBTN penaeid prawn landings was taken as response variable and, EMI, MEI, Nino 4 and Nino 1+2 were considered as the predictors, returned an adjusted R^2 value of 0.18 and the percentage deviance explained was 22.6%.

Table4.15: Details of deviance explained & adjusted R-square value for PP CPUE model and the effective degrees of freedom & significance of the explanatory variables of the model

T_PP_CPUE ~ s(EMI) + s(MEI) + s(TNI) + s(Nino4) R-sq.(adj) = 0.14 Deviance explained = 19%					
	edf	Ref.df	F	Deviance explained (%)	p-value
s(EMI)	2.396	3.050	1.852	0.05	0.13712
s(MEI)	1.000	1.000	3.756	1.52	0.05467 .
s(TNI)	2.344	2.982	1.191	1.04	0.33588
s(Nino4)	3.285	4.145	3.990	7.39	0.00365 **

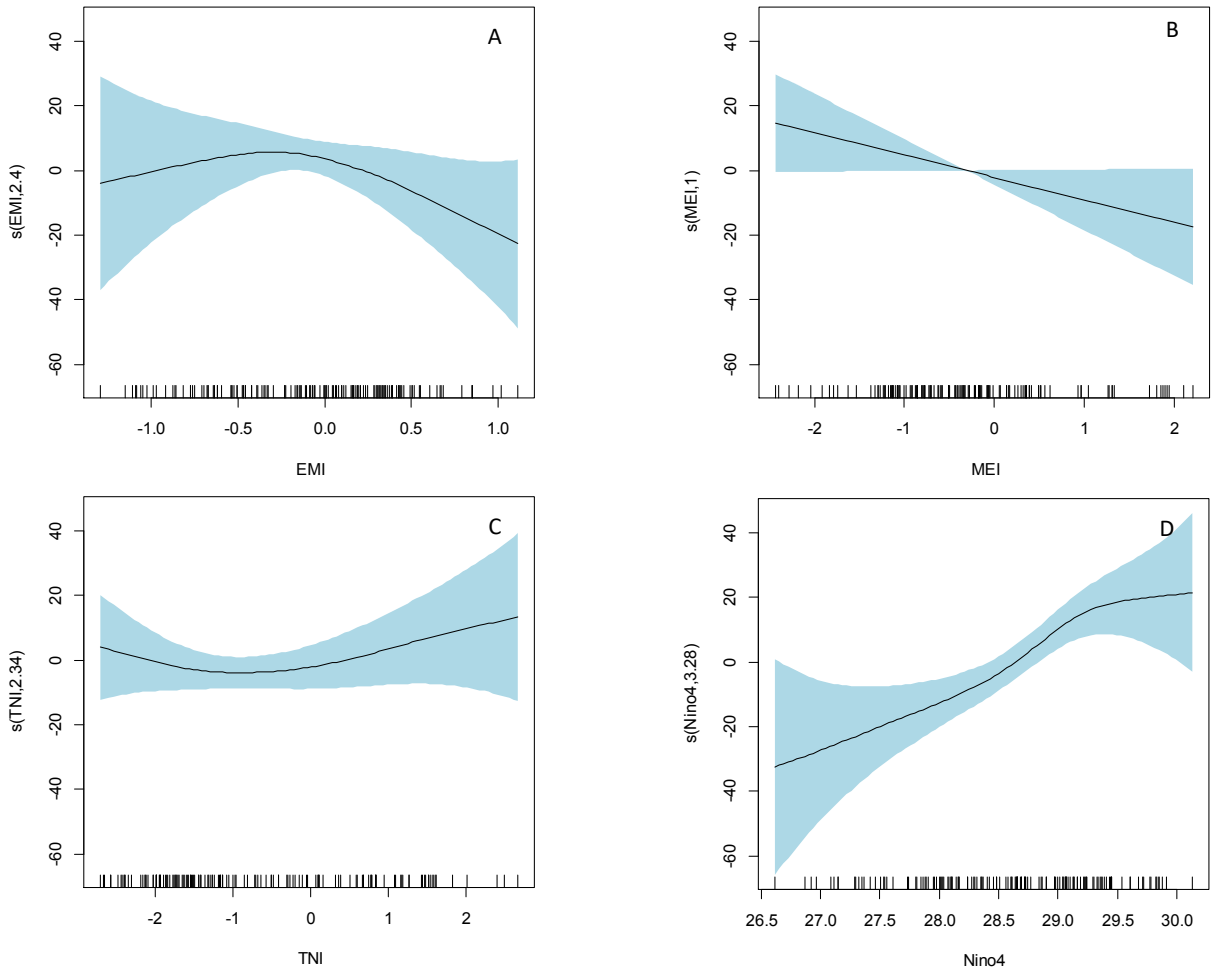

Figure 4.23: GAM model for PP CPUE showing effects of explanatory variables; EMI (A), MEI (B), TNI (C), and Nino4 (D)

Table 4.16: AIC, Adjusted R-square, and Deviance explained for the gear wise models of penaeid prawns

Model	AIC	R-sq. (adj)	Deviance explained (%)
PP_MDTN ~ s(EMI) + s(TNI) + s(Nino4)	1746.987	0.08	12.6
PP_MOTHS ~ s(Nino4) + s(Nino1.2)	1403.339	0.12	17.9
PP_MRS ~ s(EMI) + s(MEI) + s(Nino4)	1825.945	0.07	8.75
PP_MTN ~ s(EMI) + s(Nino4)	1704.147	0.03	4.37
PP_NM ~ s(DMI) + s(EMI) + s(MEI) +s(Nino4)	524.2727	0.22	28.5
PP_OBRS ~ s(DMI) + s(EMI) + s(MEI) + s(Nino4)	1481.102	0.27	32
PP_OBGN ~ s(DMI) + s(EMI) + s(TNI) + s(Nino4)	478.4332	0.09	13.1
PP_OBTN ~ s(EMI) + s(MEI) + s(Nino4) + s(Nino1.2)	1618.63	0.18	22.6

4.2.11 Impacts of ENSO events on Threadfin breams

The adjusted R^2 value of GAM taking CPUE of Threadfin breams as response variable was 0.02 and the percentage deviance explained was 3.82%. The GAM model results revealed that DMI and SOI had influence on CPUE. The parameters such as MEI, EMI, and TNI, Nino4 and Nino 1 + 2 had no effect on the CPUE of Threadfin and were removed from the final model (Table 4.17). The curve for the partial effect of DMI (edf=1.64, p<1) showed a positive effect and the curve for the partial effect of SOI (edf=1, p<1) showed a negative effect on CPUE of threadfin breams (Figure 4.24 [A,B]).

The deviance explained and adjusted R^2 value for threadfin bream CPUE model of different gears are given in the table 4.20. The GAM model, where MTN CPUE of threadfin bream landings was taken as response variable and, DMI, EMI, SOI, Nino4, Nino1.2 were considered as the predictors, returned an adjusted R^2 value of 0.11 and the percentage deviance explained was 17.9%. The adjusted R^2 value of the GAM taking NM CPUE of threadfin bream as response variable was 0.39 and the percentage deviance explained was 50.1%, the parameters such as DMI, EMI, MEI, SOI, TNI, Nino4, and Nino1+2 were considered as predictors. The GAM model, where MOTHS CPUE of threadfin bream was taken as response variable and, EMI, Nino 4 and Nino 1+2 were considered as the predictors, returned an adjusted R^2 value of 0.09 and the percentage deviance explained was 12%. The GAM model, where OBGN CPUE of Threadfin breams was taken as response variable and, DMI, EMI, MEI, TNI, Nino4, and Nino 1+2 was considered as the predictors, returned an adjusted R^2 value of 0.2 and the percentage deviance explained was 27.1%. The SOI had no significant effect in the OBGN CPUE model and was removed from the final model. The GAM model, where OBHL CPUE of threadfin bream was taken as response variable and, DMI, EMI, MEI, SOI,TNI, Nino4, and Nino 1+2 was considered as the predictors, returned an adjusted R^2 value of 0.68 and the percentage deviance explained was 76.8%.

Table 4.17: Details of deviance explained & adjusted R-square value for TB CPUE model and the effective degrees of freedom & significance of the explanatory variables of the model

T_TB_CPUE ~ s(DMI) + s(SOI) R-sq.(adj) = 0.02 Deviance explained = 3.82%					
	edf	Ref.df	F	Deviance explained (%)	p-value
s(DMI)	1.642	2.067	1.300	0.06	0.293
s(SOI)	1.000	1.000	1.314	1.04	0.254

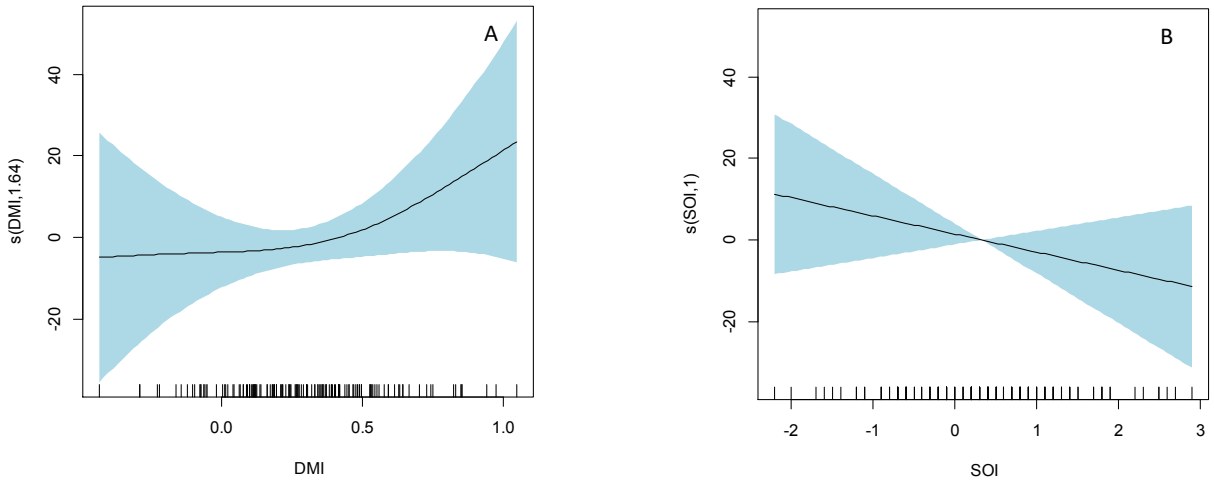

Figure 4.24: GAM model for TB CPUE showing effects of explanatory variables; DMI (A) and SOI (B)

Table 4.18: AIC, Adjusted R-square, and Deviance explained for the gear wise models of threadfin breams

Model	AIC	R-sq. (adj)	Deviance explained (%)
TB_MTN ~ s(DMI) + s(EMI) + s(SOI) + s(Nino4) + s(Nino1.2)	1314.792	0.11	17.9
TB_NM ~ s(DMI) + s(EMI) + s(MEI) + s(SOI) + s(TNI) + s(Nino4) + s(Nino1.2)	-340.9728	0.39	50.1
TB_MOTHS ~ s(EMI) + s(Nino4) + s(Nino1.2)	2125.138	0.09	12
TB_OBGN ~ s(DMI) + s(EMI) + s(MEI) + s(TNI) + s(Nino4) + s(Nino1.2)	660.7361	0.2	27.1
TB_OBHL ~ s(DMI) + s(EMI) + s(MEI) + s(SOI) + s(TNI) + s(Nino4) + s(Nino1.2)	516.1748	0.68	76.8

4.2.12 Impact on total landings

The adjusted R^2 value of GAM taking CPUE of total landings as response variable was 0.38 and the percentage deviance explained was 43.6%. The GAM model results revealed that DMI, EMI, MEI, SOI, TNI, Nino 4 and Nino 1+2 had strong influence on CPUE of total landings (Table 4.19).

The curve for the partial effect of EMI (edf=1, p<0.01), SOI (edf=1.03, p<1), TNI (edf=1, p<0.01) revealed negative effect and Nino4 (edf=1, p<0.01) had a positive effect on total CPUE (Figure 4.25 [B, D, E, F]). The curve for the partial effect of DMI (edf= 3.17, p<0.001) revealed an increasing trend, MEI (edf=3.19, p<0.05) and Nino1+2 (edf=3.26, p<1) had a decreasing trend between -1 to 1 (Figure 4.25 [A, C, G]).

The deviance explained and adjusted R^2 value for CPUE of total landings model of different gears are given in the table 4.21. The GAM model, where MDTN CPUE of total landings was taken as response variable and, DMI, EMI, SOI, Nino4 and Nino1+2 were considered as explanatory variables, returned an adjusted R^2 value of 0.20 and the percentage deviance explained was 26.6%, the parameters such as MEI and TNI had no significant influence in the model and were removed from the final model. The GAM model, where MOTHS CPUE of total landings were taken as response variable and DMI, MEI, TNI, Nino4 and Nino1+2 were considered as explanatory variables, returned an adjusted R2 value of 0.23 and the percentage deviation explained was 36.2%. The GAM model, where MRS CPUE of total landings were taken as response variable and DMI, MEI, EMI, SOI and Niino1+2 were considered as explanatory variables, returned an adjusted R2 value of 0.26 and the percentage deviation explained was 32.4%, the parameters such as TNI and Nino4 had no significant effect in the model and were removed from the final model. The GAM model, where NM CPUE of total landings were taken as response variable and DMI, MEI, TNI, Nino4 and Nino1+2 were considered as predictors, returned an adjusted R^2 value of 0.28 and the percentage deviation explained was 37.5%, the parameters such as EMI and SOI had no significant influence in the model and were removed from the final model. The GAM model, where OBBS CPUE of total landings were taken as response variable and DMI, EMI, SOI, TNI and Nino1+2 were considered as predictors, returned an adjusted R^2 value of 0.21 and the percentage deviation explained was 28.2%, the parameters such as MEI and Nino 4 had no significant influence in the model and were removed from the final model. The adjusted R^2 value of the GAM taking OBGN CPUE of total landings as response variable was 0.42 and the percentage deviance explained was 48.8%. The GAM results revealed that DMI, EMI, SOI, TNI, MEI, Nino4 and Nino1+2 strongly influence the CPUE of OBGN. The GAM model, where OBHL CPUE of total landings were taken as response variable and DMI, SOI, and Nino4 were considered as predictors, returned an adjusted R^2 value of 0.20 and the percentage deviation explained was 26.5%. The GAM model, where OBRS CPUE of total landings were taken as response variable and DMI, MEI, SOI, TNI and Nino4 were considered as predictors, returned an adjusted R^2 value of

0.314 and the percentage deviation explained was 41%, the parameters such as EMI and Nino 1+2 had no influence in the model and were removed from the final model.

Table4.19: Details of deviance explained & adjusted R-square value for Total CPUE model and the effective degrees of freedom & significance of the explanatory variables of the model

T_CPUE ~ s(DMI) + s(EMI) + s(MEI) + s(SOI) + s(TNI) + s(Nino4) + s(Nino1.2) R-sq.(adj) = 0.38 Deviance explained = 43.6%					
	edf	Ref.df	F	Deviance explained (%)	p-value
s(DMI)	3.166	3.992	5.709	13.2	0.000296 ***
s(EMI)	1.000	1.000	31.855	9.57	8.88e-08 ***
s(MEI)	3.189	3.983	1.237	11.6	0.284612
s(SOI)	1.030	1.057	5.812	3.35	0.017163 *
s(TNI)	1.000	1.000	4.443	14.7	0.036933 *
s(Nino4)	1.000	1.000	16.914	9.4	6.78e-05 ***
s(Nino1.2)	3.262	4.075	2.380	5.2e-05	0.053943 .

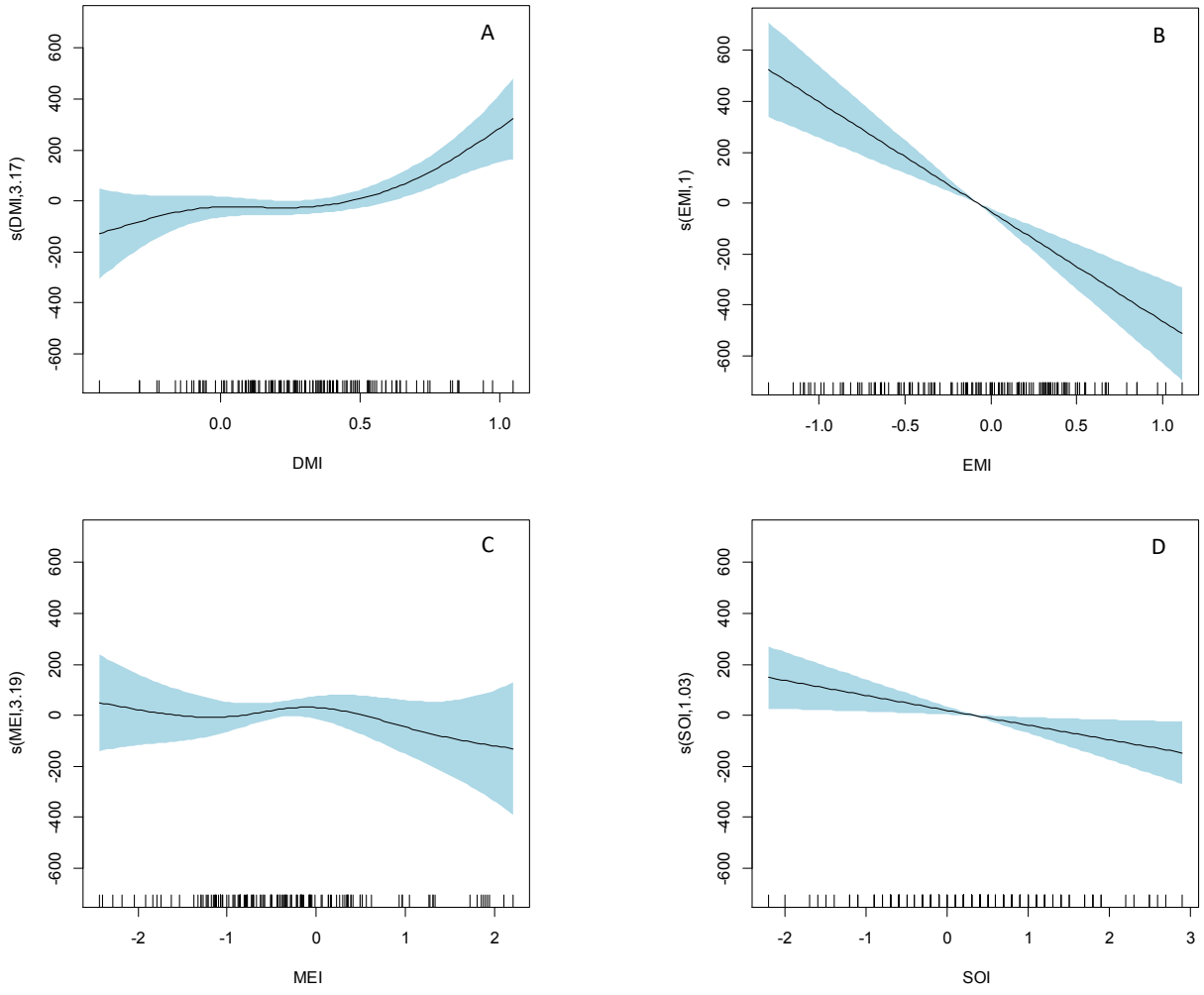

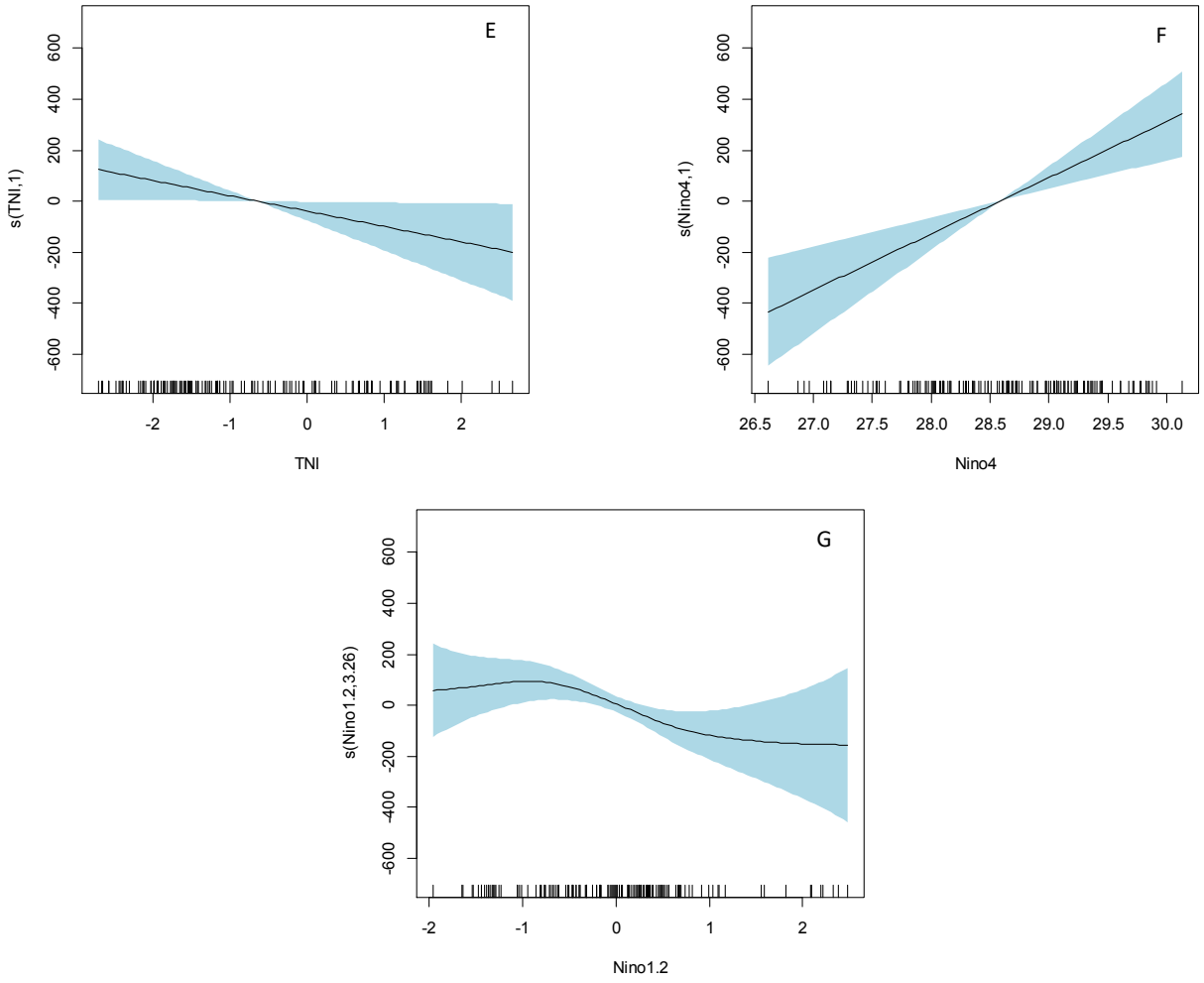

Figure 4.25: GAM model for Total CPUE showing effects of explanatory variables; DMI (A), EMI (B), MEI (C), SOI (D), TNI (E), Nino4 (F), and Nino 1+2 (G)

Table 4.20: AIC, Adjusted R-square, and Deviance explained for the gear wise models of total fish resources

Model	AIC	R-sq. (adj)	Deviance explained (%)
T_MDTN ~ s(DMI) + s(EMI) + s(SOI) + s(Nino4) + s(Nino1.2)	2408.977	0.20	26.6
T_MOTHS ~ s(DMI) + s(MEI) + s(TNI) + s(Nino4) + s(Nino1.2)	2545.705	0.23	36.2
T_MRS ~ s(DMI) + s(EMI) + s(MEI) + s(SOI) + s(Nino1.2)	2329.03	0.26	32.4
T_NM ~ s(DMI) + s(MEI) + s(TNI) + s(Nino4) + s(Nino1.2)	1036.299	0.28	37.5
T_OBBS ~ s(DMI) + s(EMI) + s(SOI) + s(TNI) + s(Nino1.2)	1982.697	0.21	28.2
T_OBGN ~ s(DMI) + s(EMI) + s(MEI) + s(SOI) + s(TNI) + s(Nino4) + s(Nino1.2)	1374.036	0.42	48.8
T_OBHL ~ s(DMI) + s(SOI) + s(Nino4)	1385.566	0.20	26.5
T_OBRS ~ s(DMI) + s(MEI) + s(SOI) + s(TNI) + s(Nino4)	2067.208	0.31	41

4.2.13 correlation analysis of ocean- atmospheric parameters

Table4.21- Correlation coefficient matrix of different ocean-atmospheric parameters

	CHL_A	SALT	SSHA	SST	RF	OCV	OCD
CHL_A							
SALT	-0.28***						
SSHA	-0.79****	0.29***					
SST	-0.82****	0.37****	0.71****				
RF	0.72****	-0.30***	-0.74****	-0.59****			
OCV	0.26**	-0.11	-0.13	-0.34****	0.25**		
OCD	-0.06	0.1	0.1	-0.05	0.22**	0.16	
LTA	0.81****	-0.33****	-0.78****	-0.78****	0.62****	0.29***	-0.1

The Chlorophyll (CHLA) was highly positively correlated (0.72) with rainfall (RF) ($p<0.001$), positively correlated (0.26) with ocean current velocity (OCV) ($p<0.05$), highly positively correlated (0.81) with local temperature anomaly (LTA) ($p<0.001$), highly negatively correlated (-0.82) with sea surface temperature (SST) ($p<0.001$), negatively correlated (-0.79) with sea surface height anomaly (SSHA) ($p<0.001$) and salinity (SALT) (-0.28, $p<0.001$). The sea surface salinity was positively

correlated with SSHA (0.29, $p<0.01$), SST (0.37, $p<0.001$), negatively correlated with RF (-0.30, $p<0.05$), OCV (-0.11, $p<1$) and LTA (-0.33, $p<0.001$).The SSHA was highly positively correlated with SST (0.71, $p<0.001$), highly negatively correlated with RF (-0.74, $p<0.001$), and LTA (-0.78, $p<0.001$). The SST was negatively correlated with RF (-0.59, $p<0.001$), and LTA (-0.78, $p<0.001$). RF was positively correlated with LTA (0.62, $p<0.001$) and LTA was positively correlated with OCV (0.29, $p<0.01$)

4.2.14 Combined Effects of Ocean-Atmospheric Parameters and ENSO on Pelagic and Demersal Fish Resources

4.2.14.1 Impact on oil sardine fishery

The adjusted R^2 value of GAM taking CPUE of oil sardine total landing as response variable was 0.32 and the percentage deviance explained was 40.1%. The GAM model results revealed that DMI, TNI, Nino4, CHLA, SST, and OCV had influence on CPUE of oil sardine. The parameters such as EMI, MEI, SOI, Nino1+2, LTA, RF, OCD, SSHA and SALT had no effect on the CPUE of oil sardine and were removed from the final model (Table 4.22). The curve for the partial effect of DMI (edf=1, $p<0.001$), and CHLA (edf=1, $p<1$) showed a positive effect on CPUE of oil sardine (Figure 4.26 [A, D]). The TNI had high edf value, so the curve is wiggly which could be seen from the figure 4.26B. The curve for the partial effect of TNI (edf=5.71, $p<0.05$) showed an increasing trend between the value -2 and-1, the curve showed decreasing trend as the value increased. The curve for the partial effect of Nino4 (edf=3.47, $p<0.001$) revealed a negative effect on CPUE (Figure 426C). The curve for the partial effect of SST (edf=2.4, $p<0.1$) showed an increasing trend up to 28°C and further increase in the value showed a decreasing trend on CPUE (Figure 4.26E). The curve for the partial effect of OCV (edf=1, $p<0.01$) showed a negative effect on CPUE of total landings of oil sardine (Figure 4.26F).

4.2.14.2 Impact on Indian mackerel

The GAM model where CPUE of Indian mackerel total landings was taken as response variable and DMI, EMI, MEI, Ninio4, Ninio1.2, CHLA, SST, LTA, RF, and OCD were considered as the predictors, returned an adjusted R^2 of 0.75 and the percentage deviance explained was 84% (Table 4.23). The parameter such as TNI, SOI, SSHA, OCV and SALT had no effect on the CPUE of Indian mackerel and were removed from the final model. The curve for the partial effect of DMI (edf=7.96), $p<0.01$) exhibited an increasing trend on the CPUE from the value 0.6 (Figure 4.27A). The curve for the partial effect of EMI (edf=2.1, $p<1$) showed an increasing trend up to the value 0, a further increase in the value had no effect on CPUE (Figure 4.27B). The curve for the partial effect of MEI (edf=8.81,

p<0.001) showed an increasing trend after the value 1 (Figure 4.27C). The curve for the partial effect of Nino4 (edf=2.02, p<1) showed a decreasing trend from the value 28.5 (Figure 4.27D). The curve for the partial effect of Nino1+2 (edf=1, p<1) had a positive effect on CPUE (Figure 4.27E). The curve for the partial effect of CHLA (edf=6.88, 0.001) showed highest CPUE of Indian mackerel at the range of 6-8 mg/m^3 (Figure 4.27F). The curve for the partial effect of SST (edf=7.09, p<0.1) had a positive effect on CPUE up to 28°C. A further increase in the value showed a decreasing trend in CPUE (Figure 4.27G). The curve for the partial effect of LTA (edf=8.17, p<0.001) had a very strong positive effect on CPUE from the value 1.5 (Figure 4.27H). The curve for the partial effect of RF (edf=5.705, p<0.1) showed an increasing trend on CPUE from the value 600mm (Figure 4.27I).

4.2.14.3 Impact on anchovy

The GAM model where the CPUE of total landings of anchovy was taken as response variable and DMI, EMI, MEI, TNI, Nino1+2, CHLA, SST, LTA, RF, SALT and OCV were considered as the predictors, returned an adjusted R^2 value of 0.58 and the percentage deviance explained was 71.1% (Table 4.24). The parameters such as SOI, Nino4, OCD, and SSHA had no effect on the CPUE of anchovy and were removed from the final model. The curve for the partial effect of DMI (edf=7.25, p<0.05) showed negative effect on CPUE up to the value 0 and a further increase in the value had not exerted much influence on CPUE (Figure 4.28A). The curve for the partial effect of EMI (edf=1.6, p<1) had a negative effect on CPUE (Figure 4.28B). The MEI (edf=7.5, p<0.01) had high edf value, so the curve was wiggly which could be seen in the figure 4.28C. The curve for the partial effect of MEI showed a strong negative effect after the value 1 and higher CPUE were observed in lower MEI values. The curve for the partial effect of TNI (edf=4.4, p<0.1) showed higher CPUE on lower negative values (Figure 4.28D). The curve for the partial effect of Nino1+2 (edf=8.3, p<0.001) revealed a positive effect on CPUE (Figure 4.28E). The curve for the partial effect of CHLA (edf=1.26, p<0.01), OCV (edf=1, p<0.001) and SST (edf=1, p<0.05) showed a positive effect on CPUE (Figure [F, K, G]). The curve for the partial effect of LTA (edf=1.9, p<1) and RF (edf=3.6, p<0.01) showed a negative effect, SALT (edf=7.08, p<0.001) showed a decreasing trend as the value increases, a further increase of value from 0.0348 psu did not have much effect on CPUE (Figure 4.28 [H, I, J]).

4.2.14.4 Impact on penaeid prawns

The adjusted R^2 value of GAM taking CPUE of total landings of penaeid prawns as response variable was 0.50 and the percentage deviance explained was 58.7%. The GAM model results revealed that DMI, TNI, Ninio4, CHLA, SST, LTA, RF, SALT, and OCV had strong influence on CPUE of penaeid

prawns. The parameters such as EMI, MEI, SOI, Nino1+2, OCD, and SSHA had no effect on the CPUE of penaeid prawns and were removed from the final model (Table 4.25). The curve for the partial effect of DMI (edf=1, p<1), TNI (edf=1, p<0.1) and Nino 4 (edf=1, p<0.05) had positive effect on CPUE of total landings of anchovy (Figure 4.29 [A, B, C]). The curve for the partial effect of CHLA (edf=4.68, p<0.001) showed decreasing trend up to 2 mg/m^3 and showed an optimum range of chlorophyll concentration between 4-6 mg/m^3 (Figure 4.29D). The curve for the partial effect of SST (2.7, p<1) showed a decreasing trend up to 29°C, a further increase in the value did not exert much effect on CPUE (Figure 4.29E). The curve for the partial effect of LTA (edf=1, p<0.05) showed a positive effect on CPUE of penaeid prawns (Figure 4.29F). The curve for the partial effect of RF (edf=8.9, p<0.001) showed a very strong positive effect on CPUE at the value 600 mm. The CPUE was highest for RF in the range of 600 to 800 mm (Figure 4.29G). The curve for the partial effect of SALT (edf=2.3, p<0.1) and OCV (edf=1, p<0.1) revealed that they had less effect on CPUE, SALT showed a decreasing trend and OCV showed a slightly increasing trend (Figure 4.29I).

4.2.14.5 Impact on threadfin breams

The adjusted R^2 value of GAM taking CPUE of total landings of threadfin breams as response variable was 0.70 and the percentage deviance explained was 81.2%. The GAM model results revealed that DMI, EMI, MEI, SOI, TNI, Ninio1+2, CHLA, SST, LTA, RF, SALT, and OCD had strong influence on CPUE of threadfin breams. The parameters such as EMI, MEI, Nino4, OCV, and SSHA had no effect on the CPUE of threadfin bream and were removed from the final model (Table 4.26). The curve for the partial effect of DMI (edf=8.9, p<0.001), EMI (edf=1.7, p<0.05), MEI (edf=5.29, p<0.05), TNI (edf=1, p<0.05), and Nino1+2 (edf=1, p<1) showed a positive effect on CPUE of threadfin breams (Figure 4.30 [A, D, E, C, B]. The curve for the partial effect of SOI (edf=2.3, p<0.1) showed a negative effect on CPUE (Figure 4.30F). The curve for the partial effect of CHLA (edf=8.14, p<0.001) showed a decreasing trend up to the value 2.5 mg/m^3, a further increase in the value resulted in an increasing trend of CPUE (Figure 4.30G). The curve for the partial effect of SST (edf=6.9, p<0.05) had an increasing trend up to 28°C (Figure 4.30H). The curve for the partial effect of LTA (edf=7.06, p<0.001) had very strong positive effect on CPUE (Figure 4.30I). The curve for the partial effect of RF (edf=2.14, p<1), SALT (edf=5.3, p<1), and OCD (edf=1.7, p<0.001) showed less variations in their curve (Figure 4.30[J, K]).

4.2.14.6 Impact on total landings

The GAM model where the CPUE of total landings was taken as response variable and DMI, Nino4, SSHA, SST, LTA, RF, and SALT were considered as the predictors, returned an adjusted R^2 value of 0.63 and the percentage deviance explained was 71.7%.The parameters such as EMI, MEI, SOI, TNI, Nino 1+2, CHLA, OCV and OCD had no effect on the CPUE of total landings and were removed from the final model (Table 4.27). The curve for the partial effect of DMI (edf=5.17, $p<0.01$) showed an increasing trend from the value 0 (Figure 4.31A). The curve for the partial effect of Nino4 (edf=3.3, $p<0.001$) showed an increasing trend up to the value 28.5, a further increase in the value showed decreasing trend on CPUE (Figure 4.31B). The curve for the partial effect of SSHA (edf=1, $p<0.05$) had a positive effect on CPUE, SST (edf=8.04, $p<0.001$) showed an increasing trend up to the value 28°C and LTA (edf=6.4, $p<0.001$) had a very strong positive effect after the value 1(Figure 4.31 [C, D, F]). The RF (edf=8.45, $p<0.001$) had high edf value, so the curve was wiggly which could be seen from the figure. The curve for the partial effect of RF showed maximum CPUE between 600 to 800 mm (Figure 4.31E). The curve for the partial effect of SALT (edf=1, $p<0.05$) was almost flat in nature (Figure 4.31G).

Table 4.22: Details of deviance explained & adjusted R-square value for OS CPUE model and the effective degrees of freedom & significance of the explanatory variables (including ocean-atmospheric parameters as explanatory variables) of the model

T_OS_CPUE ~ s(DMI) + s(TNI) + s(Nino4) + s(CHL_A) + s(SST) + s(OCV) R-sq.(adj) = 0.32 Deviance explained = 40.1%					
	edf	Ref.df	F	Deviance explained (%)	p-value
s(DMI)	1.000	1.000	13.014	2.49	0.000440 ***
s(TNI)	5.715	6.848	2.473	1.47	0.024935 *
s(Nino4)	3.466	4.346	5.613	9.49	0.000232 ***
s(CHL_A)	1.000	1.000	2.327	0.911	0.129668
s(SST)	2.399	3.062	2.211	8.31	0.087438 .
s(OCV)	1.000	1.000	7.934	0.87	0.005620 **

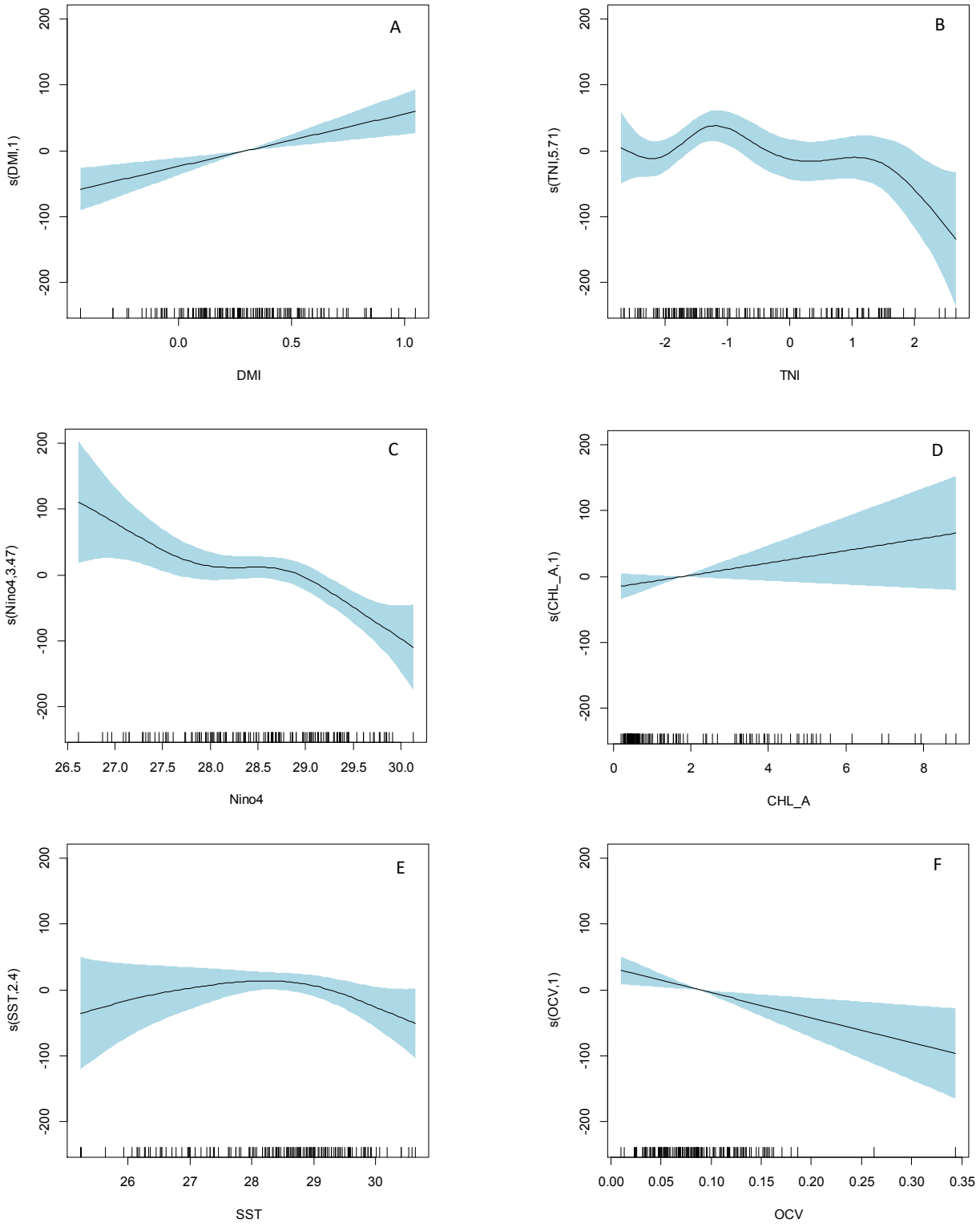

Figure4.26: GAM model for OS CPUE showing effects of explanatory variables including ocean-atmospheric parameters as explanatory variables; DMI (A), TNI (B), Nino4 (C), CHLA (D), SST (E), OCV (F).

Table 4.23: Details of deviance explained & adjusted R-square value for IM CPUE model and the effective degrees of freedom & significance of the explanatory variables (including ocean-atmospheric parameters as explanatory variables) of the model

T_IM_CPUE ~ s(DMI) + s(EMI) + s(MEI) + s(Nino4) + s(Nino1.2) + s(CHL_A) + s(SST) + s(LTA) + s(RF) + s(OCD) R-sq.(adj) = **0.75** Deviance explained = **84%**					
	edf	Ref.df	F	Deviance explained (%)	p-value
s(DMI)	7.957	8.658	2.708	7.57	0.007804 **
s(EMI)	2.102	2.669	1.276	1.97	0.252830
s(MEI)	8.811	8.978	6.572	21.3	1.39e-07 ***
s(Nino4)	2.022	2.600	1.333	3.7	0.273629
s(Nino1.2)	1.000	1.000	2.217	10.8	0.139870
s(CHL_A)	6.880	7.829	3.678	34.9	0.000755 ***
s(SST)	7.092	8.082	1.863	26.5	0.072485 .
s(LTA)	8.170	8.750	9.033	41.8	2.06e-10 ***
s(RF)	5.705	6.765	1.751	25.9	0.090415 .
s(OCD)	1.000	1.000	0.653	3.51	0.421169

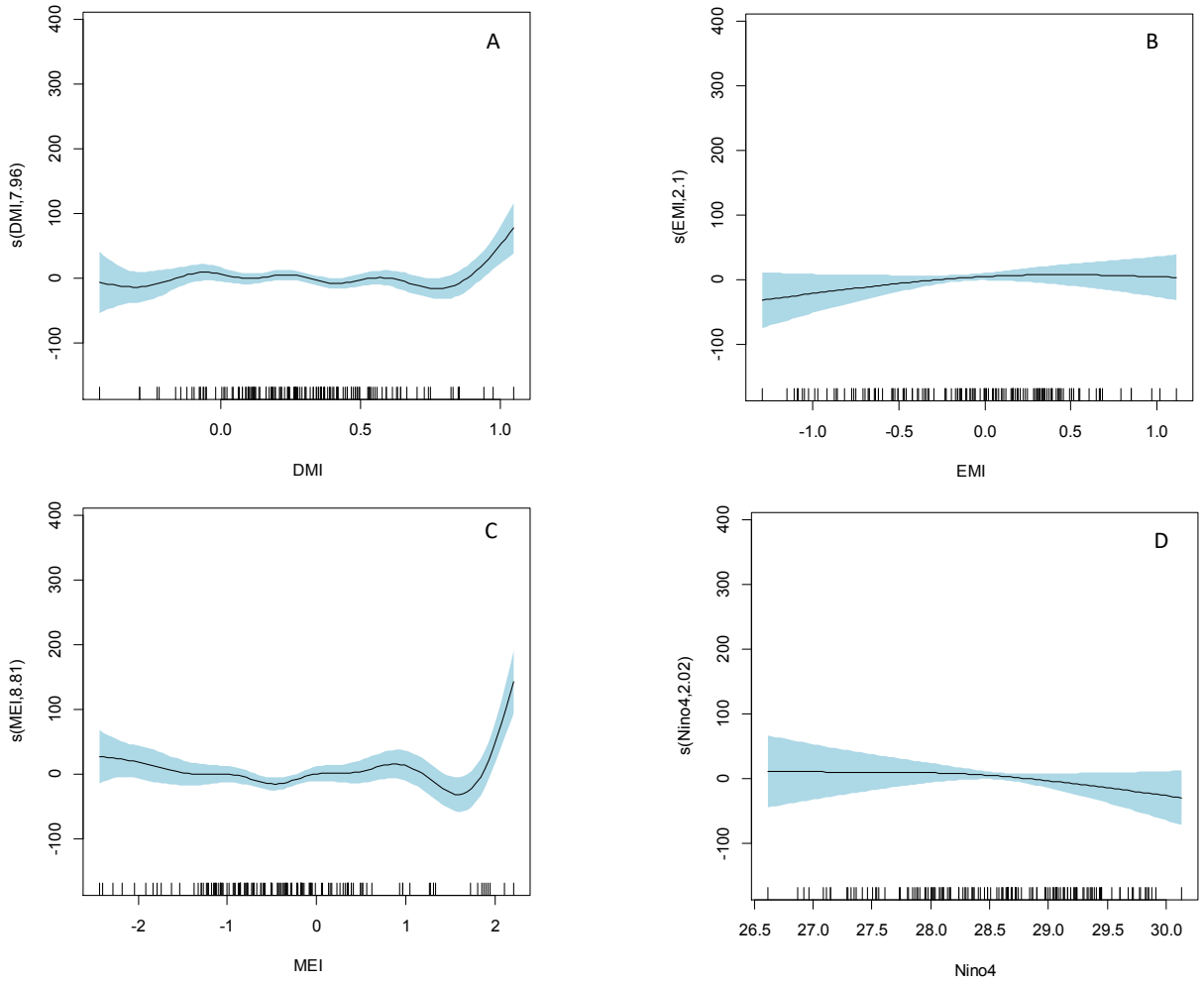

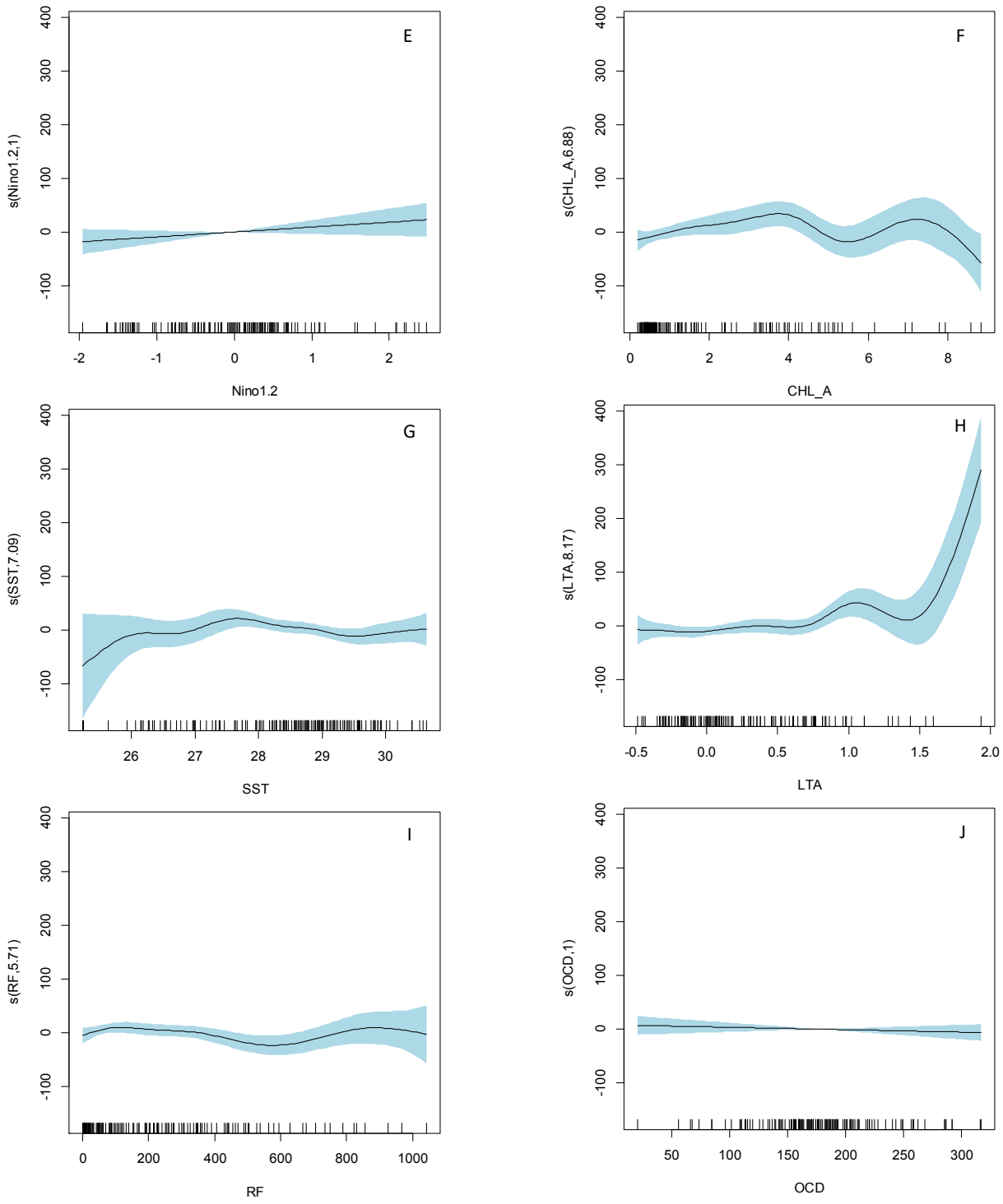

Figure4.27: GAM model for IM CPUE showing effects of explanatory variables (including ocean-atmospheric parameters as explanatory variables); DMI (A), EMI (B), MEI (C), NinO4 (D), Nino1+2 (E), CHLA_A (F), SST (G), LTA(H), RF (I), and OCD (J)

Table 4.24: Details of deviance explained & adjusted R-square value for Anchovy CPUE model and the effective degrees of freedom & significance of the explanatory variables (including ocean-atmospheric parameters as explanatory variables) of the model

T_A_CPUE ~ s(DMI) + s(EMI) + s(MEI) + s(TNI) + s(Nino1.2) + s(CHL_A) + s(SST) + s(LTA) + s(RF) + s(SALT) + s(OCV) R-sq.(adj) = 0.58 Deviance explained = 71.1%					
	edf	Ref.df	F	Deviance explained (%)	p-value
s(DMI)	7.255	8.226	2.414	6.62	0.020362 *
s(EMI)	1.630	2.047	1.518	6.37	0.223411
s(MEI)	7.565	8.433	3.393	17.3	0.001523 **
s(TNI)	4.371	5.337	1.918	5.4	0.079078 .
s(Nino1.2)	8.355	8.836	3.719	4.84	0.000561 ***
s(CHL_A)	1.262	1.455	7.071	20.5	0.005304 **
s(SST)	1.000	1.000	4.360	17.6	0.039345 *
s(LTA)	1.952	2.452	1.293	18.7	0.246091
s(RF)	3.601	4.433	3.251	25.3	0.011793 *
s(SALT)	7.086	8.079	3.800	19.8	0.000597 ***
s(OCV)	1.000	1.000	11.642	10.1	0.000929 ***

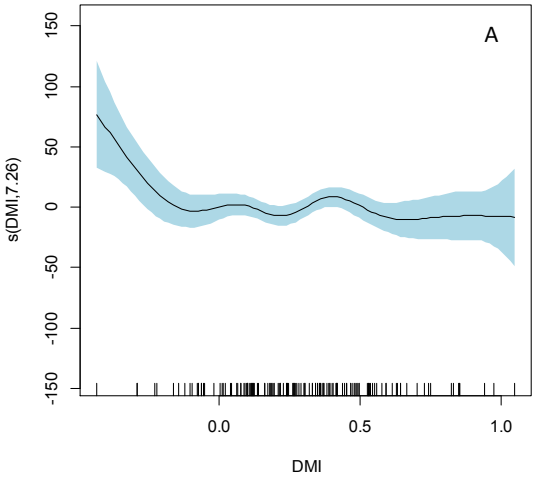

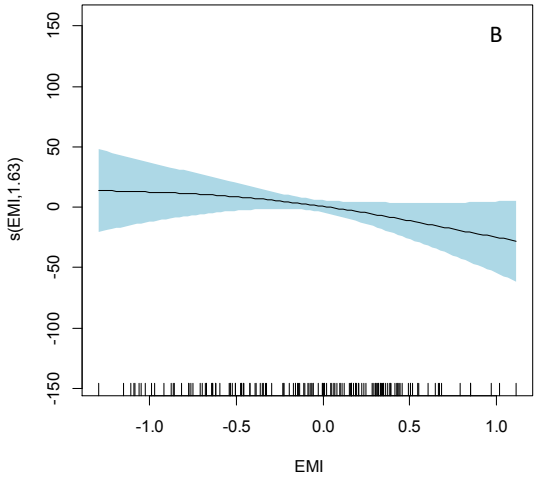

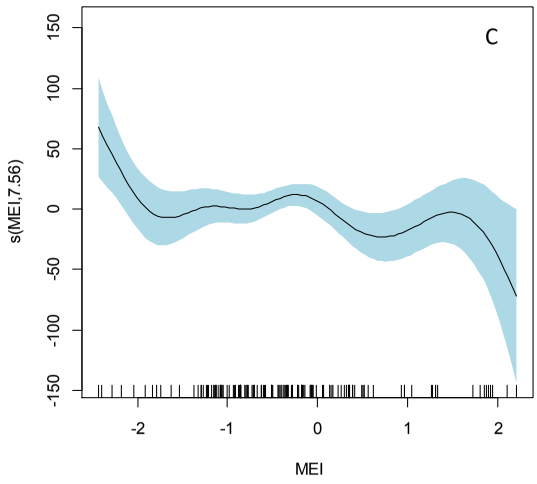
C
s(MEI,7.56)
MEI

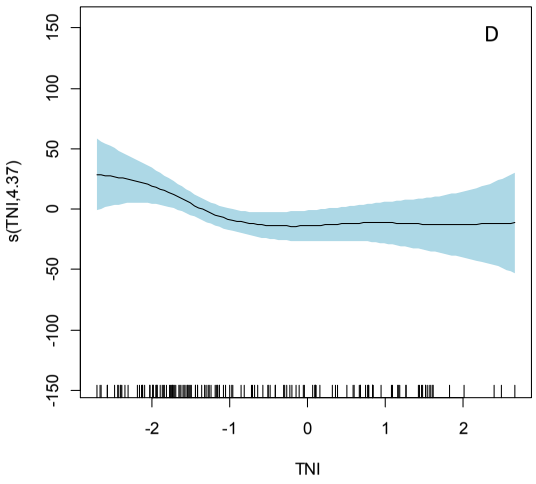
D
s(TNI,4.37)
TNI

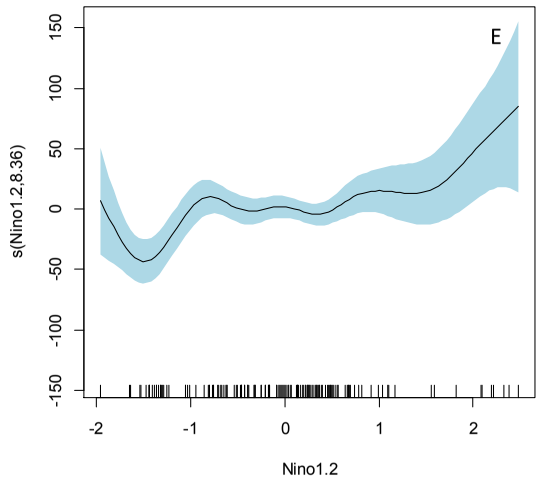
E
s(Nino1.2,8.36)
Nino1.2

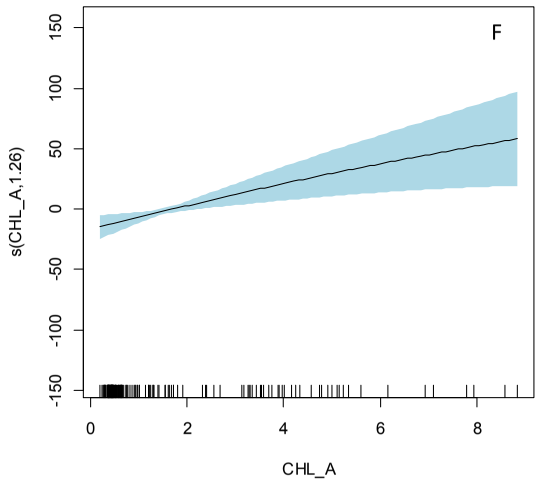
F
s(CHL_A,1.26)
CHL_A

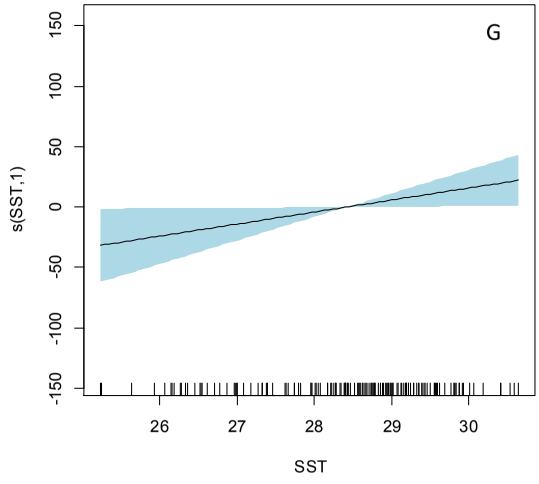
G
s(SST,1)
SST

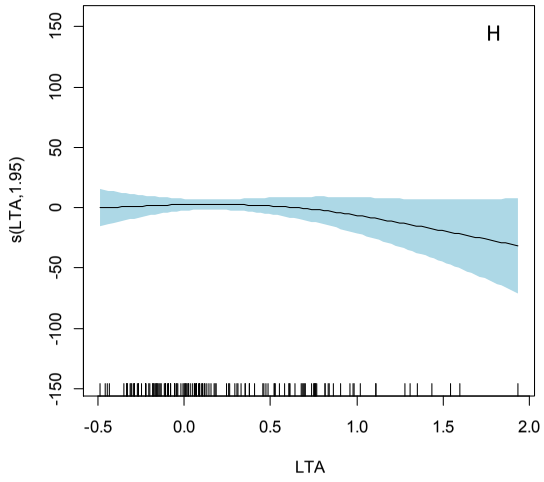
H
s(LTA,1.95)
LTA

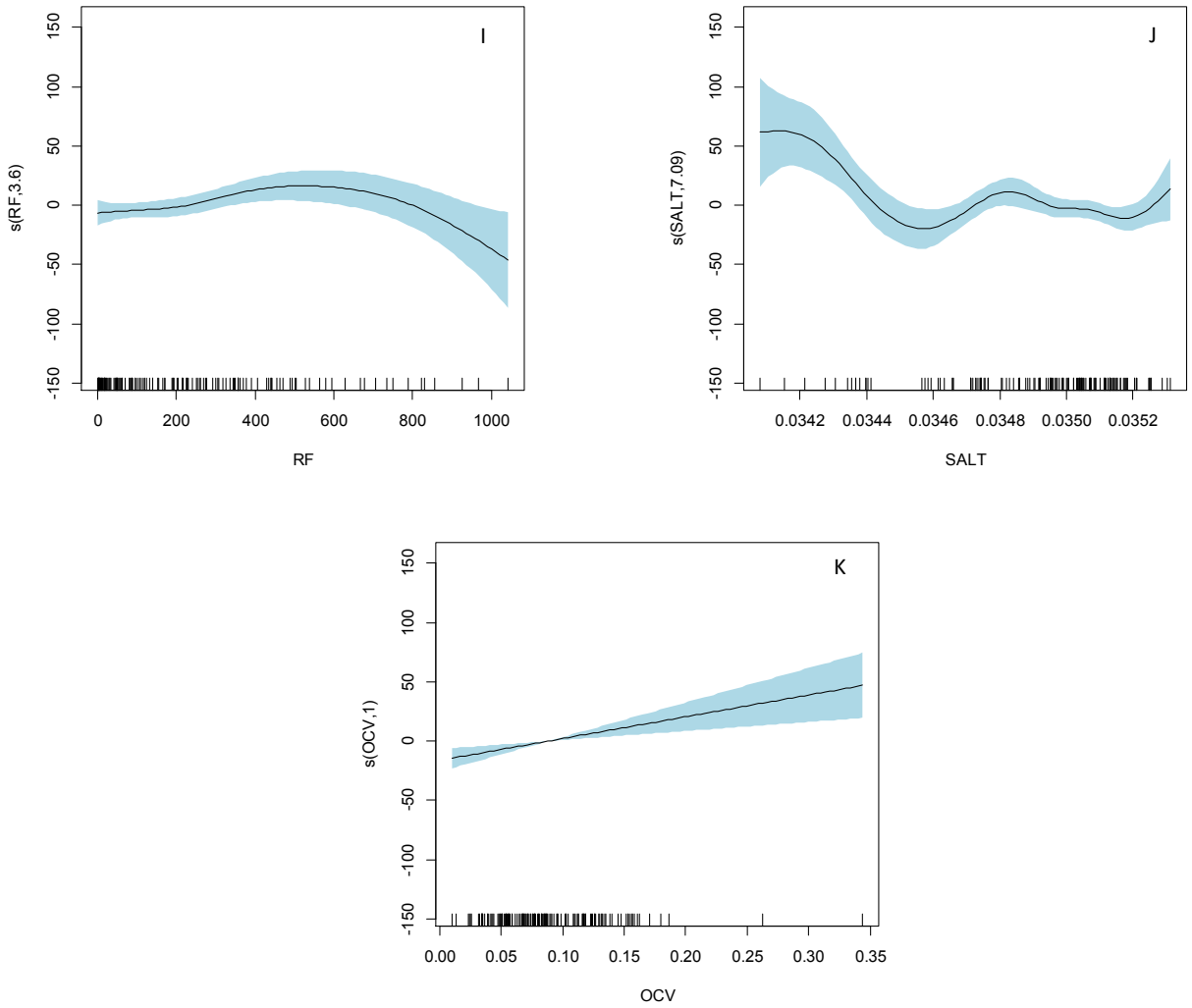

Figure4.28: GAM model for Anchovy CPUE showing effects of explanatory variables (including ocean-atmospheric parameters as explanatory variables); DMI (A), EMI (B), MEI (C), TNI (D), Nino1+2 (E), CHLA (F), SST (G), LTA (H), RF (I), SALT (J), and OCV (K)

Table 4.25: Details of deviance explained & adjusted R-square value for PP CPUE model and the effective degrees of freedom & significance of the explanatory variables (including ocean-atmospheric parameters as explanatory variables) of the model

T_PP_CPUE ~ s(DMI) + s(TNI) + s(Nino4) + s(CHL_A) + s(SST) + s(LTA) + s(RF) + s(SALT) + s(OCV) R-sq.(adj) = **0.50** Deviance explained = **58.7%**					
	edf	Ref.df	F	Deviance explained (%)	p-value
s(DMI)	1.000	1.000	2.077	0.058	0.15216
s(TNI)	1.000	1.000	2.816	1.04	0.09593 .
s(Nino4)	1.000	1.000	6.423	7.34	0.01253 *
s(CHL_A)	4.684	5.710	5.056	2.64	0.00015 ***
s(SST)	2.769	3.542	1.743	4.98	0.17854
s(LTA)	1.000	1.000	5.967	11	0.01601 *
s(RF)	8.933	8.996	11.061	33.9	1.34e-13 ***
s(SALT)	2.325	2.936	1.988	5.4	0.09990 .
s(OCV)	1.000	1.000	2.786	5.07	0.09768 .

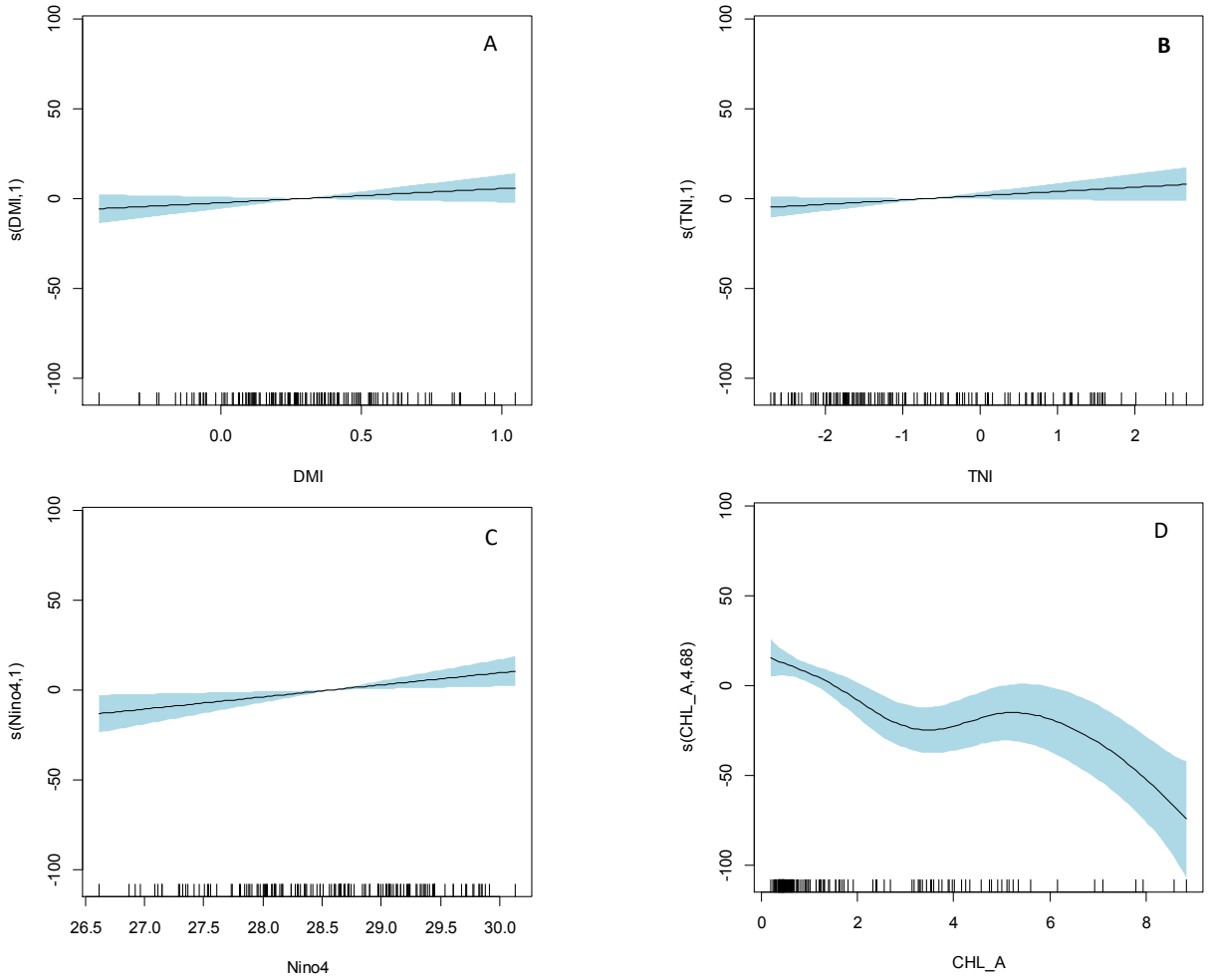

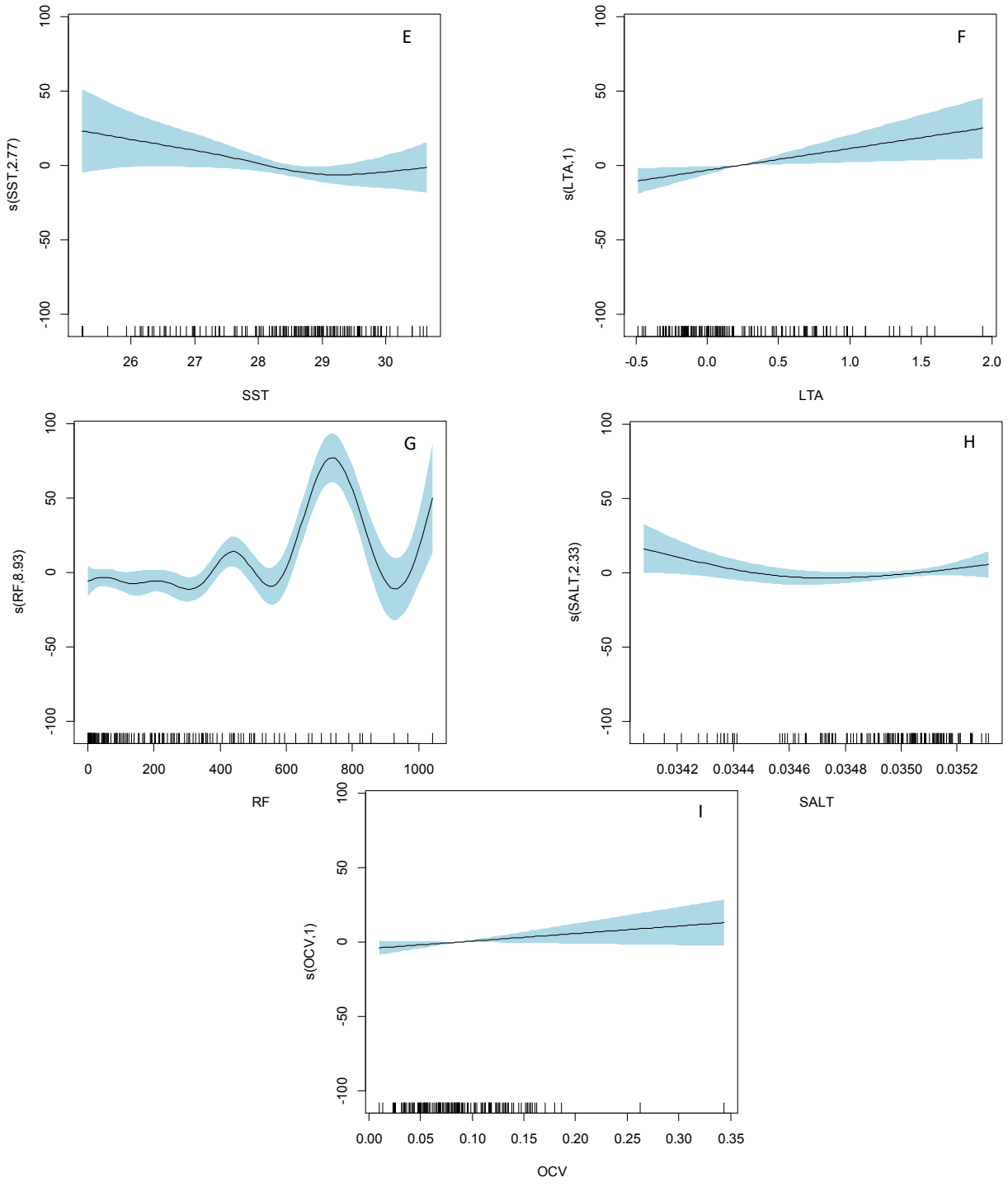

Figure4.29: GAM model for PP CPUE showing effects of explanatory variables (including ocean-atmospheric parameters as explanatory variables); DMI (A), TNI (B), Nino4 (C), CHL_A (D), SST (E), LTA (F), RF (G), SALT (H), and OCV (I)

Table 4.26: Details of deviance explained & adjusted R-square value for TB CPUE model and the effective degrees of freedom & significance of the explanatory variables (including ocean-atmospheric parameters as explanatory variables) of the model

T_TB_CPUE ~ s(DMI) + s(EMI) + s(MEI) + s(SOI) + s(TNI) + s(Nino1.2) + s(CHL_A) + s(SST) + s(LTA) + s(RF) + s(SALT) + s(OCD) R-sq.(adj) = **0.70** Deviance explained = **81.2%**					
	edf	Ref.df	F	Deviance explained (%)	p-value
s(DMI)	8.938	8.992	3.651	3.05	0.000582 ***
s(EMI)	1.719	2.148	4.017	1.74	0.020060 *
s(MEI)	5.291	6.376	2.735	0.45	0.014651 *
s(SOI)	2.301	2.960	2.365	1.5	0.070424 .
s(TNI)	1.000	1.000	5.833	0.801	0.017682 *
s(Nino1.2)	1.000	1.000	1.160	0.07	0.284192
s(CHL_A)	8.194	8.743	4.675	31.2	4.7e-05 ***
s(SST)	6.921	7.971	2.625	28.7	0.011808 *
s(LTA)	7.067	8.026	12.529	42.2	1.7e-13 ***
s(RF)	2.414	3.007	1.886	5.33	0.140785
s(SALT)	5.386	6.447	1.765	8.83	0.106105
s(OCD)	1.749	2.174	7.213	11.2	0.000915 ***

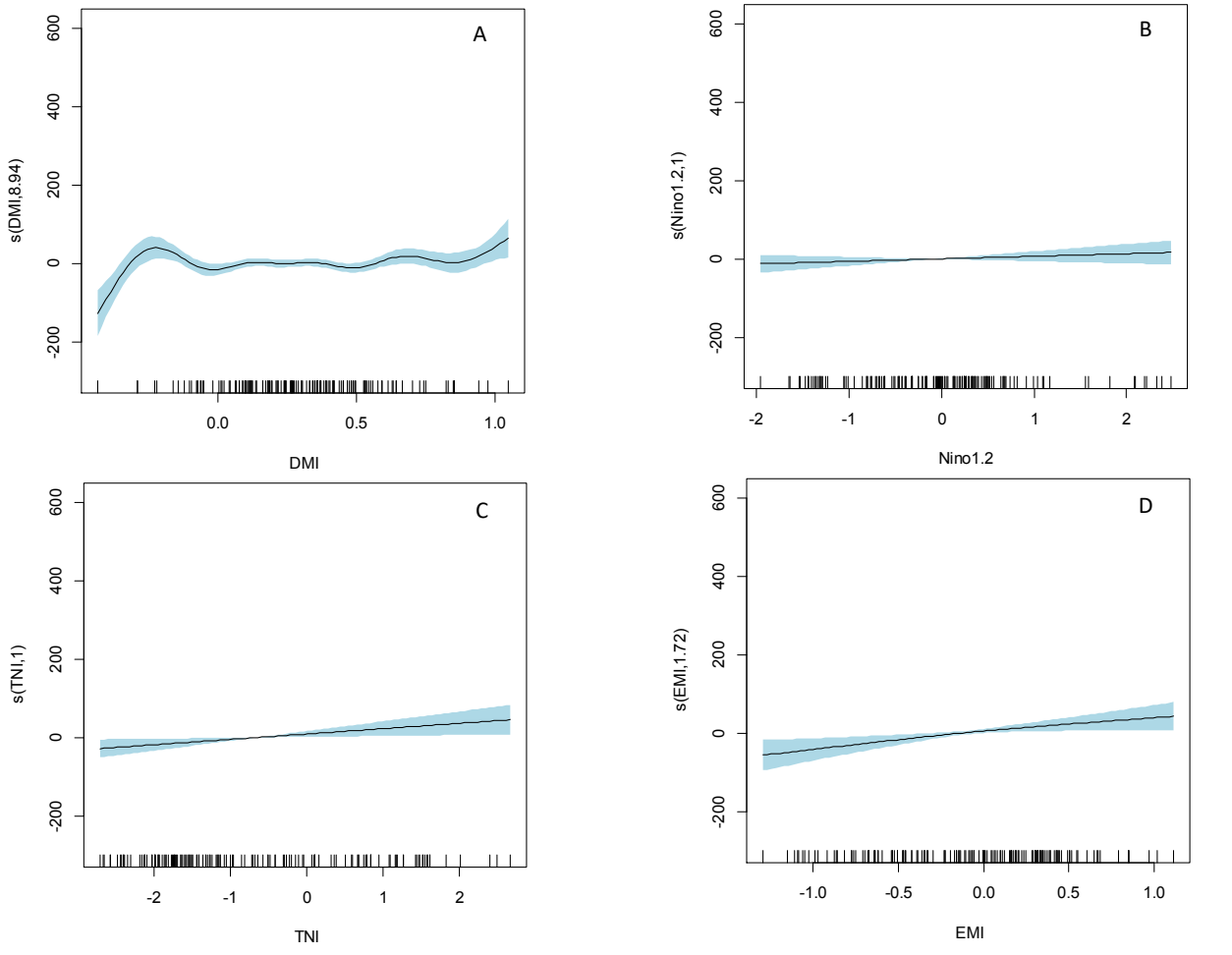

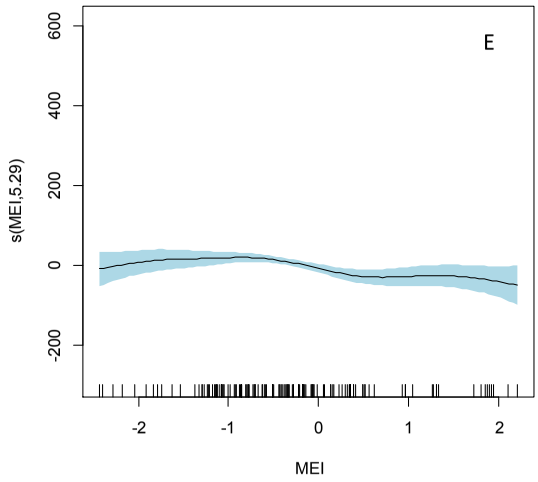
E
s(MEI,5.29)
MEI

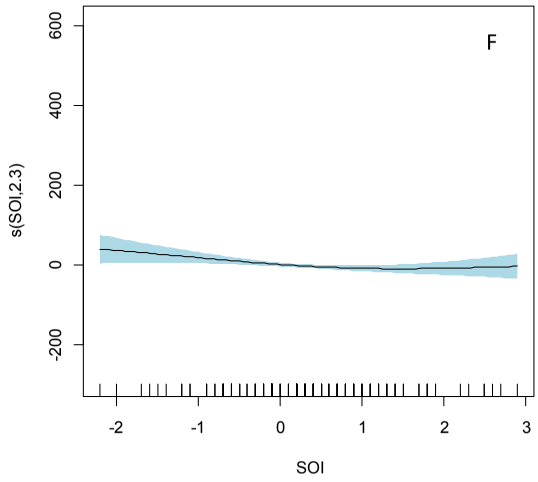
F
s(SOI,2.3)
SOI

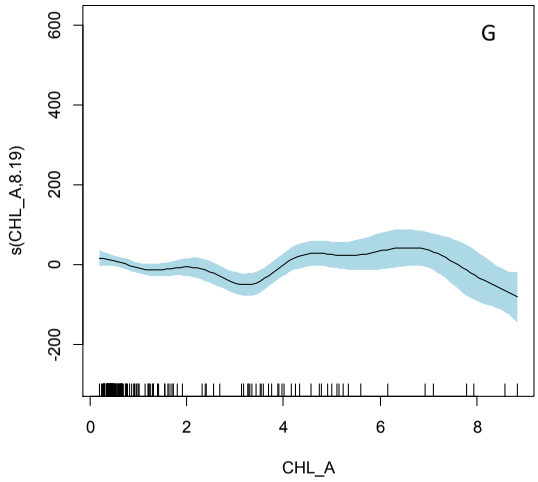
G
s(CHL_A,8.19)
CHL_A

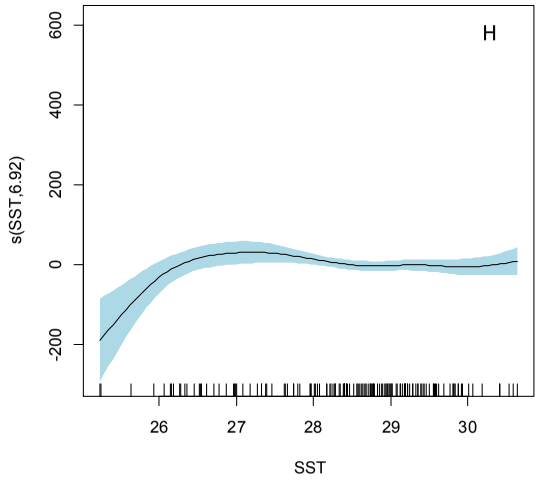
H
s(SST,6.92)
SST

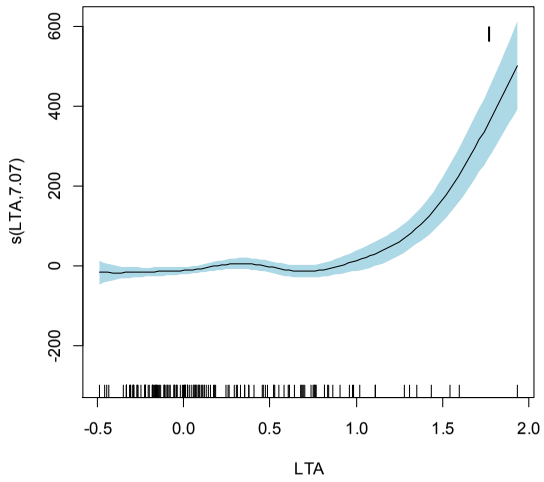
I
s(LTA,7.07)
LTA

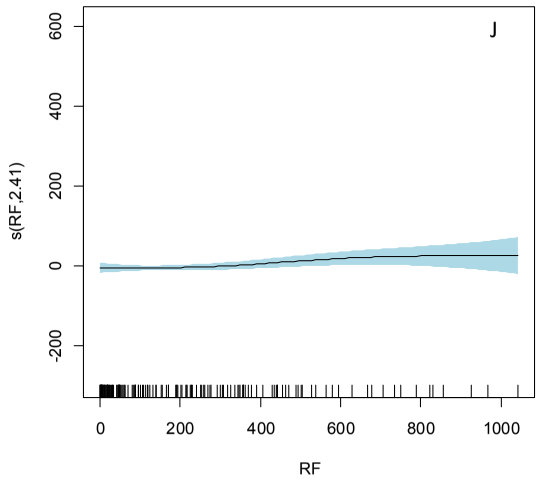
J
s(RF,2.41)
RF

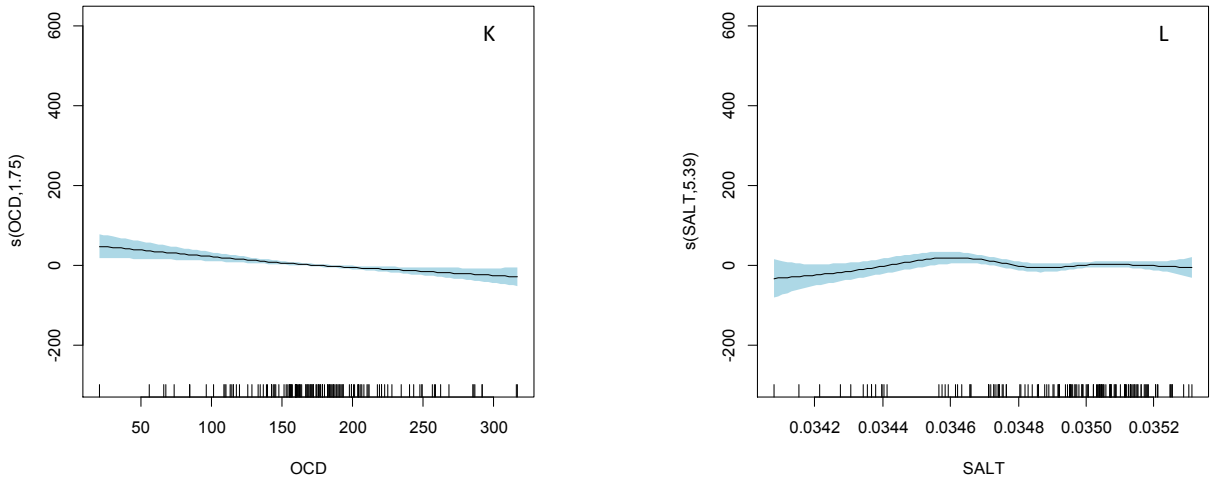

Figure4.30: GAM model for TB CPUE showing effects of explanatory variables (including ocean-atmospheric parameters as explanatory variables); DMI (A), Nino1+2 (B), TNI (C), EMI (D), MEI (E), SOI (F), CHL_A (G), SST (H), LTA (I), RF (J), OCD (K), and SALT (L)

Table 4.27: Details of deviance explained & adjusted R-square value for Total CPUE model and the effective degrees of freedom & significance of the explanatory variables (including ocean-atmospheric parameters as explanatory variables) of the model

T_CPUE ~ s(DMI) + s(Nino4) + s(SSHA) + s(SST) + s(LTA) + s(RF) +s(SALT) R-sq.(adj) = 0.63 Deviance explained = 71.7%					
	edf	Ref.df	F	Deviance explained (%)	p-value
s(DMI)	5.177	6.307	4.000	13.2	0.001019 **
s(Nino4)	3.343	4.177	7.050	9.4	3.35e-05 ***
s(SSHA)	1.000	1.000	6.554	25.8	0.011795 *
s(SST)	8.047	8.725	4.559	29	4.42e-05 ***
s(LTA)	6.436	7.500	4.188	32.4	0.000232 ***
s(RF)	8.455	8.900	3.702	23.5	0.000446 ***
s(SALT)	1.000	1.000	4.833	14.6	0.029987 *

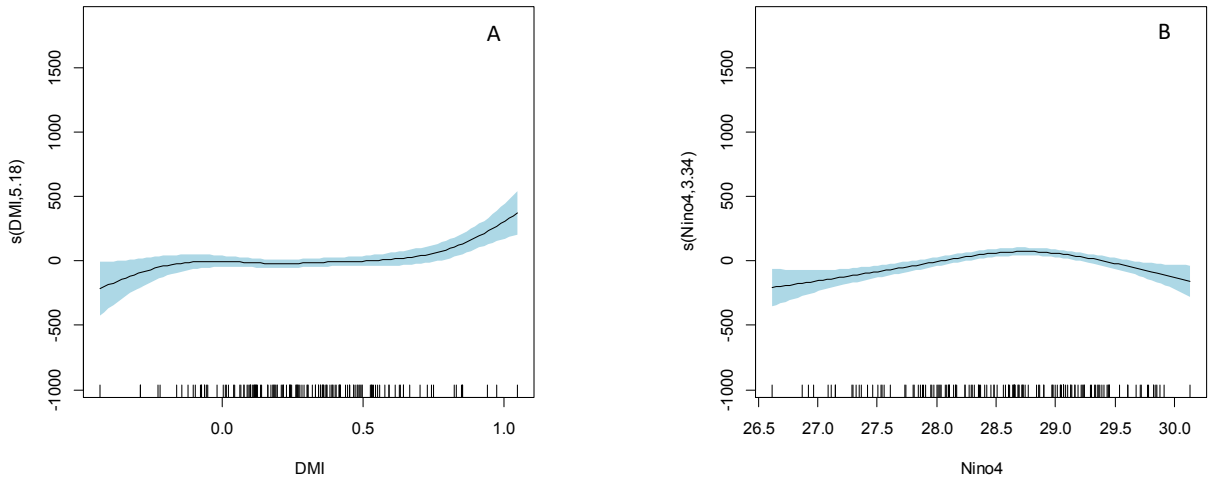

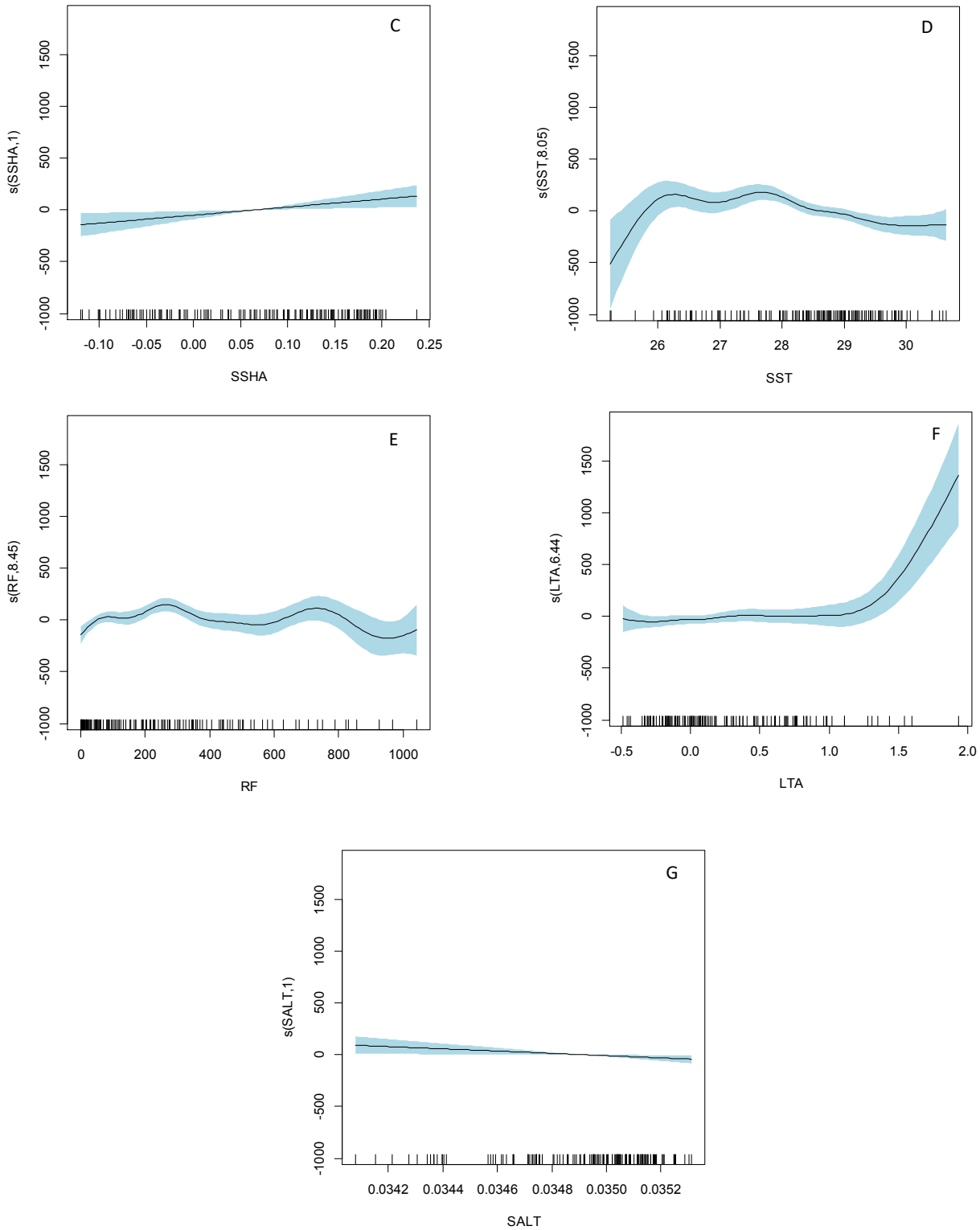

Figure4.31: GAM model for Total CPUE showing effects of explanatory variables (including ocean-atmospheric parameters as explanatory variables); DMI (A), Nino4 (B), SSHA (C), SST (D), RF (E), LTA (F), and SALT (G)

CHAPTER 5

DISCUSSION

5.1 Variations in ocean- atmosphere parameters

The variations of Ocean-atmosphere parameters such as Chlorophyll a, Local temperature anomaly, Sea surface temperature, Sea surface height anomaly, Sea surface salinity, Rainfall, Ocean current velocity and Ocean current direction along Kerala coast as affected by the ENSO episodes during 2007 to 2018 were studied. Deviance of each ocean-atmospheric parameters explained by ENSO phenomena as represented by different indices was in the order LTA (62.2%)>RF (59.9%)>SSHA (57.6%) >CHL A (52.9%)>SST (36.9%)>SALT (34%). The ENSO during premonsoon is shown to responsible for deviance in SST within the southwest coast of Indian coastal upwelling region 7°N-14°N (Krishna, 2008). In case of LTA, the order of influence of ENSO indices was TNI (20.5%)>MEI (13.6%)> EMI (9.48%) > Nino4 (8.79%)>DMI (6.88%)>SOI (2.93%). The 2010, 2016, and 2017 La Nina years reported strong upwelling in Kerala coast and the ENSO indices like MEI and EMI were found to exert maximum influence on upwelling. This result is supported by Krishna, 2008 who reported that warm ENSO events were associated with relaxation of Indian trade winds and wind induced coastal upwelling. 2018-2019 was CP weak El Nino, but 2018 exhibited strong upwelling. The ENSO index such as TNI which capture different flavours of El Nino exhibited a positive effect on upwelling in CP El Nino episode. The interannual variability of Indian Summer Monsoon (ISM) rainfall is strongly associated with the El Niño-Southern Oscillation (ENSO), experiencing below and above normal rainfall during El Niño and La Niña years respectively (Ashok *et al.* 2001).

Our investigation suggest that the monthly rainfall didn't follow a specific trend on El Nino or La Nina years. Out of 6 La Nina years observed during 2007-2018 two of them (2007-2008, 2011-2012) received above normal rain fall and 2010-2011 and 2016-2017 La Nina episodes received normal rainfall which was explained by the co-occurrence of negative IOD. The 2008-2009, and 2017-2018 years received rainfall just below the normal. This results are supported by Aneesh and Sijikumar, 2017 who observed that rainfall events were considerably reduced during the post-1980 La Nina events, due to weakening of the meridional temperature gradient over the monsoon region, which in turn reduced the monsoon rainfall and circulation. During the 2009-2010, 2018-2019 CP El Nino episodes, the region received above normal rainfall and during the very strong 2015-2016 El Nino episode, 80 mm less rainfall from normal was received.

It was observed that the chlorophyll concentrations were decreased during the El Nino episodes and were increased during the La Nina Episodes and the ENSO indices like MEI, TNI and Nino 4 were found to exert maximum influence on the chlorophyll concentration. The occurrence of seasonal bloom along west coast of India is largely affected by the ENSO events (Krishna and Rao, 2008). During 1997-98 El Nino equatorial Pacific region had positive deviations in chlorophyll concentration in the transition stage from El Nino to La Nina episodes (Yoder, 2003). Coastal upwelling off the southwest coast of India during the southwest monsoon is a well-known phenomenon that enhances the chlorophyll-a concentration (Shalin and Sanikumar, 2014). The positive IOD events resulted in an increase in chlorophyll a concentration and negative IOD events resulted in a decrease. The Indian Ocean Dipole (IOD) and the El Nino/Southern Oscillation (ENSO) are independent climate modes, which frequently co-occur, driving significant interannual changes within the Indian Ocean. The chlorophyll bloom in eastern equatorial Indian Ocean and in Bay of Bengal and negative effect of chlorophyll concentration in the region around southern tipoff India are primarily related to IOD forcing (Currie *et al.,* 2013). The EMI exhibited a negative effect on the chlorophyll a concentration. Chlorophyll concentration increased in 2010-2011, 2011-2012, and 2016-2017 La Nina episodes and didn't increase in 2008-2009 and 2017-2018 La Nina years. Chlorophyll concentration showed a hike in 2018 El Nino episode, neither hype nor dip in both 2009-2010 and 2015-2016 El Nino years. Chlorophyll a increase in 2010-2011, 2016-2017, and 2018 could be explained by the strong upwelling occurred during this time (Shafeeque, *et al.,* 2019). Chlorophyll hiked to 7mg/m^3 for both the strong (2010-2011) and moderate (2011-2012) La Nina events. Even though, 2010-2011 was a strong La Nina event and 2011-12 was a moderate La Nina event both the events resulted in a chlorophyll hike of 7mg/m^3. But, due to strong La Nina event, the 2010-2011 La Nina episode expected a more hike in the chlorophyll a concentration compared to 2011-2012 which was not happened and this could be due to the fact that 2010-2011 strong La Nina event was coincided with the negative IOD. That might have suppressed the vigorous growth of phytoplankton. The very strong El Nino episode in 2015 didn't show much dip in the chlorophyll from the normal which might be due to the co-occurrence of positive IOD.

It was observed that the SST was increased during the El Nino episodes and were decreased during the La Nina Episodes and the ENSO indices like MEI, TNI and EMI were found to exert maximum influence on the SST. The positive IOD events resulted in a decrease in SST and negative IOD events resulted in an increase. IOD events explains 12% of the SST variability in Indian Ocean (Saji *et al.,* 1999). The very strong El Nino episode in 2015-2016 resulted in a SST increase of 1°C during 2015

August to May 2016. The moderate El Nino in 2009-2010 also resulted in a SST hike of 1°C during December 2009 to May 2010. SST was decreased by 1°C during November months of 2007-2008 and 2010-2011 La Nina episodes, resulted in a decrease of 1°C during September to November months of 2016-2017 La Nina event. The SST over Indian Ocean during El Nino years show a warming trend and during La Nina a cooling trend was observed (Khole, 2003).

The ENSO episodes could explain 57% deviance in sea surface height anomaly. The ENSO indices such as EMI, MEI, TNI, and Nino 1+2 could be related to the increase in sea surface height anomaly during El Nino episodes and decrease in La Nina episodes. Devi and Sarangi, 2017 reported more positive sea surface height anomaly (SSHA range increased 20cm and above) during El Nino years in the Arabian Sea. It was seen that SSHA decreased during positive IOD events and increased during negative IOD events. Positive IOD events resulted in a decreased sea surface salinity and negative IOD resulted in an increase. The combined El Nino and positive IOD episodes resulted a freshening (negative SST anomaly) in Indian Ocean (Grunseich, *et al.,* 2011). The study revealed an increase in salinity during El Nino events and reduced salinity during La Nina episodes, but the sea surface salinity anomaly during El Nino and La Nina episodes were very less. These results are supported by Vinayachandran and Nanjundiah, 2009, who observed anomalies of sea surface salinity in Indian Ocean during El Nino or La Nina years were much weaker than salinity anomalies in IOD years.

5.2 Variations in selected pelagic and demersal fish resources

5.2.1 Variations in Oil sardine fishery

The Oil Sardine (Sardinella longiceps, Clupeidae) is an abundant coastal pelagic species, with high ecological and economic relevance. This fish species is often affected by inter-annual fluctuations and distributional shifts in the SW coast of India. The ENSO episodes could explain 31.4% deviance in the abundance of Oil sardine. In 2015, the poor maturation and recruitment of Indian Oil sardine were partially influenced by El Niño (Kripa, 2018). The GAM model output indicates the sensitivity of OS fishery to changes in DMI, EMI, SOI, TNI, and Nino 4. These ENSO indices were found to influence CPUE of OS in the order MEI (12.4)> Nino4 (9.49%)> SOI (6.84%)> EMI (3.33)> DMI (2.49) > TNI (1.47). The analysis of MEI, Nino 4, EMI, and SOI had shown that the OS abundance was decreased during El Nino and increased during La Nina. The TNI had shown the opposite trend and the DMI indicate an increase of OS during positive IOD episodes. Supraha *et al.,* (2016) reported a decrease in catch rate in oil sardine during El Nino events and hike in catch rate during La Nina event occurred after the El Nino in 1998-99.

When considering both ENSO and Ocean-atmospheric parameters DMI, TNI, Nino4, CHL A, SST, and OCV together explained the 40.1% of deviance in OS abundance over Kerala coast. These results are supported by Suprabha *et al.,* 2016, who observed that the combination of sea surface temperature and MEI could better explain deviance of oil sardine abundance. CHL A favours the OS abundance while OCV had negative impact. The chlorophyll abundance is a vulnerable factor for oil sardine fishery as it determines the feeding ground and controls its recruitment (Piontkovski, Al-Oufi, and Al-Jufaili, 2014; Zaki *et al.,* 2012). SST up to 28.3°C is favorable for OS, a further increase negatively affect the abundance. For oil sardine, Nino4 and SST could explain the deviance better than other ENSO indices and ocean –atmospheric parameters. They could be considered as the robust predictors of oil sardine abundance in this region. Increase in SST influence the marine biological systems at organismal, population, community and ecosystem levels (Vivekanandan, 2013). The oil sardines were exploited by a number of crafts including mechanized, motorized and non-motorized ones. The two principal gears exploiting oil sardines were MRS and OBRS (Kripa *et al.,* 2018). Deviance of catch per unit effort of oil sardine for different gears explained by ENSO was in the order OBRS (55.9%)> OBBS (44.4%)> NM (38.9%)> MRS (31%)> OBGN (30%). These are the gears which operate within 22 m depth. The deviance of CPUE of other gears like MDTN, MTN and MPS were found to be not well explained by ENSO. It indicated that the resource which was distant from the coastal area did not change much due to ENSO episodes or the multiday craft and gear combination changed the fishing ground to make up for the changes in the fish abundance.

5.2.2 Variations in Indian mackerel

The Indian mackerel (Rastrelliger kanagurta, Scombridae) is one of the most important pelagic fish resources of India in the context of national food security. The ENSO episodes could explain 31.7% deviance in the abundance of Indian mackerel. These ENSO indices were found to influence CPUE of IM in the order MEI (21.3%)> Nino1.2 (10.8%)> DMI 7.57%)> Nino4 (3.7%)> SOI (2.38%)> EMI (1.97%). The combination of ENSO indices and ocean-atmosphere parameters such as CHL A, SST, LTA, RF, and OCD had better explained the deviance (84%) of Indian mackerel abundance. The CPUE increased during La Nina episodes and decreased during El Nino episodes. But the most influencing ENSO indices such as MEI and Nino 1+2 showed an increasing trend on El Nino events. Positive IOD events favoured the mackerel abundance and it decreased during negative IOD events. The La Nina event favours Indian mackerel catch rate but with the less intensity than that of Oil sardine (Suprabha *et al.,* 2016). Mackerel fishery along the south west coast of India was collapsed in 1999-2000 due to La Nina event which preceded the 1997-1998 El Nino event (Krishnakumar and Bhat,

2007). These ENSO indices and ocean- atmospheric parameters were found to influence CPUE of IM in the order LTA (41.8%)> CHL A (34.9%)> SST (26.5%)> RF (25.9%)> MEI (21.3%)> Nino1.2 (10.8%) > DMI (7.57%)> Nino4 (3.7%)> EMI (1.97%). For Indian mackerel, LTA can be considered as better predictor for its abundance in this region. LTA had a positive effect on the CPUE of Indian mackerel. Increase in the CPUE was observed with increasing LTA values. Deviance of catch per unit effort of Indian mackerel for different gears explained by ENSO was in the order OBGN (46.3)> OBHL (41.1)> MRS (35.4%). The operating depth for OBGN were 25m and 30m for both MRS and OBHL. The deviance of CPUE of other gears like MDTN, MTN, MOTHS and OBBS were found to be not well explained by ENSO. It indicated that the resource which was distant from the coastal area did not change much due to ENSO episodes.

5.2.3 Variations in anchovy fishery

Anchovies are a group of small marine (coastal) schooling fishes and comprise fishes belonging to the genera Stolephorus, Coilia, Setipinna, and Thryssa. The ENSO episodes could explain 49.4% deviance in the abundance of Anchovy. These ENSO indices were found to influence CPUE of anchovy in the order MEI (17.3%)> DMI (6.62%)> EMI (6.37%)> Nino4 (5.61%)> TNI (5.4%)> Nino1.2 (4.85%). The combination of ENSO indices and ocean-atmospheric parameters had better explained the deviance (71.1%) in anchovy CPUE. Among the various elements influencing spawning and recruitment of anchovy populations, El Niño had been accounted as the most significant one (Checkley, *et al.,* 2009). GAM model result showed an increase in the CPUE during positive IOD events and decrease in negative IOD events. The ENSO indices considered in the model didn't follow same trend in El Nino or La Nina episodes. The anchovy abundance showed decreasing trend in El Nino and increase in La Nina. When considering other ocean- atmospheric parameters, order of influence on the abundance of Anchovy was in the order RF (25.3%)> CHL A (20.5%)> SALT (19.8%)> LTA (18.7%)> SST (17.6%)> OCV (10.1%). Deviance of catch per unit effort of Anchovy for different gears explained by ENSO was in the order MRS (60.1%)> OBTN (45.6%)> OBRS (43.8%)> OBBS (41.8%)> OBGN (31.4%). The operating depth for MRS, OBBS, OBGN, OBRS, and OBTN were 15, 12, 8, and 10 m respectively. All these gears operate in surface column area of coastal waters and much of the variations in the abundance was explained by ENSO episodes.

5.2.4 Variations in Penaeid Prawn fishery

The crustacean fishery in Kerala is the second largest contributor to the crustacean fishery in India (India agronet.com, 2020). Twenty species of penaeid prawns were identified in Kerala, out of the 20 species obtained 17 were of high economic value (Apsara and Pramod, 2016). Deviance in abundance of penaeid prawns could not be explained by ENSO, but combination of ENSO indices and ocean atmospheric parameters explained about 58.7% of the deviance in the abundance of penaeid prawns. They influenced the abundance of penaeid prawns in the order RF (33.9%)> LTA (11%)> Nino4 (7.34%)> SALT (5.4%)> OCV (5.07%)> SST (4.98%)> CHLA (2.64%)> TNI (1.04%)> DMI (0.06%). The rainfall between 600-800 mm was optimum for penaeid prawns and its abundance increased with positive positive LTA values. Deviance of catch per unit effort of penaeid prawn for different gears explained by ENSO was in the order OBRS (32%)> NM (28.5%). The operating depth for NM and OBRS were 7 and 10 m respectively. The deviance of CPUE of other gears like MDTN, MTN, MRS and OBTN were found to be not well explained by ENSO. This indicated that the resource which were distant from the coastal area were did not change much due to ENSO episodes.

5.2.5 Variations in Threadfin bream fishery

Threadfin bream (*Nemipterus* spp.) constitute one of the most important commercial demersal stocks targeted by trawlers in the Indian EEZ. They are abundant in 30-200 m depth range. Abundance of threadfin bream didn't follow same trend on all El Nino and La Nina episodes. Among the different factors influencing the abundance of threadfin breams, the ENSO had not been accounted as the most striking one. When considering the ocean atmospheric parameters along with the ENSO indices, it could explain 81.2% of the deviance of threadfin bream abundance. The LTA can be considered as better predictor (42.2%) for abundance of threadfin breams. The strong upwelling events favours their growth. Chlorophyll a concentration (31.2%) and SST (28.7) are other two important indicators of their abundance. Chlorophyll concentration was optimum at a range of 4 to 7 mg/m^3 and SST up to 28°C had positive effect on threadfin bream, a further increase in the SST didn't affect their abundance. Vivekanandan and Rajagopalan (2009) reported that SST between 28°C-29°C might be optimum but when it exceeded 29°C the fish are adapted to shift the spawning to season when temperature was around the preferred optima. Deviance of catch per unit effort of threadfin bream for different gears explained by ENSO was in the order OBHL (76.8%)> NM (50.1%)> OBGN (27.1%). The operating depth for these gears are within 40 m. The trawl nets are important gears for the demersal fishes like penaeid prawn and threadfin bream, as

they are found in greater depth range. But the ENSO episodes could not explain the deviance of CPUE of such gears.

5.2.6 Variations in total fish resources

The abundance of total fish resources were decreased during El Nino years and increased during La Nina episodes over Kerala coast. The GAM model of total CPUE revealed that ENSO episodes could explain 43.6% of deviance of total fish abundance. The ENSO episodes could explain the influence of total fish abundance in the order TNI (14.7%)> DMI (13.2%)> MEI (11.6%)> EMI (9.57%)> Nino4 (9.4%)> SOI (3.35%). The abundance showed a decrease during El Nino episodes and an increase during La Nina episodes. DMI index exhibited an increase during positive IOD events and decrease during negative IOD events. The SOI index showed decreasing trend on La Nina events and Nino 4 showed increasing trend during El Nino events. But both the indices had very less influence on the total fish abundance. When considering both ENSO and other ocean-atmospheric parameters, the model could explain 71.7% of deviance. They influence in the order LTA (32.4%)> SST (29%)> SSHA (25.8%)> RF (23.5%)> SALT (14.6%)> DMI (13.2%)> Nino4 (9.4%). The combined model indicated that, when considering other environmental factors which influenced total fish abundance along with ENSO, the Nino 4 index could be considered as one of the better predictors (9.4%) of fish abundance than other ENSO indices. The abundance of total fish resources was increased in La Nina years and decreased in El Nino events. Strong upwelling events favoured the fish abundance, SST up to 28°C was found to be good for fish abundance. LTA (32.4%), SST (29%) along with Nino 4 could be considered as better predictors for total fish abundance. Deviance of catch per unit effort of total fish resources for different gears explained by ENSO was in the order OBGN (48.8%)> OBRS (41%)> NM (37.5%)> MOTHS (36.2%)> MRS (32.4%)> OBBS (28.2%)> MDTN (26.6%) > OBHL (26.5%). The ENSO episodes could not explain well the deviance of CPUE of gears which were operating distant from coastal area.

CHAPTER 6

SUMMARY

El Nino southern oscillation, which affects weather patterns across the globe generally happens every 2-7 years. There were 20 major El Nino events in the last five millennia and each El Nino events were not identical. The diversity in El Nino events results in a different ecological response. This study was conducted to evaluate the impact of these diverse ENSO events during 2007-2018 on the marine fisheries of Kerala. The study indicated a strong impact on fish resources and the environment, indicating the need for increased monitoring and preparedness in fishing communities. The details of the study are summarised below.

Variations in different ENSO events

Five El Nino and six La Nina events happened during the 2007-2018 time period. Nino 3.4 and ONI indices were used to define these ENSO events. The TNI, MEI, and EMI indices were used to characterize the unique nature of each event. The El Nino events in 2006-2007, 2014-2015, 2018-2019 were weak (0.5 to 0.9SST anomaly), 2009-2010 was moderate (1.0 to 1.4) and 2015-2016 was very strong (>2.0). The La Nina episodes in 2008-2009, 2016-2017, and 2017-2018 were weak (-0.5 to -0.9), 2011-2012 was moderate (-1.0 to -1.4), 2007-2008 and 2010-2011 were strong (-1.5 to -1.9). Out of these five El Nino episodes, The El Nino event in 2006-2007 was EP type (Canonical) El Nino event, El Nino episodes in 2009-2010, 2014-2015, and 2018-2019 were CP type (El Nino Modoki) and the very strong El Nino event in 2015-2016 was Mixed type. The IOD index was used to identify the ENSO events which coincided with IOD. The El Nino episodes in 2006-2007, 2015-2016, and 2018-2019 coincided with positive IOD, and La Nina events in 2010-2011 and 2016-2017 coincided with negative IOD.

Influence of ENSO phenomenon on various ocean-atmospheric parameters

The ENSO could explain 62.2% of the deviance in the local temperature anomaly. The positive local temperature anomaly was increased during the La Nina years and there were strong upwelling events during 2010, 2016, and 2017 La Nina years. In the year 2018, there was also a strong upwelling event even though it was a weak CP El Nino year. It was due to the positive IOD event coincided with 2018 El Nino. The TNI index which captures different flavours of El Nino also showed a positive effect on LTA during El Nino events. The ENSO phenomenon as described by different indices could

explain 59.9% deviance in the monthly rainfall, but the monthly rainfall event didn't follow a specific trend during the El Nino and La Nina years. 52.9% of the deviance in the chlorophyll a concentration could be explained by ENSO. The Chlorophyll concentration was increased during La Nina episodes and in positive IOD events. But it was decreased during El Nino events, and in negative IOD events. 36.9% of the deviance in the SST could be explained by ENSO. The SST over the Kerala coast showed a warming trend during the El Nino event and a cooling trend during the La Nina events. SST showed a decreasing trend during positive IOD events and the opposite trend during negative IOD events. The ENSO episodes could explain 57.6% deviance in the sea surface height anomaly. The sea surface height was increased during El Nino events and decreased during La Nina events. SSHA was increased during negative IOD events and decreased during negative IOD events. The ENSO could explain the 34% deviance in the monthly sea surface salinity over the Kerala coast. The mean monthly sea surface salinity was increased during El Nino and decreased during La Nina events. But the variations of salinity during ENSO episodes were very less.

Impact of El Nino and La Nina on major pelagic and demersal resources of Kerala

The abundance of major pelagic fish resources like oil sardine, Indian mackerel, and anchovy and demersal fish resources like threadfin breams and penaeid prawns during ENSO episodes were studied.

The ENSO episodes could explain 31.4% deviance in the abundance of oil sardine. The oil sardine abundance was decreased during El Nino episodes and was increased during La Nina episodes. In the same line, the abundance was increased during positive IOD events and decreased during negative IOD events. The ENSO episodes and the ocean-atmospheric parameters together explain 40.1% of the deviance in the abundance of oil sardine. The resource in the near shore area were much affected by the ENSO and the resource that were distant from the coastal area did not change much due to ENSO episodes.

The ENSO episodes could explain 31.7% of the deviance in the abundance of Indian mackerel. The abundance of Indian mackerel was increased during La Nina events and decreased during El Nino events. Positive IOD events favoured the mackerel abundance and it decreased during negative IOD events. The ENSO episodes and the ocean-atmospheric parameters together explain 84% of the deviance in the abundance of Indian mackerel. The resource that were distant from the coastal area did not change much due to ENSO episodes.

The ENSO episodes could explain 49.4% of the deviance in the abundance of anchovy. The anchovy abundance showed a decreasing trend during El Nino episodes and an increasing trend during La Nina episodes. All the gears operating in the coastal waters were most affected by the ENSO events. The GAM model with combination of ENSO indices and ocean-atmospheric parameters as predictors explained 71.1% deviance in the anchovy abundance. The ocean-atmospheric parameters like rainfall and local temperature anomaly were the most influencing ones.

The combination of ENSO indices and ocean-atmospheric parameters had better predictability on the abundance of penaeid prawns, and it explained 58.7% of the deviance. The ENSO episodes alone did not much affect the abundance of penaeid prawns. The monthly rainfall amount and the local temperature anomaly were the better predictors of the abundance of penaeid prawns in this region.

The GAM model with combination of ENSO and ocean-atmospheric parameters as predictors could explain 81.2% deviance of the abundance of threadfin breams. Among the different factors influencing the abundance of threadfin breams, the ENSO indices were the least influential. The surface chlorophyll-a concentration and sea surface temperature could be considered as better predictors of their abundance.

The ENSO episodes could explain 43.6% of the deviance in the abundance of total fish resources over the Kerala coast. The total fish abundance was decreased during El Nino events and increased during La Nina events. The combination of ENSO and ocean-atmospheric parameters had better predictability on the abundance of total fish resources and it could explain 71.7% of the deviance of the abundance of total fish resources. The local temperature anomaly and SST were the influential predictors of total fish abundance.

General Conclusion

The study indicated that the warm and cold phase of ENSO partially influence the abundance of the major commercially important fish resources of Kerala. The El Nino (warm) episodes have negative and the La Nina (cold) episodes have a positive effect on the major pelagic fish resources such as oil sardine, Indian mackerel, and anchovy. The major demersal fish resources such as threadfin bream and penaeid prawns are not much affected by the ENSO events.

The gear-wise analysis indicated that the ENSO events are mainly affecting the fisheries in non-mechanized and motorized sector, which could have severe impact on the economy and livelihood of the coastal community.

The study brought out the intricate relationship between the ENSO phenomenon and the ocean-atmospheric variables. The changes in ocean-atmospheric parameters like chlorophyll, SST, upwelling, and rainfall during ENSO events and the, associated variations in fisheries were understood.

REFERENCES

Agri South Africa (AgriSA), 2016. A Raindrop in the Drought: Agri SA's Status Report on the Current Drought Crisis, (February). pp. 1-27.

Aneesh, S., and Sijikumar, S. 2016. Changes in the south Asian monsoon low level jet during recent decades and its role in the monsoon water cycle. *Journal of Atmospheric and Solar-Terrestrial Physics, 138(139), pp.47–53.* doi:10.1016/j.jastp.2015.12.009

Annamalai, H., Xie S. P. and McCreary, J. P. 2004 Impact of Indian Ocean Sea Surface Temperature on Developing El Niño. *Jour. of Climate*. 18(2), pp.302-319. doi: 10.1175/JCLI-3268.1.

Apsara S. K., and Pramod K. R. B., 2016. Diversity of penaeid shrimps in the trawl fishery of south-west coast of India. *Journal of Aquatic Biology & Fisheries.* 4, pp. 163-165.

Arcos, D.F., Cubillos, L.A. and Núñez, S.P. 2001. The Jack mackerel fishery and El Niño 1997-1998 effects off Chile. *Progress in Oceanography*, 49 (1-4), pp.597-617. doi: 10.1016/S0079-6611(01)00043-X.

Arntz, W. E. 1986. 1984 El Nin˜o and Peru positive aspects. *Oceanus*, 27, pp.36–39.

Arntz, W. E. 1986. The two faces of El Ni˜no 1982–83, *Meeresforsch.*, 31, pp.1–46,

Arntz, W. E., Gallardo, V. A., Gutiérrez, D., Isla, E., Levin, L. A. et al... 2006. El Niño and similar perturbation effects on the benthos of the Humboldt, California, and Benguela Current upwelling ecosystems. *Advances in Geosciences,* 6, pp.243-265. doi: 10.5194/adgeo-6-243-2006.

Arntz, W. E., Tarazona, J., Gallardo, V. A., Flores, L. A., and Salzwedel, H. 1991. Benthos communities in Oxygen deficient shelf and upper slope areas of the Peruvian and Chilean Pacific coast and changes caused by El Niño. *Geological Society Special Publications*, 58, pp.131-154. DOI: 10.1144/GSL.SP.1991.058.01.10

Arthur, R. 2000. Coral bleaching and mortality in three Indian reef regions during an El Niño southern oscillation event. *Current Sci.,* 79 (12), pp. 1723-1729

Ashok, K., Behera, S. K., Rao, S. A., Weng, H., and Yamagata, T. 2007 El Ni~no Modoki and its possible teleconnection. *Journal of Geophysical Research: Oceans*, 112(11), pp.1-27. doi: 10.1029/2006JC003798.

Ashok, K., Guan, Z, and Yamagata T. 2001. Impact of Indian Ocean dipole on the relationship between the Indian monsoon rainfall and ENSO, *Geophys. Res. Lett.,* 28(23), pp. 4499– 4502. doi: 10.1029/2001GL013294.

Ashok, K., Guan, Z, Saji, N. H., Yamagata T. 2004. Individual and combined influences of ENSO and the Indian Ocean dipole on the Indian summer monsoon. *J Clim*. 17(16), pp.3141–3155. doi: 10.1175/1520-0442(2004)017<3141:IACIOE>2.0.CO;2.

Ayers, J. M. and Strutton, P. G. 2013. Nutrient variability in Subantarctic Mode Waters forced by the Southern Annular Mode and ENSO. *Geophysical research letters*, 40(13), pp.3419–3423. doi:10.1002/grl.50638

Barber, R. T. and Kogelshatz, J. E. 1989. Nutrients and productivity during the 1982/83 El Niño. Monterey Bay Aquarium Research Institute, Pacific Grove, California, 93950 USA, pp. 21–53.

Baudoin, M.A., Vogel, C., Nortje, K., and Nai, M. 2017. Living with drought in South Africa: lessons learnt from the recent El Niño drought period. *International Journal of Disaster Risk Reduction*, 23, pp.128-137. doi: 10.1016/j.ijdrr.2017.05.005.

Bayer, A. M., Danysh, H. E., Garvich, M., Gonzálvez, G., Checkley, W., Alvarez, M., and Gilman, R. H., 2014. An unforgettable event: A qualitative study of the 1997-98 El Niño in northern Peru', *Disasters*, 38(2), pp. 351–374. doi: 10.1111/disa.12046.

Bertram, D. F., Harfenist, A., Cowen, L.L.E., Koch, D., Drever, M.C., Hipfner, J. M., and Lemon, M.J.F., 2017. Latitudinal temperature-dependent variation in timing of prey availability can impact Pacific seabird populations in Canada.

Bjerknes J (1969) Atmospheric teleconnections from the equatorial Pacific. Mon Weather Rev 97:163–172.

Brainard, R., E., Oliver, T., McPhaden, M., J., Cohen, A., Venegas, R., Heenan, A., Ángel, B., V., Rotjan, R., Mangubhai, S., Flint, E., and Hunter S., A., 2018. Ecological impacts of the 2015/16 el niño in the Central equatorial pacific. *Bulletin of the American Meteorological Society*. 99, pp.

Brander, K. M., 2007. Global fish production and climate change. Proc Natl Acad Sci USA 104(50), pp.19709–19714

Brown, B. E., and Suharsono. 1990. Damage and recovery of coral reefs affected by El Nifio related seawater warming in the Thousand Islands, Indonesia. Coral Reefs. 894), pp.163-170. doi: 10.1007/BF00265007.

Carre, M., Bentaleb, I., Fontugne, M., and Lavallee, D. 2005. Strong El Niño events during the early Holocene: stable isotope evidence from Peruvian seashells The Holocene. 15(1), pp. 42-47.

Cashin, P.A., Mohaddes, K., Raissi, M., 2017. Fair weather or foul? The macroeconomic effects of El Niño. J. Int. Econ. 106, pp.37–54

Central Marine Fisheries Research Institute (CMFRI), 2019, Annual Report 2018-19, ICAR-CMFRI, Kochi. p.320

Central Marine Fisheries Research Institute (CMFRI). 2012. Marine fisheries census 2010 Part I India. ICAR-Central Marine Fisheries Research Institute, Kochi, p.110.

Changnon, S. A. 1999. Impacts of 1997–98 El Niño–generated weather in the United States. Bulletin of the American Meteorological Society, pp. 1819-1827.

Chavez, F.P., Pennington, J.T., Castro, C.G., Ryan, J.P., Michisaki, R.P., Schlining, B., Walz, P., Buck, K.R., McFadyen, A. and Collins, C.A. 2002. Biological and chemical consequences of the 1997–1998 El Niño in central California waters. Progress in Oceanography, 54, pp.205–232

Checkley, *et al.,* 2009. Climate Change and Small Pelagic Fish. Scripps Institution of Oceanography, University of California, San Diego, La Jolla,California, USA. pp. 1-1026.

Chi, J., Du, Y., Zhang, Y. *et al.* 2019. A new perspective of the 2014/15 failed El Niño as seen from ocean salinity. *Sci Rep* 9, p.2720.https://doi.org/10.1038/s41598-019-38743-z

Claar, D. C., Szostek, L., McDevitt-Irwin, J. M., Schanze, J. J., and Baum, J. K. 2018. Global patterns and impacts of El Niño events on coral reefs: A meta- analysis. PLoS ONE 13(2) pp.1-22. doi: 10.1371/journal.pone.0190957.

Costa, A. K. R., Pereira, L. C. C., Costa, S. F. S., Leite, N. R., Flores-Montes, M., and Costa, R. M. 2016. Spatiotemporal variation in salinity during drought years in an Amazonian estuary (Taperaçu). Journal of Coastal Research, 75(1), pp.48-52.

Cravatte, S. T., Delcroix, D., Zhang, M., McPhaden, and Leloup, J. 2009. Observed freshening and warming of the western Pacific Warm Pool. Clim. Dyn., 33, pp.565–589.

Csirke, J., Guevara, R., Cardenas, G., Niquen, M., and Chipollini, A., 1994. Situationof resources anchovy (Engraulis ringens) & sardine (Sardinops sagax) at beginning of 1994 and perspectives for fishing in Peru, with special reference to northern-center region of Peru. Bolletin del Instituto Mar Peru. 15 (1), pp.2–23.

Currie, J. C., Lengaigne, M., Vialard, J., Kaplan, D. M., Aumont, O., Naqvi, S. W. A., and Maury, O., 2013, Indian Ocean Dipole and ElNino/ Southern oscillation impacts on regional chlorophyll anomalies in Indian Ocean. Biogeosciences (1726-4170) (Copernicus Gesellschaft Mbh), 10(10), pp. 6677-6698. https://doi.org/10.5194/bg-10-6677-2013,

Davis, J. L. D., 2000.Changes in a tidepool fish assemblage on two scales of environmental variation: seasonal and El Ni˜no Southern Oscillation, *Limnol. Oceanogr.,* 45, pp.1368–1379.

Delcroix, T. 1998. Observed surface oceanic and atmospheric variability in the tropical Pacific at seasonal and ENSO timescales: A tentative overview. *J. Geophys. Res. Oceans*. 103, pp.18611–18633.

Devi, K. N. and Sarangi, R. K. 2017. Time-series analysis of chlorophyll-a, sea surface temperature, and sea surface height anomalies during 2003–2014 with special reference to El Niño, La Niña, and Indian Ocean Dipole (IOD) Years. *International Journal of Remote Sensing*, 38(20), pp.5626–5639. doi:10.1080/01431161.2017.1343511

Dilley, M. and Heyman, B. A. 2005. ENSO disaster: Droughts, floods and El Niño Southern Oscillation warm events. *Disasters*. 19(3), pp.181-193.

Dogliotti, A.I., Ruddick, K., Guerrero, R. 2016. Seasonal and inter-annual turbidity variability in the Río de la Plata from 15 years of MODIS: El Niño dilution effect, *Estuarine, Coastal and Shelf Science.* Elsevier Ltd, 182, pp. 27–39. doi: 10.1016/j.ecss.2016.09.013.

Domı´nguez, G. E., Va´zquez, R. J., Pin˜a, G. V., and Palomino, A. B. 2000. Changes in the structure of a coastal fish assemblage exploited by a small scale gillnet fishery during an el Niño–la Nina event. *Estuarine, Coastal and Shelf Science.* 51, pp.773–787b doi:10.1006/ecss.2000.0724, available online at http://www.idealibrary.com.

Duke, N. C. and Larkum, A.W. 2019. Mangroves and Seagrass – an impression, (February). pp. 219-228. https://www.researchgate.net/publication/330552125

Fisher, J. L., Peterson, W. T., and Rykaczewski, R. R. 2015. The impact of El Niño events on the pelagic food chain in the northern California Current. Global Change Biology, 21(12), pp.4401-4414. doi:10.1111/gcb.13054

Folland, C. K., Renwick, J. A., Salinger, M. J., and Mullan, A. B. 2002. Relative influences of the interdecadal Pacific oscillation and ENSO on the South Pacific convergence zone. *Geophys. Res. Lett.,* 29 (13), doi:10.1029/2001GL014201.

Food and Agriculture Organisation (FAO) and International Collective in Support of Fishworkers (ICSF) Trust. 2018. Cyclone Ockhi Disaster risk management and sea safety in the Indian marine fisheries sector. Rome, FAO. p.72.

Food and Agriculture Organisation (FAO). 2007. The world's mangroves 1980-2005. A thematic study prepared in the framework of the Global Forest Resources Assessment 2005 FAO. Rome, p.80

Food and Agriculture Organisation (FAO). 2020. El Niño Southern Oscillation (ENSO) effects on fisheries and aquaculture. FAO Fisheries and Aquaculture Technical Paper No. 660. Rome, FAO. https://doi.org/10.4060/ca8348en

Francisco, A. S. and Netto S. A. 2020. El Nin˜ o–Southern Oscillations and Pacific Decadal Oscillation as Drivers of the Decadal Dynamics of Benthic Macrofauna in Two Subtropical Estuaries (Southern Brazil). *Ecosystems* https://doi.org/10.1007/s10021-019-00475-6

George, G., Jayasankar, J., Shah, P., Joseph, T., Raj, M., S., Shafeeque, M., Platt, T., and Sathyendranath, S. 2019. How Oceanography Influences Fishery Biology? - A Case of Distribution Differences in Carnivorous and Planktivorous Fishes along the Coastal Waters of Eastern Arabian Sea. ICAR-CMFRI, pp. 319-352.

Gierach, M. M., Lee, T., Turk, D., and McPhaden, M. J. 2012. Biological response to the 1997–98 and 2009–10 El Niño events in the equatorial Pacific Ocean, *Geophys. Res. Lett.,* 39, L10602, doi:10.1029/2012GL051103.

Glantz, M. H., 2001. Currents of Change: Impacts of El Niño and La Niña on Climate and Society. *Cambridge University Press; Cambridge*

Glynn, P. W., Maté, J. L., Baker, A. C., and Calderón, M. O., 2001. Coral bleaching and mortality in Panama and Ecuador during the 1997–1998 El Niño–Southern Oscillation event: Spatial/temporal patterns and comparisons with the 1982–1983 event. *Bull. Mar. Sci.,* 69, pp.79–109.

Goes, J. I., Thoppil, P. G., Gomes, R., and Fasullo, J. T., 2005. Warming of the Eurasian landmass is making the Arabian Sea more productive, *Science,* 308(5721), pp.545–547.

Gordon, L. 2015. Blame El Niño for poisonous sea snake found on Ventura County beach, *LA Times*, pp. 2–9. Available at: http://www.latimes.com/local/lanow/la-me-ln-venomous-sea-snake-found-20151016-story.html.

Grove, R. and Adamson, G. 2018. El Niño in world history. London, Palgrave Macmillan UK. (available at http://link.springer.com/10.1057/978-1-137-45740-0_1).

Gutierrez, L. 2017. Impacts of El Niño-Southern Oscillation on the wheat market: A global dynamic analysis. PLoS One. 12(6), pp. 1–27. doi: 10.1371/journal.pone.0179086.

Haddad, M., Taibi, H., and Arezki, S. M. M. 2013. On the recent global mean sea level changes: Trend extraction and El Niño's impact. Comptes Rendus Geoscience, 345(4), p. 167-175.

Harris, L. S., Varela, D. E., Whitney, F. W., and Harrison, P. J. 2009. Nutrient and phytoplankton dynamics off the west coast of Vancouver Island during the1997/98ENSOevent. Deep-Sea ResearchII 56, pp.2487–2502.

Heidelberg, K. B., O'Neil, K. L., Bythell, J. C., and Sebens, K. P. 2010. Vertical distribution and diel patterns of zooplankton abundance and biomass at Conch Reef, Florida Keys (USA). Journal of Plankton Research, 32, pp.75–91.

Howard, R., Bell II, and Pike, D. A. 2014. Thermal tolerances of sea turtle embryos: current understanding and future directions. Endanger Species Res., 26, pp.75–86

Hsiang, S. M., and Meng, K. C., 2015. Tropical economics. Am. Econ. Rev. 105 (5), pp.257–261

Humphries, G. R.W., Velarde, E., Anderson, D. W., Haase, B., and Sydeman, W. 2015. Seabirds as early warning indicators of climate events in the Pacific. PICES Press. 23, pp.18–20

Intergovernmental Panel on Climate Change (IPCC), 2014. Fifth Assessment Report: Climate Change 2014: Impacts, adaptation, and vulnerability. Part A: Global and sectoral aspects. *Cambridge University Press, Cambridge*. p.1132.

Intergovernmental Panel on Climate Change (IPCC), 2018. Proposed outline of the special report in 2018 on the impacts of global warming of 1. 5 ° C above pre-industrial levels and related global greenhouse gas emission pathways, in the context of strengthening the global response to the threat of climate cha', Ipcc - Sr15, 2(October), pp. 17–20. Available at: www.environmentalgraphiti.org

Izumo, T., Vialard, J., Lenagaigne, M., Montegut, C. B., Behera, S.K., Luo, J., Cravatte, S., Masson, S.,and Yamagata,T. 2010. Influence of the state of the Indian Ocean Dipole on the following year's El Niño. *Nature Geo science letters.* 3, pp 168-172.DOI: 10.1038/NGEO760

Kao, H. Y., Yu, J.Y. 2009. Contrasting eastern-Pacific and central-Pacific types of ENSO. *Journal of Climate,* 22, pp.615–632.

Khole, M. 2003, Variability of sea surface temperature over Indian Ocean during El Nino and La Nina years, Mausam, 54(4), pp.829-836.

Kiladis, G. N. and Diaz, H. F. 1989. Global climatic anomalies associated with extremes in the Southern Oscillation, *J. Clim.,* 2, pp.1069– 1090.

Klein, S. A., Soden, B. J., and Lau, N. C. 1999. Remote sea surface temperature variations during ENSO: evidence for a tropical atmospheric bridge. *J Clim* 12, pp.917–932. https://doi. org/10.1175/1520-0442(1999)012<0917:RSSTVD>2.0.CO;2

Kluger, L. C., Kochalski, S., Aguirre-Velarde, A., Vivar, I., and Wolff, M. 2018. Coping with abrupt environmental change: the impact of the coastal El Ni~no 2017 on artisanal fisheries and mariculture in North Peru. *Journal of Marine Science*, 76(4), pp.1122–1130. doi:10.1093/icesjms/fsy171

Kripa, V., 2018. Effect of Environmental Variations on Fishery Biology and Fisheries: The Indian Oil Sardine - A Case Study. CMFRI, Kochi-Manual

Kripa, V., Mohamed, K. S., Koya, K. P. S., Jeyabaskaran, R., Prema, D., Padua, S., Kuriakose, S., Anilkumar, P. S., Nair, P. G., Ambrose T. V., Dhanya, A. M., Abhilash, K. S., Bose. J., Divya,

N. D., Shara, A. S., and Vishnu, P. G. 2018 Overfishing and Climate Drives Changes in Biology and Recruitment of the Indian Oil Sardine Sardinella longiceps in Southeastern Arabian Sea. *Front. Mar. Sci*. 5, p.443.doi: 10.3389/fmars.2018.00443

Krishna, K., M. and Rao, S., R. 2008. Seasonal and interannual variability of sea surface chlorophyll a concentration in the Arabian Sea. Journal of Applied Remote Sensing 2(1), 023501. https://doi.org/10.1117/1.2837118

Krishna. K., M. 2008. Coastal upwelling along the southwest coast of India; ENSO modulation. *Ocean Science Discussions*, European Geosciences Union, , 5 (1), pp.123-134. ⟨hal-00298496⟩

Krishnakumar, P. K., and Bhat, G. S. 2007. Seasonal and interannual variations of oceanographic conditions off Mangalore coast (Karnataka, India) in the Malabar upwelling system during 1995-2004 and their influences on the pelagic fishery. Fisheries Oceanography, 17(1), 45–60. doi:10.1111/j.1365-2419.2007.00455.x

Kug, J. S., Jin, F. F., and An, S. I., 2009. Two types of El Ni~no events: cold tongue El Ni~no and warm pool El Ni~no. *Journal of Climate*, 22, pp.1499–1515.

Kumar, K., Rajagopalan, B., Hoerling, M., Bates, G., and Cane, M. 2006. Unraveling the Mystery of Indian Monsoon Failure during El Niño. *Science,* 314, pp.115–119.

Kumar, P. S., Pillai, G. N., and Manjusha, U. 2014. El Niño Southern Oscillation (ENSO) impact on tuna fisheries in Indian Ocean. *SpringerPlus*, 3(1), p. 1. doi: 10.1186/2193-1801-3-730.

Le Quéré, C., Moriarty, R., Andrew, R. M., Peters, G. P., and Ciais, P., et al. 2015. Global carbon budget 2014. Earth Syst. Sci. Data 7, 47–85. doi: 10.5194/essd-7-47-2015

Lee, T., McPhaden M. J., 2010. Increasing intensity of El Ni~no in the central-equatorial Pacific. *Geophysical Research Letters*, 37, L14603.

Lehodey, P., Bertignac, M., Hampton, J., Lewis, A., and Picaut, J. 1997. El Niño southern oscillation and tuna in the western Pacific. *Nature* 389, pp.715–718.

Lehodey, P., Senina, I., and Murtugudde, R. 2008. A spatial ecosystem and populationsdynamics model (SEAPODYM) – modeling of tuna and tuna-like populations. *Prog Ocean.* 78, pp.304–318

Li, T., Zhang, Y. S., Chang, C. P., and Wang, B. 2001. On the relationship between Indian Ocean sea surface temperature and Asian summer monsoon, *Geophys. Res. Lett.,* 28, pp.2843– 2846.

Lin, I. I., Camargo, S., Patricola, C. M., Boucharel, J., Chand, S., Klotzbach, P., Chan, J. C. L., et al. 2020. ENSO and tropical cyclones. In McPhaden, M. J., Santoso A., and Cai, W., eds. AGU Monograph: ENSO in a changing climate. Wiley, New York.

López-Medellín, X., *et al.,* 2011. Oceanographic anomalies and sea-level rise drive mangrove inland in the Pacific coast of Mexico. *Journal of Vegetation Science*. 22(1), pp.143-151

Lovelock, C. E., Feller, I.C., Ellis, J., Schwarz, A. M., Hancock, N., Nichols, P., and Sorrell, B. 2007. Mangrove growth in New Zealand estuaries: the role of nutrient enrichment at sites with contrasting rates of sedimentation. *Oecologia,* 153, pp. 633-641.

Maes, C., Picautand, J., and Belamari, S. 2005. Importance of salinity barrier layer for the buildup of El Niño. *J. Climate*, 18, pp.104–118, doi:10.1175/JCLI-3214.1.

Maity, R., and Nagesh Kumar D. 2006, Bayesian dynamic modeling for monthly Indian summer monsoon rainfall using El Nin˜o–Southern Oscillation (ENSO) and Equatorial Indian Ocean Oscillation (EQUINOO), *J. Geophys. Res.,* 111 (7), pp. 1-12 doi:10.1029/2005JD006539.

Maity, R., and Nagesh Kumar, D. 2006. Bayesian dynamic modeling for monthly Indian summer monsoon rainfall using El Niño–Southern Oscillation (ENSO) and Equatorial Indian Ocean Oscillation (EQUINOO). *Journal of Geophysical Research*, 111(D7). doi: 10.1029/2005jd006539

Marin Jarrin, J. and Salinas-de-Leon, P. 2020. Effects of the 2016 El Niño on the Galapagos Artisanal Coastal Fin-Fish Fishery. *Jour. Galapagos Research*. 69, pp. 25-33

McPhaden, M. J., Lee, T., and McClurg, D. 2011. El Ni~no and its relationship to changing background conditions in the tropical Pacific Ocean. *Geophysical Research Letters*, 38, L15709.

McPhaden, M. J., Zebiak, S. E., and Glantz, M. H. 2006. ENSO as an integrating concept in earth science. Science, 314(5806), pp.1740–1745. (available at https://doi.org/10.1126/ science.1132588).

Miller, K. A. 2007. Climate variability and tropical tuna: management challenges for highly: migratory fish stocks. *Mar Policy*. 31(1), pp.56–70

Mini, K. G. (2014) 'Sampling Methodology Employed By Cmfri', pp. 109–112.

Montero N, Santidrián Tomillo, P., Saba, V., Marcovaldi, M. A. G., López-Mendilaharsu, M., Santos, A. S., and Fuentes, M. M. P. B., 2019. Effects of local climate on loggerhead hatchling production in Brazil: implications from climate change. *Sci Rep*., 9, pp.8861

Muis, S., Haigh, I. D., Guimarães Nobre, G., Aerts, J. C. J. H., and Ward, P. J. 2018. Influence of El Niño-Southern Oscillation on global coastal flooding. *Future*, *6*, pp.1311–1322. https://doi. org/10.1029/2018EF000909

Murtugudde, R. G., Signorini, S. R., Christian, J. R., Busalacchi, A. J., McClain, C. R., and Picaut J. 1999. Ocean color variability of the tropical Indo-Pacific basin observed by SeaWiFS during 1997–1998, J. Geophys. Res., 104(18), pp.351–18.

N˜ iquen, M. and Bouchon, M. 2004. Impact of El Niño events on pelagic fisheries in peruvianwaters. *Deep-Sea Research II*. 51, pp.563–574

Naidu, P. D., Kumar, M. R. and Babu, V. R., 1999. Time and space variations of monsoonal upwelling along the west and east coasts of India. *Cont. Shelf Res.*, 19(4), pp.559-572.

National Fisheries Development Board (NFDB), 2019. About Indian Fisheries, Department of Fisheries, Ministry of Fisheries, Animal Husbandry & Dairying, Gov. of India. [on line]. Available: http://nfdb.gov.in/about-indian-fisheries.htm. [2019-07-18]. Obura, D., and S. Mangubhai, 2011: Coral mortality associated with thermal fluctuations in the Phoe¬nix Islands, 2002–2005. Coral Reefs, 30, pp.607–619, doi: 10.1007/s00338-011-0741-7

NOAA, 2017: Global coral bleaching event likely end¬ing. News & Features [online], National Oceanic and Atmospheric Administration. [Available on¬line at www.noaa.gov/media-release/global-coral -bleaching-event-likely-ending.].

Nobre, G. G., Muis, S., Veldkamp, T. I. E., and Ward, P. J. 2019. Achieving the reduction of disaster risk by better predicting impacts of El Niño and La Niña. *Progress in Disaster Science*. 2, p.6

Obura, D., Mangubhai, S. 2011. Coral mortality associated with thermal fluctuations in the Phoenix Islands, 2002-2005. *Coral Reefs.* 30, pp.607-619.

Ormaza-González, F. I., Cervetto, A. M., Martínez, R. M. B., Domínguez, M. A. H., Bravo, M. R. P., and Maldonado, V. M. J., 2016. Can small pelagic fish landings be used as predictors of high-frequency oceanographic fluctuations in the 1–2 El Niño region? *Adv. Geosci.,* 42, pp.61–72

Park J, Kim I-H, Fong J. J., Koo K-S, Choi W-J, Tsai T-S, et al. 2017. Northward dispersal of sea kraits (Laticauda semifasciata) beyond their typical range. PLoS ONE 12(6), pp.1-9. https://doi.org/10.1371/journal.pone.0179871.

Perea, L.A., Buitron, B., Mecklenburg, E., 1998. Reproductive state, partial fecundity and frequency of it spawns from the Peruvian anchoveta to autumn beginnings 1998. *Inf. Inst. Mar Peru*. 135, pp.147–152.

Pereira, L.C., Oliveira, S.M., Costa, R.M., Costa, K., Vila-Concejo, A. 2013. What happens on an equatorial beach on the Amazon coast when La Niña occurs during the rainy season?. *Estuarine, Coastal and Shelf Science,* 135, p. 116-127.

Peter A. Thompson, Pru Bonham, Paul Thomson, Wayne Rochester, Martina A. Doblin, Anya M. Waite, Anthony Richardson, Cecile S. Rousseaux. 2015. Climate variability drives plankton community composition changes: the 2010–2011 El Niño to La Niña transition around Australia. *Journal of Plankton Research*, 37(5), 966–984, https://doi.org/10.1093/plankt/fbv069

Piontkovski, Al-Oufi, and Al-Jufaili, 2014. Seasonal and interannual changes of Indian oil sardine, Sardinella longiceps landings in the governorate of Muscat (the Sea of Oman). Marine Fisherirs Review. 76(3), pp.50-59.

Plisnier, P. D., Serneels, S., Lambin, E. F., 2000. Impact of ENSO on East African ecosystems: a multivariate analysis based on climate and remote sensing data. *Global Eco Biogeo* 9(6), pp.481–497.

Qu, T. and Yu, J. Y. 2014. ENSO indices from sea surface salinity observed by Aquarius and Argo. *J Oceanogr.* 70, pp.367–375 DOI 10.1007/s10872-014-0238-4

Quasem, A. A. and Alam, G. M. 2016. Impact of El-Niño on Agro-economics in Malaysia and the Surrounding Regions: An Analysis of the Events from 1997-98. *Asian Journal of Earth Sciences*, 9, pp.1-8

Racault, M. F., Sathyendranath, S., Brewin, R. J. W., Raitsos, D. E., Jackson, T., and Platt, T. 2017. Impact of El Niño Variability on Oceanic Phytoplankton. *Front. Mar. Sci.* 4(MAY), p.133. doi: 10.3389/fmars.2017.00133

Rao, G. S., Sathianandan, T. V., Kuriakose, S., Mini, K. G., Najmudeen, T. M., Jayasankar, J. and Mathew, W. T., 2016. Demographic and socio-economic changes in the coastal fishing community of India. *Indian J. Fish.* 63(4), pp.1-9.

Rasmussen, A. R., Murphy, J. C., Ompi, M., Gibbons, J. W., Uetz, P. 2011. Marine reptiles. PLoS ONE. 6(11), doi: 10.1371/journal.pone.0027373.

Rasmusson, E. M., and Carpente, T. H., 1983. The relationship between eastern equatorial Pacific sea surface temperature and rainfall over India and Sri Lanka, *Mon. Weather Rev.*, 111, pp.517–528.

Reina, R. D., Spotila, J. R., Paladino, F. V., and Dunham, A. E., 2009. Changed reproductive schedule of eastern Pacific leatherback turtles Dermochelys coriacea following the 1997– 98 El Niño to La Nina transition. *Endangered Species Research.* 7, pp.155–161.

Reina, R.D., Mayor, P.A., Spotila, J. R., Piedra, R., and Paladino, F. V. 2002. Nesting ecology of the leatherback turtle, Dermochelys coriacea, at Parque Nacional Marino Las Baulas, Costa Rica: 1988–1989 to 1999–2000. *Copeia*., pp.653–664.

Riascos, J. M., Solı´s, M. A., Pacheco, A. S., and Ballesteros, M. 2017. Breaking out of the comfort zone: El Nin˜o-Southern Oscillation as a driver of trophic flows in a benthic consumer of the Humboldt Current ecosystem. *Proc. R. Soc. B: Biological Sciences*, 284(1857). doi: 10.1098/rspb.2017.0923.284: 20170923.

Richard, Y., Trzaska, S., Roucou, P., and Rouault, M. 2000. Modification of the southern African rainfall variability/ENSO relationship since the late 1960s, Clim. Dyn. 16, pp.883–895.

Ropelewski, C.F. and Jones, P.D., 1987: An extension of the Tahiti-Darwin Southern Oscillation Index. *Monthly Weather Review* 115, pp.2161-2165.

Rossi, S. and Soares, M. de O. 2017. Effects of El Niño on the Coastal Ecosystems and Their Related Services', *Mercator*, 16(12), pp. 1–16. doi: 10.4215/rm2017.e16030.

Roxy, M. K., Modi, A., Murtugudde, R., Valsala, V., Panickal, S., Prasanna Kumar, S., Ravichandran, M., Vichi, M., and Lévy M. 2016. A reduction in marine primary productivity driven by rapid warming over the tropical Indian Ocean, *Geophys. Res. Lett.,* 43, pp. 826–833, doi: 10.1002/2015GL066979.

Rueda, M. R. 2018. The Impact of Early Life Shocks on Human Capital Formation: Evidence from El Ni˜noFloods in Ecuador, Journal of Health Economics (2018), https://doi.org/10.1016/j.jhealeco.2018.07.003

Saba, V. S., Santidrian Tomillo, P., Reina, R. D., Spotila, J. R., Musick, J. A., Evans, D. A., and Paladino, F. V. 2007. The effect of the El Ni~no southern oscillation on the reproductive frequency of eastern Pacific leatherback turtles. *Journal of Applied Ecology*. 44, pp.395–404.

Saji, N., H., Goswamy, B., N., Vinayachandran,P., N., and Yamagata, T., 1999. A dipole mode in tropical Indian Ocean, *Nature,* 401(6751), pp.360-363.

Santidrián Tomillo, P., Fonseca, L. G., Ward, M., Tankersley, N., Robinson, N. J., Orrego, C. M., Paladino, F. V. and Saba, V. S. 2020. The impacts of extreme El Niño events on sea turtle nesting populations. *Climatic Change.* 159, pp.163–176.

Santidrian Tomillo, P., Robinson, N. J., Sanz-Aguilar, A., Spotila, J. R., Paladino, F. V., And Tavecchia, G. 2017. High and variable mortality of leatherback turtles reveal possible anthropogenic impacts. *Ecology,* 98(8), pp. 2170–2179.

Santidrian Tomillo, P., Saba, V. S., Blanco, G. S., Stock, C. A., Paladino, F. V., and Spotila, J. R. 2012. Climate driven egg and hatchling mortality threaten survival of Eastern Pacific leatherback turtles. PLoS ONE 7:e37602.

Sathianandan, T. V., Jayasankar, J., Vivekanandan, E., Narayankumar, R., and Pillai, N. G. K. 2008. Estimates on potential yield and maximum sustainable fleet size for marine fisheries in Kerala. *J. Mar. Biol. Ass. India*, 50 (2), pp.196 – 201.

Shafeeque, M., Shah, P., Platt, T., Sathyendranath, S., Menon, N. N., Balchand, A. N., and George, G. 2019. Effect of precipitation on Chlorophyll-*a* in an upwelling-dominated region along the west coast of India. *Journal of Coastal Research*. 86 (SI), pp.218–224.

Shah, P., Sajeev, R., and Gopika, N., 2015. Study of upwelling along the west coast of India - A climatological approach. *J. Coast. Res.* Florida, 31(5), pp.1151–1158.

Shalin, S. and Sanilkumar, K. V. 2014 Variability of chlorophyll-a off the southwest coast of India. International Journal of Remote Sensing, 35(14), 5420–5433. doi:10.1080/01431161.2014.926411

Shetye, S., Kurian, S., Gauns, M., and Vidya, P., J. 2019. 2015–16 ENSO contributed reduction in oil sardines along the Kerala coast, south-west India. *Marine ecology*. 40(6), pp. 1–9. DOI: 10.1111/maec.12568

Siderius, C., Gannon, K. E., Ndiyoi , M., Opere , A., Batisani , N., Olago , D., Pardoe, J., and Conway, D. 2018. Hydrological Response and Complex Impact Pathways of the 2015/2016 El Niño in Eastern and Southern Africa. *Earth's Future*, 6(1) https://doi.org/10.1002/2017EF000680

Smith, S. C. and Ubilava, D. 2017. The El Niño Southern Oscillation and economic growth in the developing world. *Global Environmental Change* 45(May), pp.151-164.

Smitha, B. R., Sanjeevan, V. N., Vimalkumar, K. G. and Revichandran, C., 2008. On the upwelling off the southern tip and along the west coast of India. *J. Coast. Res.*, 24(3), pp.95-102.

Srinath, M., Kuriakose, S. and Mini, K. G., 2005. Methodology for the estimation of marine fish landings in India. *CMFRI Special publication*, 86, pp.1-57.

Suarez, J. S., Ortiz, W. R., Gay-García, C., Torres-Jácome, J. Y., 2004. ENSO–tuna relationsin the eastern Pacific Ocean and its prediction as a non-linear dynamic system, Atmosfera 17(4), pp.245–258

Supraba, V. *et al.,* 2016. Climate influence on oil sardine and Indian mackerel in souththh-eastern Arabian Sea, (January).

Syamsuddin, M., Sunarto, and Yuliadi, L., 2018. How do El Niño Southern Oscillation events impact on small pelagic fish catches in the west Java Sea. *IOP Conf. Ser.: Earth Environ. Sci.* 176(1), 012014

Tamaddum, K. A., Kalra, A., Bernardez, M., and Ahamad, S. 2019. Effects of ENSO on Temperature, Precipitation, and Potential Evapotranspiration of North India's Monsoon: An Analysis of Trend and Entropy. *Water (Switzerland)*, 11(2). doi: 10.3390/w11020189.

Tang, W. and Yueh, S. 2017. The role of sea surface salinity in ENSO related water cycle anomaly. *Geophysical Research Abstracts*. 19, p. 18230.

Thomsen S. K., Mazurkiewicz, D. M., Stanley, T. R., Green, D. J. 2018. El Nin˜o/ Southern Oscillation-driven rainfall pulse amplifies predation by owls on seabirds via apparent

competition with mice. *Proc. R. Soc. B: Biological Sciences*, 285(1889). doi: 10.1098/rspb.2018.1161.

Thorne L. H. *et al*. 2015. Foraging behavior links climate variability and reproduction in North Pacific albatrosses. *Mov. Ecol.* 3, pp.1–15. (doi:10.1186/ s40462-015-0050-9).

Thorne L. H., Conners, M. G., Hazen, E. L., Bograd, S. J., Antolos, M., Costa, D. P., and Shaffer, S. A. 2016. Effects of El Nin˜o-driven changes in wind patterns on North Pacific albatrosses. *J. R. Soc. Interface,* 13: 20160196. http://dx.doi.org/10.1098/rsif.2016.0196.

Timmermann, A., Oberhuber, J., Bacher, A., Esch, M., Latif, M., and Roeckner, E. 1999. Increased El Nino frequency in a climate model forced by future greenhouse warming. *Nature*, 398, pp.694-696

Trenberth, K, E., 1997. The definition of El Nino. *American meteorological society*, 78, pp.2771-2777.

Trenberth, K. E., and Stepananiak, D. P., 2001. Indices of El Nino Evolution. J. Climate. 14 (8), pp.1697–1701.

Trenberth, K.E. 2013. El Niño Southern Oscillation (ENSO). Reference module in Earth Sciences and Environmental Sciences. *Elsevier*, p. 1-12,

Van Der Velde, M. *et al.* 2006. El Niño-Southern Oscillation determines the salinity of the freshwater lens under a coral atoll in the Pacific Ocean, *Geophysical Research Letters*, 33(21), pp. 1–5. doi: 10.1029/2006GL027748.

Vargas-Ángel, B., Looney, E. E., Vetter, O. J., and Coccagna, E. F. 2011. Severe, widespread El Niño–associ¬ated coral bleaching in the US Phoenix islands. *Bull. Mar. Sci.,* 87, pp.623–638.

Vinayachandran, P. N. and Nanjundiah, R. S. 2009. Indian Ocean sea surface salinity variations in a coupled model, *Climate Dynamics*, 33(2–3), pp. 245–263. doi: 10.1007/s00382-008-0511-6.

Vineetha, G., Karati, K. K., Raveendran, T. V., Babu, I. K. K., Riyas, C., Mushin, M. I., Shihab, B. K., Simon. C., Anil, P., 2018. Responses of the zooplankton community to peak and warning periods of El Niño 2015–2016 in Kavaratti reef ecosystem, northern Indian Ocean. Environ Monit. Assess. 190 (8). doi: 10.1007/s10661-018-6842-9.

Vivekanandan, E. and Rajagopalan, M. 2009. Impact of rise in seawater temperature on the spawning of threadfin breams, *Global climate change and Indian agriculture*, pp. 93–96. Available at: http://eprints.cmfri.org.in/8436/

Vivekanandan, E., 2013. Climate change: Challenging the sustainability of marine fisheries and ecosystems. *Journal of Aquatic Biology and Fisheries*, 1 (1&2), pp.54-67.

Wang, G. et al., 2017. Continued increase of extreme El Nino frequency long after 1.5°C warming stabilization. Nature Climate Change, 7(8), pp.568–572, doi:10.1038/nclimate3351.

Ward, R.D., Friess, D.A., Day, R.H., and Mackensie, R.A. 2016. Impacts of climate change on mangrove ecosystems: a region by region overview. *Ecosystem Health and Sustainability*, 2(4), pp.1-25.

Weng, H., Ashok, K., Behera, S. K., Rao, S. A., and Yamagata, T. 2007. Impacts of recent El Ni~no Modoki on dry/wet conditions in the Pacific rim during boreal summer. *Climate Dynamics,* 29(2-3), pp.113–129.

Wilkinson, C. R., LindeÂn, O., Cesar, H., Hodgson, G., Rubens, J., and Strong, A. E. 1999. Ecological and socioeconomic impacts of 1998 coral mortality in the Indian Ocean. An ENSO impact and a warning of future change? *Ambio.* 28, pp.188-196.

Wingfield, J.C., Hau, M., Boersma, P.D., Romero, L.M., Hillgarth, N., Ramenofsky, M., Wrege, P., Scheibling, R., Kelley, J.P., Walker, B., Wikelski, M., 2017. Effects of El Niño and La Niña Southern Oscillation Events on the Adrenocortical Responses to Stress in Birds of the Galapagos Islands., *General and Comparative Endocrinology*, 259, pp. 20–33. doi: 10.1016/j.ygcen.2017.10.015.

Wolter, K., and Timlin, M. S. 1998. Measuring the strength of ENSO events: How does 1997/98 rank? *Weather*, 53(9), pp.315–324. doi:10.1002/j.1477-8696.1998.tb06408.x

Wood, S.N. and Augustin, N.H., 2002. GAMs with integrated model selection using penalized regression splines and applications to environmental modelling. *Ecological Modelling*, 157 (2-3), pp.157-177.

Xue, Y., *et al.,* 2016.West African monsoon decadal variability and drought and surface-related forcings: Second West African Monsoon Modeling and Evaluation Project Experiment (WAMME II). *Clim. Dyn.*, 47(11), pp.3517-3545, doi: 10.1007/s00382-016-3224-2.

Yeh, S. W., Kirtman, B. P., Kug, J. S., Park, W., Latif, M. 2011. Natural variability of the central Pacific El Ni~no event on multi-centennial timescales. *Geophysical Research Letters*, 38, L02704.

Yeh, S. W., Kug, J. S., Dewitte, B., Kwon, M. H., Kirtman, B. P., and Jin, F. F. 2009. El Ni~no in a changing climate. Nature, 461(7263), pp.511–514.

Yoder, J. A., & Kennelly, M. A. (2003). *Seasonal and ENSO variability in global ocean phytoplankton chlorophyll derived from 4 years of SeaWiFS measurements. Global Biogeochemical Cycles, 17(4), n/a–n/a.* doi:10.1029/2002gb001942

Yu, J. Y. and Kim, S. T. 2012. Short Communication Identifying the types of major El Ni˜no events since 1870. *Int. J. Climatol*. 33(8), pp. 2105–2112. DOI: 10.1002/joc.3575

Zacharia, P. U., Mohamed, K. S., Sathianandan, T. V., Asokan, P. K., Krishnakumar, P. K., Abdurahiman, K. P., Durgekar, N. R., and Veena, S. 2011. Alpha, beta and gamma diversity of fished marine taxa along the southwest coast of India during 1970-2005. *J. Mar. Biol. Assoc.* 53(1), pp.21-26.

Zaki, S., Jayabalan, N., Al-Kiyumi, F., Al-Kharusi, L., and Al-Habsi, S., 2012. Maturation and spawning of the Indian oil sardine *Sardinella longiceps* Val. from the Sohar coast, Sultanate of Oman. *Journal of the Marine Biological Association of India*, 54 (1), 100-107.

Zebiak, S. E., Orlove, B., Muñoz, Á. G., Vaughan, C., Hansen, J., Troy, T., and Garvin, S. 2014. Investigating El Niño-Southern Oscillation and society relationships. *Wiley Interdisciplinary Reviews: Climate Change,* 6(1), pp.17–34. doi:10.1002/wcc.294

Zhang, N., Feng, M., Hendon, H. H., Hobday, A. J. and Zinke, J. 2017. Opposite polarities of ENSO drive distinct patterns of coral bleaching potentials in the southeast Indian Ocean. *Scientific Reports*, 7(1), p. 2443.

Zhao, M., Hendon, H. H., Yin, Y., and Alves, O. 2016 Variations of Upper-Ocean Salinity Associated with ENSO from PEODAS Reanalysis. Journal of Climate. 29, pp. 2077-2094.

Zhu, J., Huang, B., Zhang, R. *et al.* 2014. Salinity anomaly as a trigger for ENSO events. *Sci Rep.,* 4**,** p.6821. https://doi.org/10.1038/srep06821

Impact of El Nino and La Nina on selected commercially important marine fishery resources of Kerala

by

RESNA. K

(2015-20-016)

THESIS

Submitted in partial fulfilment of the

requirements for the degree of

B.Sc. – M.Sc. (Integrated) Climate Change Adaptation

Faculty of Agriculture

Kerala Agricultural University

ACADEMY OF CLIMATE CHANGE EDUCATION AND RESEARCH

VELLANIKKARA, THRISSUR – 680 656

KERALA, INDIA

2020

ABSTRACT

The El Nino Southern Oscillation (ENSO) is one of the most important coupled ocean-atmospheric phenomenon that causes global climate variability on inter annual time scales. El Nino has become very visible in recent years as a dominant source of inter annual climate variability around the world and will stay as the dominant mode of interannual climate variability with great influence on human populations and ecosystems. ENSO episodes are known to change the environmental characteristics of coastal waters which are the major habitats of the fish resources which are harvested all along the Indian coasts. The impact of diverse ENSO events during 2007-2018 on the marine fisheries of Kerala were studied. The monthly catch of major pelagic and demersal fishes like oil sardine, Indian mackerel, anchovy, penaeid prawns, and threadfin breams by major gears for the period 2007-2018 were collected and catch per unit effort (CPUE) were estimated. The ENSO indices like EMI, MEI, SOI, TNI, Nino4, Nino 1+2 and DMI and ocean-atmospheric parameters such as sea surface temperature (SST), rainfall (RF), chlorophyll a (CHL_A), local temperature anomaly (LTA), salinity (SALT), sea surface height anomaly (SSHA), and ocean current velocity (OCV) were analysed. The relationship of ENSO and those ocean-atmospheric parameters to variations in abundance of oil sardine, Indian mackerel, anchovy, penaeid prawns and threadfin breams were explored with Generalized Additive Model. The GAM results indicated that The ENSO could explain 62.2% of the deviance in the local temperature anomaly (R^2.adj = 0.56), 59.9% of the deviance in the monthly rainfall (R^2.adj = 0.53), 57.9% of the deviance in the sea surface height anomaly (R^2.adj = 0.52), 52.9% of the deviance in the chlorophyll a concentration (R^2.adj = 0.45), and 36.9% of the deviance in sea surface temperature (R^2.adj =0.30). The ENSO episodes could also explain 31.4% deviance in the abundance of oil sardine (R^2.adj =0.25), 31.7% of the deviance in abundance of Indian mackerel (R^2.adj =0.25), and 49% of the deviance in the abundance of anchovy (R^2.adj =0.39). The study also indicated that a combination of ENSO indices and ocean-atmospheric parameters could explain better the deviance in the abundance of fish resources. The combined model explained 40.1% deviance of oil sardine (R^2.adj =0.32), 84% deviance of Indian mackerel (R^2.adj =0.75), 71.1% deviance of anchovy (R^2.adj =0.58), 58.7% deviance of penaeid prawns (R^2.adj =0.5), and 81.2% deviance of threadfin breams (R^2.adj =0.7). The ENSO episodes alone could explain 43.6% deviance (R^2.adj = 0.38) and a combination of ENSO and ocean-atmospheric parameters could explain 71.7% of the deviance (R^2.adj =0.63) in the abundance of total fish resources the over the Kerala coast.